1

Project	**IEEE 802.16 Broadband Wireless Access Working Group <http://ieee802.org/16>**
Title	**Draft IEEE 802.16m Evaluation Methodology**
Date Submitted	**2007-10-22**
Source(s)	Editor: Roshni Srinivasan, Intel Corporation roshni.m.srinivasan@intel.com Jeff Zhuang, Motorola (Section 3) jeff.zhuang@motorola.com Louay Jalloul, Beceem Communications (Section 4) jalloul@beceem.com Robert Novak, Nortel Networks (Section 5,6,7,8) rnovak@nortel.com Jeongho Park, Samsung Electronics (Section 10) jeongho.jh.park@samsung.com
Re:	Evaluation Methodology for P802.16m-Advanced Air Interface
Abstract	This document is an update to C802.16m-07/080r3 according to the comment resolution conducted by TGm in Session #51.
Purpose	Updated evaluation methodology for the P802.16m draft
Notice	*This document does not represent the agreed views of the IEEE 802.16 Working Group or any of its subgroups*. It represents only the views of the participants listed in the "Source(s)" field above. It is offered as a basis for discussion. It is not binding on the contributor(s), who reserve(s) the right to add, amend or withdraw material contained herein.
Release	The contributor grants a free, irrevocable license to the IEEE to incorporate material contained in this contribution, and any modifications thereof, in the creation of an IEEE Standards publication; to copyright in the IEEE's name any IEEE Standards publication even though it may include portions of this contribution; and at the IEEE's sole discretion to permit others to reproduce in whole or in part the resulting IEEE Standards publication. The contributor also acknowledges and accepts that this contribution may be made public by IEEE 802.16.
Patent Policy	The contributor is familiar with the IEEE-SA Patent Policy and Procedures: <http://standards.ieee.org/guides/bylaws/sect6-7.html#6> and <http://standards.ieee.org/guides/opman/sect6.html#6.3>. Further information is located at <http://standards.ieee.org/board/pat/pat-material.html> and <http://standards.ieee.org/board/pat>.

Table of Contents

Index of Tables

Index of Figures

1 Abbreviations and Acronyms

2

3GPP	3G Partnership Project
3GPP2	3G Partnership Project 2
AAS	Adaptive Antenna System also Advanced Antenna System
ACK	Acknowledge
AES	Advanced Encryption Standard
AG	Absolute Grant
AMC	Adaptive Modulation and Coding
A-MIMO	Adaptive Multiple Input Multiple Output (Antenna)
AMS	Adaptive MIMO Switching
AoA	Angle of Arrival
AoD	Angle of Departure
ARQ	Automatic Repeat reQuest
ASN	Access Service Network
ASP	Application Service Provider
BE	Best Effort
CC	Chase Combining (also Convolutional Code)
CCI	Co-Channel Interference
CCM	Counter with Cipher-block chaining Message authentication code
CDF	Cumulative Distribution Function
CDL	Clustered Delay Line
CINR	Carrier to Interference + Noise Ratio
CMAC	block Cipher-based Message Authentication Code
CP	Cyclic Prefix
CQI	Channel Quality Indicator
CSN	Connectivity Service Network
CSTD	Cyclic Shift Transmit Diversity
CTC	Convolutional Turbo Code
DL	Downlink
DOCSIS	Data Over Cable Service Interface Specification
DSL	Digital Subscriber Line
DVB	Digital Video Broadcast
EAP	Extensible Authentication Protocol
EESM	Exponential Effective SIR Mapping
EIRP	Effective Isotropic Radiated Power
ErtVR	Extended Real-Time Variable Rate
EVM	Error Vector Magnitude
FBSS	Fast Base Station Switch
FCH	Frame Control Header
FDD	Frequency Division Duplex
FD-FDD	Full Duplex - Frequency Division Duplex

FFT	Fast Fourier Transform
FTP	File Transfer Protocol
FUSC	Fully Used Sub-Channel
HARQ	Hybrid Automatic Repeat reQuest
HD-FDD	Half Duplex – Frequency Division Duplex
HHO	Hard Handover
HMAC	keyed Hash Message Authentication Code
HO	Handover
HTTP	Hyper Text Transfer Protocol
IE	Information Element
IEFT	Internet Engineering Task Force
IFFT	Inverse Fast Fourier Transform
IR	Incremental Redundancy
ISI	Inter-Symbol Interference
LDPC	Low-Density-Parity-Check
LOS	Line of Sight
MAC	Media Access Control
MAI	Multiple Access Interference
MAN	Metropolitan Area Network
MAP	Media Access Protocol
MBS	Multicast and Broadcast Service
MCS	Modulation and Coding Scheme
MDHO	Macro Diversity Hand Over
MIMO	Multiple Input Multiple Output (Antenna)
MMS	Multimedia Message Service
MPC	Multipath Component
MPLS	Multi-Protocol Label Switching
MS	Mobile Station
MSO	Multi-Services Operator
NACK	Not Acknowledge
NAP	Network Access Provider
NLOS	Non Line-of-Sight
NRM	Network Reference Model
nrtPS	Non-Real-Time Polling Service
NSP	Network Service Provider
OFDM	Orthogonal Frequency Division Multiplex
OFDMA	Orthogonal Frequency Division Multiple Access
PER	Packet Error Rate
PF	Proportional Fair (Scheduler)
PKM	Public Key Management
PUSC	Partially Used Sub-Channel
QAM	Quadrature Amplitude Modulation

QPSK	Quadrature Phase Shift Keying
RG	Relative Grant
RMS	Root Mean Square
RR	Round Robin (Scheduler)
RRI	Reverse Rate Indicator
RTG	Receive/transmit Transition Gap
rtPS	Real-Time Polling Service
RUIM	Removable User Identify Module
SCM	Spatial Channel Model
SDMA	Space (or Spatial) Division Multiple Access
SF	Spreading Factor
SFN	Single Frequency Network
SGSN	Serving GPRS Support Node
SHO	Soft Handover
SIM	Subscriber Identify Module
SINR	Signal to Interference + Noise Ratio
SISO	Single Input Single Output (Antenna)
SLA	Service Level Agreement
SM	Spatial Multiplexing
SMS	Short Message Service
SNR	Signal to Noise Ratio
S-OFDMA	Scalable Orthogonal Frequency Division Multiple Access
SS	Subscriber Station
STC	Space Time Coding
TDD	Time Division Duplex
TDL	Tapped Delay Line
TEK	Traffic Encryption Key
TTG	Transmit/receive Transition Gap
TTI	Transmission Time Interval
TU	Typical Urban (as in channel model)
UE	User Equipment
UGS	Unsolicited Grant Service
UL	Uplink
UMTS	Universal Mobile Telephone System
VoIP	Voice over Internet Protocol
VPN	Virtual Private Network
VSF	Variable Spreading Factor
WiFi	Wireless Fidelity
WAP	Wireless Application Protocol
WiBro	Wireless Broadband (Service)
WiMAX	Worldwide Interoperability for Microwave Access

References

[1] IST-4-027756 WINNER II, D 5.10.2, "Spectrum requirements for systems beyond IMT-2000", v.0.5

[2] A. F. Molisch, "Wireless Communications", IEEE-Press Wiley, 2005.

[3] Erceg, et al, "Channel models for fixed wireless applications", IEEE 802.16.3c-01/29r4, 17/7/2001

[4] Recommendation ITU-R M.1225, "Guidelines for evaluation of radio transmission technologies for IMT-2000", 1997

[5] 3GPP-3GPP2 Spatial Channel Ad-hoc Group, "Spatial Channel Model Text Description," V7.0, August 19, 2003

[6] 3GPP TR 25.996, "Spatial channel model for Multiple Input Multiple Output (MIMO) Simulations"

[7] G. Calcev, D. Chizhik, B. Goransson, S. Howard, H. Huang, A. Kogiantis, A. F. Molisch, A. L. Moustakas, D. Reed and H. Xu, "A Wideband Spatial Channel Model for System-Wide Simulations", IEEE Trans. Vehicular Technology, vol. 56, pp. 389-403, 2007.

[8] Daniel S. Baum et al, "An Interim Channel Model for Beyond-3G Systems – Extending the 3GPP Spatial Channel Model (SCM)", Proc. IEEE VTC'05, Stockholm, Sweden, May 2005.

[9] A. F. Molisch, H. Asplund, R. Heddergott, M. Steinbauer, and T. Zwick, "The COST259 directional channel model – I. overview and methodology," IEEE Trans. Wireless Comm., vol. 5, pp. 3421–3433, 2006.

[10] H. Asplund, A. A. Glazunov, A. F. Molisch, K. I. Pedersen, and M. Steinbauer, "The COST259 directional channel model II - macrocells," IEEE Trans. Wireless Comm., vol. 5, pp. 3434–3450, 2006.

[11] L. Correia (ed.), "Flexible Personalized Wireless Communications", Wiley, 2001.

[12] A. F. Molisch and H. Hofstetter, "The COST273 Channel Model," in "Mobile Broadband Multimedia Networks ", (L. Correia, ed.), Academic Press, 2006.

[13] IST-WINNER II Deliverable D1.1.1 v1.0, "WINNER II Interim Channel Models", December 2006.

[14] M. Steinbauer, A. F. Molisch, and E. Bonek, "The double-directional radio channel," IEEE Antennas and Propagation Mag., pp. 51–63, August 2001.

[15] G. J. Foschini and M. J. Gans, "On limits of wireless communications in a fading environment when using multiple antennas," Wireless Personal Communications, vol. 6, pp. 311–335, Feb. 1998.

[16] P. Almers, et al. "Survey of channel and radio propagation models for wireless MIMO systems," Eurasip J. Wireless Comm. Networking, vol. in press, 2007.

[17]   T-S Chu, L.J. Greenstein, "A quantification of link budget differences between the cellular and PCS bands", IEEE Trans VT-48, No.1, January 1999, pp.60-65

[18]   "Digital mobile radio towards future generation systems", COST Action 231 Final Report, EUR 18957

[19]   D. Parsons, "The Mobile Radio Propagation Channel", Chapter.4, p.88, Pentech Press, 1992

[20]   Y. Oda, K. Tsunekawa, M. Hata, "Advanced LOS path-loss model in microcellular mobile communications" , IEEE Trans AP-51, pp.952-956, May 2003

[21]   "Universal Mobile Telecommunications System (UMTS) ; Selection procedures for the choice of radio transmission technologies of the UMTS (UMTS 30.03 version 3.2.0)", ETSI technical report TR 101 112 v3.2.0 (1998-04)

[22]   Jakes, W.C "Microwave mobile communications", Wiley, New York, 1974

[23]   M. Patzold, "Mobile Fading Channels", John Wiley, 2002

[24]   3GPP, R1-061001 "LTE Channel Models and link simulations"

[25]   https://www.ist-winner.org/phase_model.html

[26]   RUNCOM, "Coverage capacity simulations for OFDMA PHY in ITU-T channel models, " IEEE C802.16d-03/78r1, November, 2003

[27]   RUNCOM, "Coverage simulation for OFDMA PHY mode," IEEE C8021.6e-03/22r1.

[28]   Sony, Intel, "TGn Sync TGn Proposal MAC Simulation Methodology", IEEE 802.11-04/895r2, November 2004.

[29]   ST Micro-Electronics "Time Correlated Packet Errors in MAC Simulations", IEEE Contribution, 802.11-04-0064-00-000n, Jan. 2004.

[30]   Atheros, Mitsubishi, ST Micro-Electronics and Marvell Semiconductors, "Unified Black Box PHY Abstraction Methodology", IEEE Contribution 802.11-04/0218r1, March 2004.

[31]   3GPP TR 25.892 V2.0.0 "Feasibility Study for OFDM for UTRAN enhancement,"

[32]   WG5 Evaluation Ad-hoc Group, "1x EV-DV Evaluation Methodology – Addendum (V6)," July 25, 2001

[33]   Ericsson, "System level evaluation of OFDM- further considerations", TSG-RAN WG1 #35, R1-03-1303, November, 2003

[34]   Nortel, "Effective SIR Computation for OFDM System-Level Simulations," TSG-RAN WG1 #35, R03-1370, November 2003.

[35]   Nortel "OFDM Exponential Effective SIR Mapping Validation, EESM Simulation Results for System-Level Performance Evaluations," 3GPP TSG-RAN1 Ad Hoc, R1-04-0089, January, 2004.

[36]   K. Brueninghaus et al, "Link performance models for system level simulations of broadband radio access," IEEE PIMRC, 2005.

[37]   L. Wan, et al, "A fading insensitive performance metric for a unified link quality model," WCNC, 2006.

[38]   DoCoMo, Ericsson, Fujitsu, Mitsubishi Electric, NEC, Panasonic, Sharp, Toshiba Corporation, R1-060987, "Link adaptation schemes for single antenna transmissions in the DL, 3GPP-LTE WG1 meeting #44-bis, Athens, March 2006.

[39]   G. Caire, "Bit-Interleaved Coded Modulation", *IEEE Transactions on Information Theory*, Vol. 44, No.3, May 1998.

[40]   J. Kim, et al, "Reverse Link Hybrid ARQ: Link Error Prediction Methodology Based on Convex Metric", Lucent Technologies, 3GPP2 contribution, TSG-C WG3 20030401-020, April 2003.

[41]   S. Tsai, "Effective-SNR Mapping for Modeling Frame Error Rates in Multiple-State Channels", Ericsson, 3GPP2-C30-20030429-010.

[42]   IEEE P 802.20™ PD-09 Version 1.0, "802.20 Evaluation Criteria – version 1.0," September 23, 2005

[43]   P. Barford and M Crovella, "Generating Representative Web Workloads for Network and Server Performance Evaluation" In Proc. ACM SIGMETRICS International Conference on Measurement and Modeling of Computer Systems, pp. 151-160, July 1998.

[44]   S. Deng. "Empirical Model of WWW Document Arrivals at Access Link." In Proceedings of the 1996 IEEE International Conference on Communication, June 1996

[45]   R. Fielding, J. Gettys, J. C. Mogul, H. Frystik, L. Masinter, P. Leach, and T. Berbers-Lee, "Hypertext Transfer Protocol - HTTP/1.1", RFC 2616, HTTP Working Group, June 1999. ftp://ftp.Ietf.org/rfc2616.txt.

[46]   B. Krishnamurthy and M. Arlitt, "PRO-COW: Protocol Compliance on the Web", Technical Report 990803-05-TM, AT&T Labs, August 1999, http://www.research.att.com/~bala/papers/procow-1.ps.gz. 29 30 31 32 33 34 35 36 37

[47]   B. Krishnamurthy, C. E. Wills, "Analyzing Factors That Influence End-to-End Web Performance", http://www9.org/w9cdrom/371/371.html

[48]   H. K. Choi, J. O. Limb, "A Behavioral Model of Web Traffic", Proceedings of the seventh International Conference on Network Protocols, 1999 (ICNP '99), pages 327-334.

[49]   F. D. Smith, F. H. Campos, K. Jeffay, D. Ott, "What TCP/IP Protocol Headers Can Tell Us About the Web", Proc. 2001 ACM SIGMETRICS International Conference on Measurement and Modeling of Computer Systems, pp. 245-256, Cambridge, MA June 2001.

[50]   3GPP2/TSG-C30-20061204-062A, "cdma2000 Evaluation Methodology (V6)", Maui, HI., December 2006

[51]   J. Cao, William S. Cleveland, Dong Lin, Don X. Sun., "On the Non-stationarity of Internet Traffic", Proc. ACM SIGMETRICS 2001, pp. 102-112, 2001.

[52]   K. C. Claffy, "Internet measurement and data analysis: passive and active measurement", http://www.caida.org/outreach/papers/Nae/4hansen.html.

[53]   3GPP2-TSGC5, HTTP and FTP Traffic Model for 1xEV-DV Simulations

[54]   3GPP TSG-RAN1#48   R1-070674, LTE physical layer framework for performance verification, Orange, China Mobile, KPN, NTT DoCoMo, Sprint, T-Mobile, Vodafone, Telecom Italia, February 2007.

[55]   WINNER Project, IST-2003-507581 WINNER D1.3 version 1.0, "Final usage scenarios."

[56]   3GPP TS 25.101v7.7.0, "User Equipment (UE) Radio Transmission and Reception (FDD)"

[57]   3GPP TSG RAN WG1#44, R1-060385, "Cubic Metric in 3GPP-LTE", February 13-17, 2006, Denver, USA

[58]   http://www-tkn.ee.tu-berlin.de/research/trace/ltvt.html

[59]   F. Fitzek and M. Reisslein. MPEG-4 and H.263 traces for network performance evaluation (extended version). Technical Report TKN-00-06, Technical University Berlin, Dept. of Electrical Eng., Germany, October 2000.

[60]   W. R. Stevens, "TCP/IP Illustrated, Vol. 1", Addison-Wesley Professional Computing Series, 1994.

[61]   "Part 16: Air interface for fixed and mobile broadband wireless access systems. Amendment 2: Physical and Medium Access Control Layers for Combined Fixed and Mobile Operation in Licensed Bands", IEEE standard for local and metropolitan area networks, 2005.

[62]   IEEE 802.16e-2005 - IEEE Standard for Local and metropolitan area networks Part 16: Air Interface for Fixed and Mobile Broadband Wireless Access Systems. Amendment 2: Physical and Medium Access Control Layers for Combined Fixed and Mobile Operation in Licensed Bands and Corrigendum 1.

[63]   "Next Generation Mobile Networks Radio Access Performance Evaluation Methodology", June, 2007 (www.Ngmn-cooperation.com/docs/NGMN Evaluation Methodology V1.2.pdf)

[64]   FCC regulations: http://www.hallikainen.com/FccRules/2007/27/53/, http://www.access.gpo.gov/nara/cfr/waisidx_06/47cfr27_06.html (see 27.53 emission limits).

[65]   UMTS Forum, 3G Offered Traffic Report, 30 June 2003.

[66]   ITU R M.2072, World mobile telecommunication market forecast.

[67]   B. H. Kim, and Y. Hur, "Application Traffic Model for WiMAX Simulation," POSDATA, Ltd, April 2007.

[68]   L. A. Dabbish, R. E. Kraut, S. Fussell and S. Kiesler, "Understanding Email Use:

Predicting Action on a Message," Proceedings of the ACM Conference on Human Factors in Computing Systems (CHI'05), NY: ACM Press, pp.691-700.Ffff.

[69]   V. Bolotin, Y. Levy, and D. Liu," Characterizing Data Connection and Messages by Mixtures of Distributions on Logarithmic Scale, ITC 99, Edinburgh.

[70]   G.. Brasche, B. Walke, " Concepts Services, and Protocols of the New GSM Phase 2+ General Packet Radio Service, IEEE Communications Magazine, August 1997.

[71]   M. S. Borella," Source Models of Network Game Traffic", Computer Communications, 23 (4), pp. 403-410.

[72]   IEEE C802.16m-07/181 "Wideband Extension of the ITU profiles with desired spaced-frequency correlation", Alcatel-Lucent, Malaga, Spain, September 2007.

[73]   L. Jalloul, " On the Expected Value of the Received Bit Information Rate", IEEE C802.16m-07/195, Malaga, Spain, September 2007.

1 **Editor's Notes**

2 This document is a revision to C802.16m-07_080r3 based on the resolution of
3 comments by TGm in Session #51. C802.16m-07_080r3 was developed by the
4 evaluation methodology ad-hoc groups through harmonization of contributions and
5 resolution of comments in TGm sessions #48, #49, #50 and #51.

6

7 The drafting ad-hoc groups have marked some text with brackets and left other text
8 unbracketed. Unbracketed text in black identifies content that has been harmonized and
9 adopted through comment resolution. Square brackets [ ] identify text that requires
10 further harmonization. Bracketed text has also been color coded in green. Editors' notes
11 in red capture actions that may be necessary for further updates.

12

13

1. Introduction

A great deal can be learned about an air interface by analyzing its fundamental performance in a link-level setting which consists of one base station and one mobile terminal. This link-level analysis can provide information on the system's fundamental performance metrics. The actual performance, in real-world settings, where multiple base stations are deployed in a service area and operating in the presence of a large number of active mobile users, can only be evaluated through a system-level analysis. The extension of the link-level analysis methods to a system-level analysis may start with adding multiple users in a single-cell setting. This technique is generally straightforward and provides a mechanism for initial understanding of the multiple-access characteristics of the system. Ultimately, however, quantifying the system level performance, although difficult, carries with it the reward of producing results that are more indicative of the system performance.
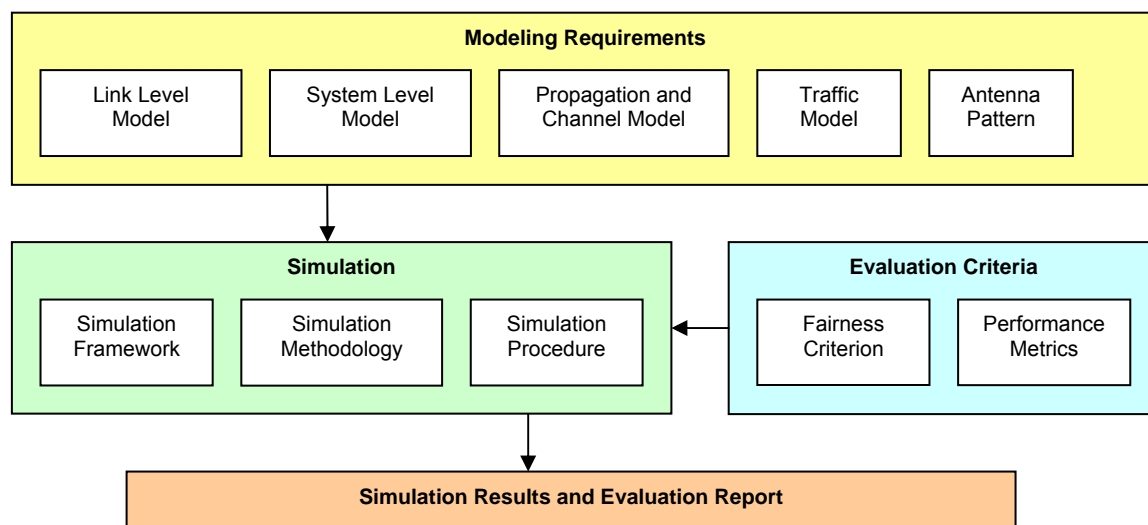
Figure 1 : Simulation Components

Since system level results vary considerably with different propagation and interference environments, as well as with the number and distribution of users within the cells, it is important that the assumptions and parameters used in the analysis be reported carefully lest the quoted network-level performance be misleading.

The objective of this evaluation methodology is to define link-level and system-level simulation models and associated parameters that shall be used in the evaluation and comparison of technology proposals for IEEE 802.16m. Proponents of any technology proposal using this methodology shall follow the evaluation methods defined in this document and report the results using the metrics defined in this document. The methods provided in this evaluation methodology document may be extended or

1 enhanced in order to align with IMT EVAL or to further evaluate specific proposals not
2 covered by this document.
3
4 Evaluation of system performance of a mobile broadband wireless access technology
5 requires system simulation that accurately captures the dynamics of a multipath fading
6 environment and the architecture of the air-interface. The main simulation components
7 are illustrated in Figure 1.

8 **2. System Simulation Requirements**

9 **2.1.   Antenna Characteristics**
10 This section specifies the antenna characteristics, e.g. antenna pattern, orientation, etc.
11 for antennas at the BS and the MS.

12 **2.1.1.   BS Antenna**

13 **2.1.1.1.   BS Antenna Pattern**
14
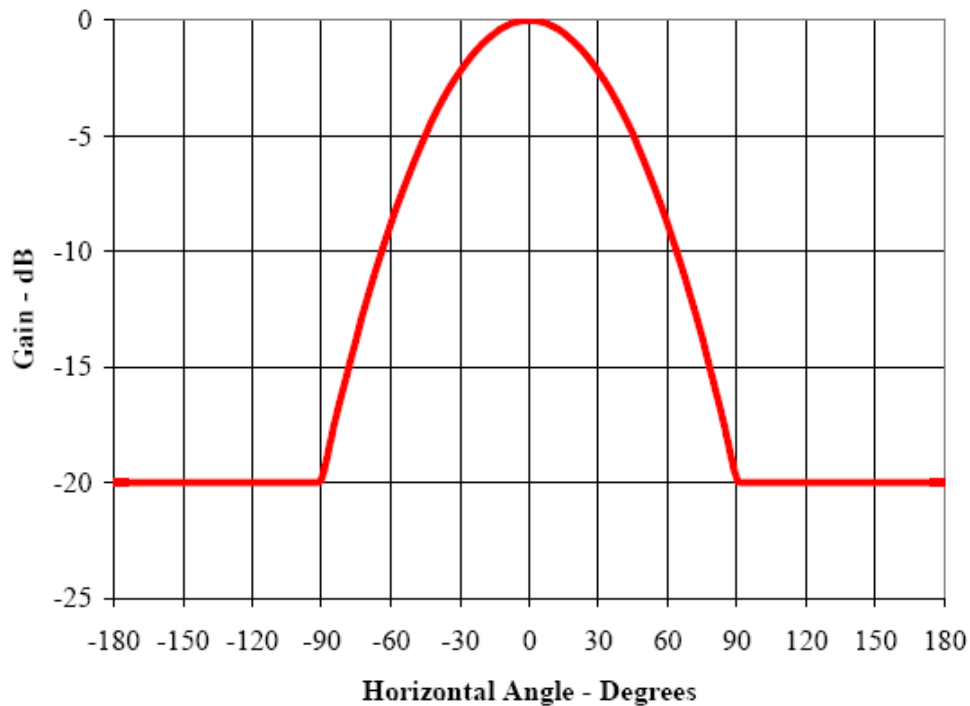
15
16 **Figure 2: Antenna Pattern for 3-Sector Cells**
17
18 The antenna pattern used for each BS sector is specified as

19
$$A(\theta) = -\min\left[12\left(\frac{\theta}{\theta_{3\,dB}}\right)^2, A_m\right] \qquad (1)$$

1   where $A(\theta)$ is the antenna gain in dBi in the direction θ, $-180^\circ \leq \theta \leq 180^\circ$, and min [.]

2   denotes the minimum function, θ_{3dB} is the 3 dB beamwidth (corresponding to

3    $\theta_{3dB} = 70^\circ$), and A_m= 20 dB is the maximum attenuation. Figure 2 shows the BS

4   antenna pattern for 3 sector cells to be used in system level simulations.

5

6   A similar pattern will be used for elevation in simulations that need it. In this case the

7   antenna pattern will be given by:

8
$$A_e(\varphi) = -\min\left[12\left(\frac{\varphi}{\varphi_{3\,dB}}\right)^2, A_m\right] \qquad (2)$$

9   where $A_e(\phi)$ is the antenna gain in dBi in the elevation direction ϕ, $-90^\circ \leq \phi \leq 90^\circ$. ϕ_{3dB}

10   is the elevation 3 dB value, and it may be assumed to be 15°, unless stated otherwise.

11

12   The combined antenna pattern at angles off the cardinal axes is computed as

13   $A(\theta) + A_e(\phi)$.

14   **2.1.1.2.   BS Antenna Orientation**

15   The antenna bearing is defined as the angle between the main antenna lobe center and

16   a line directed due east given in degrees. The bearing angle increases in a clockwise

17   direction. Figure 3 shows the hexagonal cell and its three sectors with the antenna

18   bearing orientation proposed for the simulations. The center directions of the main

19   antenna lobe in each sector point to the corresponding side of the hexagon.
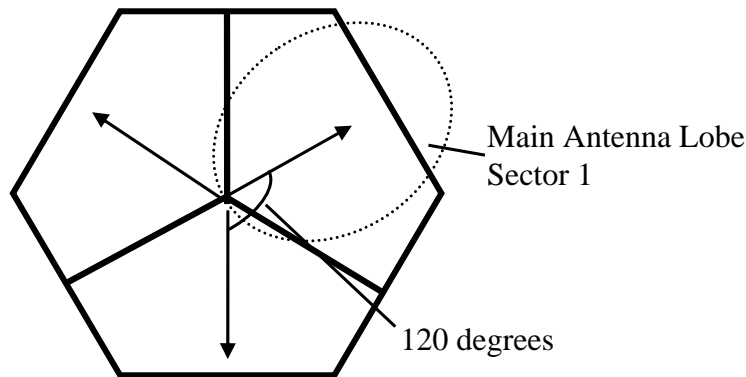
20
21   **Figure 3 : Antenna bearing orientation diagram**
22

23   A uniform linear antenna array is assumed at the BS with an inter-element spacing of 4

24   wavelengths. For cross-polarized antennas, an antenna array with an inter-element

25   spacing of 4 wavelengths is assumed with two co-located dual polarized elements and

26   XPD as defined in the CDL tables of Section 3.2.5.

1   **2.1.2.   MS Antenna**

2   The MS antenna is assumed to be omni directional.

3

4   A uniform linear antenna array is assumed at the MS with an inter-element spacing of
5   1/2 wavelength. For cross-polarized antennas, an antenna array with an inter-element
6   spacing of 1/2 wavelength is assumed with two co-located dual polarized elements and
7   XPD as defined in the CDL tables of Section 3.2.5.

8   **2.2.   Simulation Assumptions**

9   The purpose of this section is to outline simulation assumptions that proponents will
10   need to provide in order to facilitate independent assessment of their proposals. The
11   current tables for downlink and uplink simulation assumptions are templates that may
12   be extended for a complete description of simulation assumptions. Baseline
13   assumptions are specified for calibration and comparison with the reference system as
14   defined by the 802.16m requirements. Additional assumptions relevant to a proposal
15   may be provided by proponents to describe details that may be necessary for an
16   evaluation of the proposal.

17

Topic	Description	Baseline System Assumptions	Proposal Specific Assumptions (To be provided by Proponent)
Basic modulation	Modulation schemes for data and control	QPSK, 16QAM, 64QAM	
Duplexing scheme	TDD, HD-FDD or FD-FDD	TDD	
Subchannelization	Subcarrier permutation	PUSC	
Resource Allocation Granularity	Smallest unit of resource allocation	PUSC: Non-STC: 1 slot, STC: 2 slots (1 slot = 1 subchannel x 2 OFDMA symbols)	
Downlink Pilot Structure	Pilot structure, density etc.	Specific to PUSC subchannelization scheme	
Multi-antenna Transmission Format	Multi-antenna configuration and transmission scheme	MIMO 2x2 (Adaptive MIMO Switching Matrix A & Matrix B) Beamforming (2x2)	
Receiver Structure	MMSE/ML/MRC/ Interference Cancellation	MMSE (Matrix B data zone) MRC (MAP, Matrix A data zone)	
Data Channel Coding	Channel coding schemes	Convolutional Turbo Coding (CTC)	

Control Channel Coding	Channel coding schemes and block sizes	Convolutional Turbo Coding (CTC), Convolutional Coding (CC) for FCH only	
Scheduling	Demonstrate performance / fairness criteria in accordance to traffic mix	Proportional fairness for full buffer data only *, 10 active users per sector, fixed control overhead of 6 symbols, 22 symbols for data, 5 partitions of 66 slots each, latency timescale 1.5s	
Link Adaptation	Modulation and Coding Schemes (MCS), CQI feedback delay / error	QPSK(1/2) with repetition 1/2/4/6, QPSK(3/4), 16QAM(1/2), 16QAM(3/4), 64QAM(1/2), 64QAM(2/3), 64QAM(3/4) 64QAM(5/6), CQI feedback delay of 3 frames / CQI feedback error **[TBD]**	
Link to System Mapping	EESM/MI	MI (RBIR) **	
HARQ	Chase combining/ incremental redundancy, synchronous/asynchronous, adaptive/non-adaptive ACK/NACK delay, Maximum number of retransmissions, retransmission delay	Chase combining asynchronous, non-adaptive, 1 frame ACK/NACK delay, ACK/NACK error, maximum 4 HARQ retransmissions, minimum retransmission delay 2 frames***	
Power Control	Subcarrier power allocation	Equal power per subcarrier	
Interference Model	Co-channel interference model, fading model for interferers, number of major interferers, threshold, receiver interference awareness	Average interference on used tones in PHY abstraction (refer to section 4.5.8)	
Frequency Reuse	Frequency reuse pattern	3 Sectors with frequency reuse of 1 ****	
Control Signaling	Message/signaling format, overheads	Compressed MAP with sub-maps	

Table 1: System-level simulation assumptions for the downlink

* Details of PF scheduler implementation are given in Appendix F.
** EESM may be used for liaison with NGMN after beta values are calibrated.
*** HARQ retransmission shall occur no earlier than the third frame after the previous transmission.

1　**** All technical proposals shall use frequency reuse factor of 1. A coverage vs.
2　capacity trade-off, as defined in Section 13.2.3.7 shall be shown for all 802.16m
3　technical proposals evaluating other reuse schemes (e.g., frequency reuse of 3).
4

Topic	Description	Baseline Assumptions Where Applicable	Proposal Specific Assumptions (To be filled by Proponent)
Basic Modulation	Modulation schemes for data and control	QPSK, 16QAM	
Duplexing Scheme	TDD, HD-FDD or FD-FDD	TDD	
Subchannelization	Subcarrier permutation	PUSC	
Resource Allocation Granularity	Smallest unit of resource allocation	PUSC: 1 slot, (1 slot = 1 subchannel x 3 OFDMA symbols)	
Uplink Pilot Structure	Pilot structure, density etc.	Specific to PUSC subchannelization scheme	
Multi-antenna Transmission Format	Multi-antenna configuration and transmission scheme	Collaborative SM for two MS with single antenna	
Receiver Structure	MMSE/ML Interference cancellation	MMSE	
Data Channel Coding	Channel coding schemes	Convolutional Turbo Coding (CTC)	
Control Channel Coding	Channel coding schemes	CDMA Codes (PUSC 2 symbols) for initial ranging and handover, CDMA Codes (PUSC 1 symbol) for periodic ranging and bandwidth request, CQICH (6 bits)	
Scheduling	Demonstrate performance / fairness criteria in accordance to traffic mix	Proportional fairness for full buffer data only *, 10 active users per sector, fixed control overhead of 3 symbols, 15 symbols for data, 5 partitions of 35 slots each, latency timescale 1.5s	
Link Adaptation	Modulation and Coding Schemes (MCS)	QPSK(1/2) with repetition 1/2/4/6, QPSK(3/4), 16QAM(1/2), 16QAM(3/4)	
Link to System Mapping	EESM/MI	MI(RBIR) **	

HARQ	Chase combining/ incremental redundancy, synchronous asynchronous, adaptive/non-adaptive ACK/NACK delay, maximum number of retransmissions, retransmission delay	Chase combining asynchronous, non-adaptive, ACK/NACK delay N/A, ACK/NACK error, maximum 4 HARQ retransmissions, minimum retransmission delay 2 frames***	
Power Control	Open loop / closed loop		
Interference Model	Co-channel interference model, fading model for interferers, number of major interferers, threshold, receiver interference awareness	Average interference on used tones in PHY abstraction (refer to section 4.5.8)	
Frequency Reuse	Frequency reuse pattern	3 Sectors with frequency reuse of 1 ****	
Control Signaling	Message/signaling format, overheads	Initial ranging, periodic ranging, handover ranging, bandwidth request, fast feedback/CQI channel, sounding	

Table 2: System-level simulation assumptions for the uplink

* Details of PF scheduler implementation are given in Appendix F.
** EESM may be used for liaison with NGMN after beta values are calibrated.
*** HARQ retransmission shall occur no earlier than the third frame after the previous transmission.
**** All technical proposals shall use frequency reuse factor of 1. A coverage vs. capacity trade-off, as defined in Section 13.2.3.7 shall be shown for all 802.16m technical proposals evaluating other reuse schemes (e.g., frequency reuse of 3).

2.3.   Test Scenarios

The following table summarizes the test environments and associated assumptions and parameters that are required for system level simulations. For purposes of FDD system evaluation, a **TBD** test scenario shall be used. Proponents are required to present performance results for both mandatory test scenarios defined in Table 3.

Scenario/ Parameters	Baseline Configuration (Calibration & SRD)	NGMN Configuration	Urban Macrocell
Requirement	Mandatory	Optional *	Mandatory
Site-to-Site Distance	1.5 km	0.5 km	1 km
Carrier Frequency	2.5 GHz	2.5 GHz	2.5 GHz

Operating Bandwidth	10 MHz for TDD	10 MHz for TDD	10 MHz for TDD / 5 MHz per uplink and downlink for FDD
BS Height	32 m	32 m	32 m
BS Tx Power per sector	46 dBm	46 dBm	46 dBm TDD 43 dBm FDD
MS Tx Power	23 dBm	23 dBm	23 dBm
MS Height	1.5 m	1.5 m	1.5 m
Penetration Loss	10 dB	20 dB	10 dB
Path Loss Model	Loss (dB) = $130.62+37.6\log_{10}(R)$ (R in km) **	Loss (dB) = $130.62+37.6\log_{10}(R)$ (R in km) **	Refer to Section 3.2.3.1
Lognormal Shadowing Standard Deviation	8 dB	8 dB	8 dB
Correlation Distance for Shadowing	50m	50m	50m
Mobility	0-120 km/hr	3 km/hr	0-120 km/hr
Channel Mix	ITU Ped B 3 km/hr – 60% ITU Veh A 30 km/hr – 30% ITU Veh A 120 km/hr – 10%	ITU Ped B 3 km/hr	TBD
Spatial Channel Model	ITU with spatial correlation (Refer to Section 3.2.9)	ITU with spatial correlation (Refer to Section 3.2.9)	Urban Macrocell CDL (Refer to Table 9 in Section 3.2.5.1) with spatial correlation (Appendix A)
EVM	**[30 dB]**	N/A	**[30 dB]**

Table 3: Test Scenarios

* Used for liaison with NGMN
** Refer to Section 3.2.3.8

2.4.   Reference System Calibration

The purpose of this section is to provide guidelines for simulation parameters that proponents will need to use in order to evaluate performance gains of their proposals relative to the reference system as defined in the 802.16m requirements document. The purpose of calibration is to ensure that, under a set of common assumptions and

models, the simulator platforms that will be used by various proponents can produce results that are similar.

2.4.1.   Base Station Model

Parameter	Description	Value
P_{BS}	MAX transmit power per sector/carrier	46 dBm @ 10 MHz bandwidth
H_{BS}	Base station height	32m
G_{BS}	Gain (boresight)	17 dBi
S	Number of sectors	3
θ_{BS}	3-dB beamwidth	$S = 3 : \theta_{BS} = 70^0$
G_{FB}	Front-to-back power ratio	20 dB
M_{TX}	Number of transmit antennas	2
M_{RX}	Number of receive antennas	2
d_{BS}	BS antenna spacing	4λ
NF_{BS}	Noise figure	5 dB
HW_{BS}^{*}	Cable loss	2 dB

Table 4: BS equipment model

* Implementation loss must be justified and accounted for separately.

2.4.2.   Mobile Station Model

Parameter	Description	Value
P_{SS}	RMS transmit power/per SS	23 dBm
H_{SS}	Subscriber station height	1.5 m
G_{SS}	Gain (boresight)	0 dBi

$\{\theta_{SS}\},\ G(\{\theta_{SS}\})$	Gain as a function of Angle-of-arrival	Omni
N_{TX}	Number of transmit antennas	1
N_{RX}	Number of receive antennas	2
d_{SS}	SS antenna spacing	$\lambda/2$
NF_{SS}	Noise figure	7 dB
$HW_{SS}{}^{*}$	Cable Loss	0 dB

Table 5: MS Equipment Model

* Implementation loss must be justified and accounted for separately.

2.4.3.   OFDMA Parameters

Parameter	Description	Value : 802.16e Reference System	Value: 802.16m
f_c	Carrier frequency	2.5 GHz	
BW	Total bandwidth	10 MHz	
N_{FFT}	Number of points in full FFT	1024	
F_s	Sampling frequency	11.2 MHz	
Δ_f	Subcarrier spacing	10.9375 kHz	
$T_o = 1/\Delta_f$	OFDMA symbol duration without cyclic prefix	91.43 us	
CP	Cyclic prefix length (fraction of T_o)	1/8	
T_s	OFDMA symbol duration with cyclic prefix	102.86 us for CP=1/8	
T_F	Frame length	5 ms	
N_F	Number of OFDMA symbols in frame	47	

R_{DL-UL}	Ratio of DL to UL (TDD mode)	Full buffer data only: 29 symbols: 18 symbols VoIP only: DL to UL ratio suitably chosen to support bidirectional VoIP	
T_{duplex}	Duplex time	TTG: 296 PS for 10 MHz RTG: 168 PS for 10 MHz PS = $4/F_S$	
DL_{Perm}	DL permutation type	PUSC	
UL_{Perm}	UL permutation type	PUSC	

Table 6: OFDMA Air Interface Parameters

3. Channel Models

3.1.   Introduction

Channel models suitable for evaluation of 802.16m system proposals are described in this section, wherein the model considers parameters specific to 802.16m including bandwidths, operating frequencies, cell scenario (environment, cell radius, etc), and multi-antenna configurations. Both system level and link level models are described in detail with a purpose of fulfilling the needs to conduct effective link- and system-level simulations that can generate trustworthy and verifiable results to assess performance related to the 802.16m system requirements.

Section 3.1.1, Section 3.1.2, Section 3.1.3 and Section 3.1.4 are informative only. The detailed specifications of system and link level models are in section 3.2. Section 3.2.9 describes the channel model to be used for calibration and baseline simulations as defined in the test scenarios in Table 3.

3.1.1.   General Considerations (Informative)

The channel models defined in this document are to provide sufficient details for the purpose of evaluating the system proposals to 802.16m. Since 802.16m is also targeting IMT-Advanced, the system requirements, deployment scenario, and operational bandwidth and frequency of a future IMT-advanced system should also be considered.

In the ITU-R recommendation ITU-R M.1645 the framework for systems beyond IMT-2000 (IMT-Advanced) envisions data rates of up to 1Gbps for nomadic/local area wireless access, and up to 100 Mbps for mobile access. As a reference, the European WINNER project has devised a method for determining spectrum requirements for IMT-Advanced, and their conclusions are given in [1]. In that report it is stated that in order to achieve the above performance targets of IMT-Advanced, sufficiently wide bandwidth and possibly multiple such wideband RF channels may be needed. Candidate bands for IMT-Advanced are to be considered in 2007 at the WRC-07 conference. When considering candidate bands, the WINNER report further suggests that the utilization of bands above 3 GHz may be necessary, but these bands could present significant

technical challenges if used for wide area mobile access, due to the increase in path loss with frequency.

The terrain environment in which 802.16m systems may be deployed (i.e., outdoor, indoor, macro-, micro-, and pico-cell, etc.) dictates the channel modeling, affecting not only parameters but also the model itself. Therefore, channel modeling needs to consider various radio environments and propagation scenarios in which 802.16m system may be deployed.

3.1.2.   Overview of Channel Modeling Methodology (Informative)

The channel behavior is described by its long-term and short-term fading characteristics where the former often depends on the geometrical location of a user in a wireless network and the latter defines the time-variant spatial channels.

In general, there are two ways of modeling a channel: *deterministic* and *stochastic* [2]. The deterministic category encompasses all models that describe the propagation channel for a specific transmitter location, receiver location, and environment. Deterministic channel models are site-specific, as they clearly depend on the location of transmitter, receiver, and the properties of the environment. They are therefore most suitable for network planning and deployment.

In many cases, it is not possible or desirable to model the propagation channel in a specific environment. Especially for system testing and evaluation, it is more appropriate to consider channels that reflect "typical", "best case", and "worst case" propagation scenarios. A stochastic channel model thus prescribes *statistics* of the channel impulse responses (or their equivalents), and during the actual simulation, impulse responses are generated as *realizations* according to those statistics.

For a simulation-based study, stochastic channel modeling is more suitable. Almost all the existing channels models are stochastic ones, such as the SUI model proposed for IEEE 802.16d [3], the ITU model for IMT-2000 [4], the 3GPP SCM model [5][6][7] and SCME (Spatial Channel Model Extensions) model [8], the COST 259 model [9][10][11], the COST 273 model[12], and the WINNER model[13].

Essential to the evaluation of multiple-antenna techniques, which are envisioned to be a key enabling technology for 802.16m and IMT-Advanced, is the modeling of MIMO channels that can be represented as double-directional channels [15]or as vector (or matrix) channels[14]. The former representation is more related to the physical propagation effects, while the latter is more on the "mathematical" effect of the channel on the system [16]. The double-directional model is a physical model in which the channel is constructed from summing over multiple waves or rays. Thus it can also be referred to as a "ray-based model". The vector or matrix channel is a mathematical or analytical model in which the space-time channel as seen by the receiver is constructed mathematically, assuming certain system and antenna parameters. In this approach, the channel coefficients are correlated random process in both space and time, where the correlation is defined mathematically.

A realization of a *double-directional channel* is characterized by its double-directional impulse response. It consists of N propagation waves between the transmitter and the

receiver sites. Each wave is delayed in accordance to its excess-delay τ_ℓ, weighted with the proper complex amplitude $a_\ell e^{j\phi_\ell}$. Note that the amplitude is a two-by-two matrix, since it describes the vertical and horizontal polarizations and the cross-polarization; neglecting a third possible polarization direction is admissible in macro- and microcells. Finally, the waves are characterized by their Angle of Departure (AoD) $\Omega_{T,\ell}$ and Angle of Arrival (AoA) $\Omega_{R,\ell}$.[1] The channel impulse response matrix $\underline{h}$, describing horizontal and vertical polarization is then

$$\underline{h}(t,\tau,\Omega_T,\Omega_R) = \sum_{\ell=1}^{N} \underline{h}_\ell(t,\tau,\Omega_T,\Omega_R) = \sum_{\ell=1}^{N} \underline{a}_\ell e^{j\phi_\ell} \delta(\tau - \tau_\ell)\delta(\Omega - \Omega_{T,\ell})\delta(\Psi - \Omega_{R,\ell}) \qquad (3)$$

The number of waves N can become very large if all possible paths are taken into account; in the limit, the sum has to be replaced by an integral. For practical purposes, waves that are significantly weaker than the considered noise level can be neglected. Furthermore, waves with similar AoDs, AoAs, and delays can also be merged into "effective" paths, known also as taps.

In general, all multipath parameters in the channel impulse response, $\tau_\ell, \Omega_{R,\ell},\ \Omega_{T,\ell}, \underline{a}_\ell,$ and $e^{j\phi_\ell}$ will depend on the absolute time t; also the set of waves or multipath components (MPCs) contributing to the propagation will vary, $N \to N(t)$. The variations with time can occur both because of movements of scatterers, and movement of the mobile station or MS (the BS is assumed fixed).

A mathematical wideband *matrix* channel response describes the channel from a transmit to a receive antenna array. It is characterized by a matrix $\underline{H}$ whose elements H_{ij} are the (non-directional) impulse responses from the $j-$th transmit to the i-th receive antenna element. They can be computed for any antenna constellation as

$$H_{i,j} = h(\tau, \vec{x}_{R,i}, \vec{x}_{T,j}) = \sum_{\ell=1}^{N} \vec{g}_R(\Omega_R) \cdot \underline{h}(\tau_\ell, \Omega_{R,\ell}, \Omega_{T,\ell}) \cdot \vec{g}_T(\Omega_T) \cdot e^{j\left\langle \vec{k}(\varphi_{R,\ell})\vec{x}_{R,i} \right\rangle} e^{j\left\langle \vec{k}(\varphi_{T,\ell})\vec{x}_{T,j} \right\rangle}, \qquad (4)$$

where $\vec{x}_R$ and $\vec{x}_T$ are the vectors of the chosen element-position measured from an arbitrary but fixed reference points $\vec{x}_{R,0}$ and $\vec{x}_{T,0}$ (e.g., the centers of the arrays) and $\vec{k}$ is the wave vector so that

$$\left\langle \vec{k}(\Omega) \cdot \vec{x} \right\rangle = \frac{2\pi}{\lambda}(x\cos\vartheta\cos\varphi + y\cos\vartheta\sin\varphi + z\sin\vartheta). \qquad (5)$$

where ϑ and φ denote elevation and azimuth, respectively. The functions $\vec{g}_R(\Omega_R)$ and $\vec{g}_T(\Omega_T)$ are the antenna patterns at transmitter and receiver, respectively, where the two entries of the vector $\vec{g}$ describe the antenna pattern for horizontal and vertical polarization.

---

[1]We stress that the (double-directional) channel is reciprocal. While the directions of multipath components at the base station and at the mobile station are different, the directions at one link end for the transmit case and the receive case must be identical. When we talk in the following about AoAs and AoDs, we refer to the directions at two different link ends.

3.1.3. Calibration Model (Informative)

A link level channel model is used mainly for calibrating point-to-point MIMO link performance at various SINR points of interest, with extensions to multiple links in the case of interference. Note that any particular link level channel does not contain the information of large-scale fading or how often a particular kind of link condition occurs in a wireless system.

A link level channel can be naturally developed as a typical representation of a propagation scenario under a particular system setting (e.g., a macrocell outdoor system with a representative BS and MS antenna configuration). A link-level channel modeling methodology should be consistent with the system level modeling methodology.

Conventional Tapped Delay Line (TDL) models, such as the three-tap ones used for the IEEE 802.16d SUI TDL [3] and the six-tap ITU models for IMT-2000 [4], need to be extended to include the spatial channel modeling to capture the relationship among all the channels between multiple transmit and receive antennas. For example, SCME models [8] define TDLs where each tap consists of multiple rays in the space that can be further grouped into 3 or 4 mid-taps. WINNER II clustered delay line (CDL) models [13] for systems beyond-3G also defined delay line model with additional angular information specified for each tap.

A few important observations need to be considered:

1. The six-tap ITU models were developed for 5 MHz bandwidth channels, and as the bandwidth increases, the resolution in the delay domain increases so that more taps are required for higher bandwidth channel models. Each resolvable tap consists of a number of multipath components so that the tap fades as the mobile moves. As bandwidth increases there will be fewer multipath components per resolvable tap so that the fading characteristics of the taps are likely to change. The tap fading is likely to become more Ricean in nature (i.e., increasing K-factor with bandwidth) and the Doppler spectrum will not have the classic "bathtub" shape. This also means that the coherence times or distances for the tap fading will most likely be longer for higher bandwidths. The above observation suggests that measurement data under bandwidths up to 100MHz needs to be collected and analyzed to obtain the appropriate channel statistics which may vary according to transmission bandwidth.

2. The model should be flexible to incorporate various antenna effects such as the potential antenna gain imbalance, antenna coupling, and polarization. Ideally the model would include both azimuth and elevation angle (i.e., antenna tilt).

3.1.4. System Level Channel Modeling Considerations (Informative)

System level simulation is a tool widely used to understand and assess the overall system performance. In system-level modeling, all possible link conditions are modeled along with their occurrence probability. System models include additionally the large-

scale location-dependent propagation parameters such as path loss and shadowing, as well as the relationship among multiple point-to-point links.

Channel models that allow effective and efficient system level simulations are of particular interest in the evaluation methodology discussion. In a typical system level simulation, the geometry of a wireless deployment is first defined (e.g., typically a cellular topology is assumed), based on which the long-term fading behaviors and large-scale parameters are derived. After that, the short-term time-variant spatial fading channels are generated.

As mentioned previously, there are in general two types of methodologies to generate short-term fading channels. The first is a physical model in which the channel is constructed from summing over multiple rays that are parameterized according to the geometrics. The physical modeling is independent of the antenna configuration, which means that the actual mathematical channel perceived by a receiver will need to further incorporate the antenna configuration, traveling speed, velocity, and so on.

As an example of a physical model, the 3GPP SCM model [5] has been widely used in system simulation. It models the physical propagation environment using paths and sub-paths with randomly specified angles, delays, phases, and powers. The MIMO channel coefficients for simulation are derived after defining the antenna configuration and array orientation at both MS and BS. Time-variation is realized after defining MS travel direction and speed. Other ray-based channel models for system level simulation include, but not limited to, SCME [8] and WINNER channel model [13]. The ray-based physical models are powerful as they are independent from any particular assumption of antenna configurations.

The other modeling methodology is mathematical or analytical modeling in which the space-time channel as seen by the receiver is constructed mathematically, assuming certain system and antenna parameters. In this method, the channel coefficients are correlated random process in both space and time, where the correlation is defined mathematically.

Mathematical modeling tries to analytically model the statistical behavior of a channel, represented by probability distributions and power profiles of delays and angles. On the other hand, in a ray-based modeling, the statistical behavior is satisfied through the summation of multiple rays with random parameters. The two approaches can be viewed as two different simulation implementations, especially if they are based on the same probability distributions and power profiles. The system performance results are expected to be very close with both models.

Both approaches could be considered for system simulation purpose. A few important considerations for system simulations are:

- *Simulation run-time*. A system level simulation typically involves the generation of spatial channels from a MS position to multiple base stations (e.g., 19 cells or 57 sectors in a three-sector cellular network). Multi-user scheduling is also commonly simulated, in which the channel conditions of multiple MSs (e.g., 10, 20, or more) are required in the scheduler to determine how to distribute

resources among them. Therefore, it is important if a model can result in the reduction of run-time without sacrificing the truthfulness to reality.

- *Consistency with link-level models*. Link level models should reflect particular (e.g., typical) link conditions experienced in various propagation scenarios. A link level study relies on the system level model to understand the likelihood of the particular link condition, while system level study sometimes relies on the link-level study results in order to model the actual link performance.

- *Comparison of results and statistical convergence*. A channel model should facilitate comparison of system study results from independent sources. A channel model should ensure the statistical behavior of a channel to converge quickly without having to run a larger number of realizations (run-time concern). As an example, if a model defines some second order statistics as random variables themselves (e.g., angular spread, delay spread, etc.), the simulation may require more realizations and thus longer time to get convergence.

3.2.   System Level Channel Model

This section focuses on the system-level simulation procedure and parameters for modeling the long- and short-term behavior of spatial channels between a MS and one or more BSs. The procedure and all the required parameters for the purposes of simulation will be described in sufficient detail.

For assumptions and parameters related to test scenarios, as required in system level simulation, refer to Section 2 of this evaluation methodology document. The deployment parameters include, among others, cell radius and topology, BS transmission power, BS antenna pattern, orientation, height, gain, and front-to-back ratio, MS transmission power, MS antenna pattern, height, and gain.

Once the deployment parameters are specified, a system level simulation typically involves the random drop of users in a radio environment of interest. The set of users comprises of a specified mix of different speeds and channel scenarios. Then, the long-term parameters of the link between a set of BS and a MS, such as path loss and shadowing factor, are generated. The short-term time-varying spatial fading channel coefficients are generated in the final step. Typically, multiple links between an MS and multiple BSs are needed, among which there is one desired link and multiple interference links. The shadowing factor of these links can be correlated.

Following the introduction of the general approach to spatial channel modeling, the remaining subsections will define the channel modeling procedure and parameters, as well as channel scenarios and speed mix recommended for system simulation.

3.2.1.   Spatial Channel Modeling

The general modeling approach is based on the geometry of a network layout. The large-scale parameters such as path loss and shadowing factor are generated according to the geometric positions of the BS and MS. Then the statistical channel behavior is defined by some distribution functions of delay and angle and also by the

power delay and angular profiles. Typically, an exponential power delay profile and Laplacian power angular profile are assumed with the function completely defined once the RMS delay spread and angular spread (both Angle of Departure (AoD) and Angle of Arrival (AoA)) are specified. The RMS delay and angular spread parameters can be random variables themselves, with a mean and deviation as in SCM. The RMS delay and angular spread can be mutually correlated, together with other large-scale parameters such as shadowing factors.

According to the exact profile and distribution functions defined by the particular RMS delay and angular spread values, a finite number of channels taps are generated randomly with a per-tap delay, mean power, mean AoA and AoD, and RMS angular spread. They are defined in a way such that the overall power profile and distribution function are satisfied. Each tap is the contribution of a number of rays (plane waves) arriving at the same time (or roughly the same time), with each ray having its own amplitude, AoA, and AoD.

The number of taps and their delay and angles may be randomly defined, but a reduced-complexity model can specify the delays, mean powers, and angles of the channel taps in a pre-determined manner when typical values are often chosen. Similar to the well-known TDL version of the WSSUS (Wide-Sense Stationary Uncorrelated Scattering) model, where the power delay profile is fixed, a "spatial" TDL reduced-complexity model additionally defines the spatial information such as per-tap mean AoA, AoD, and per-tap angular spread (thus the power angular profile). Spatial TDL models are also referred to as Cluster Delay Line or CDL models as each tap is modeled as the effect of a cluster of rays arriving at about the same time. Each tap suffers from fading in space and over time. The spatial fading process will satisfy a pre-determined power angular profile. Due to the simplicity of reduced complexity modeling, it is recommended for system level simulation.

The actual realization of a time-varying spatial channel can be performed in two ways:

- Ray-based: The channel coefficient between each transmit and receive antenna pair is the summation of all rays at each tap and at each time instant, according to the antenna configuration, gain pattern, and the amplitude, AoA, AoD of each ray. The temporal channel variation depends on the traveling speed and direction relative to the AoA/AoD of each ray.

- Correlation based: The antenna correlation for each tap is computed first according the per-tap mean AoA/AoD, per-tap power angular profile, and antenna configuration parameters (e.g.., spacing, polarization, etc.). The per-tap Doppler spectrum depends on the traveling speed and direction relative to the mean per-tap AoA/AoD, as well as the per-tap power angular profile. The MIMO channel coefficients at each tap can then be generated mathematically by transforming typically the i.i.d. Gaussian random variables according to the antenna correlation and the temporal correlation (correspondingly the particular Doppler spectrum). The approach of pre-calculating and storing all the correlations and time-varying fading processes may also be used in system simulation.

Correlation based method should be used as the mandatory baseline channel modeling approach.

3.2.2.   Radio Environment and Propagation Scenarios

The terrain or radio environment, such as indoor, urban, or suburban, dictates the radio propagation behavior. Even in similar terrain environments, there may be different propagation behavior or scenarios.

For the simulation of IEEE 802.16m systems, the following test scenarios are defined:

1. **Urban macrocell (mandatory)**: This scenario is characterized by large cell radius (approximately 1-6 km BS to BS distance), high BS antenna positions (above rooftop heights, between 10-80 m, typically 32 m), moderate to high delay and angle spread and high range of mobility (0 – 350 km/h). In a typical urban macrocell a mobile station is located outdoors at street level with a fixed base station clearly above surrounding building heights. As for propagation conditions, non- or obstructed line-of-sight is a common case, since street level is often reached by a single diffraction over the rooftop. The building blocks can form either a regular Manhattan type of grid, or have more irregular locations. Typical building heights in urban environments are over four floors. Buildings height and density in typical urban macrocell are mostly homogenous. As a variant, the *optional* **bad urban macrocell** describes cities with buildings with distinctly inhomogeneous building heights or densities. The inhomogeneities in city structures can be the result of, for example, large water areas separating the built-up areas, or the high-rise skyscrapers in an otherwise typical urban environment. Increased delay and angular dispersion can also be caused by mountains surrounding the city. The base station is typically located above the average rooftop level, but within its coverage range there can also be several high-rise buildings exceeding the base station height. From the modeling point of view this differs from typical urban macrocell by an additional far scatterer cluster.

2. **Suburban macrocell (optional)**: This scenario is characterized by large cell radius (approximately 1-6 km BS to BS distance), high BS antenna positions (above rooftop heights, between 10-80 m, typically 32 m), moderate to high delay spreads and low angle spreads and high range of mobility (0 – 350 km/h). In suburban macrocells, base stations are located well above the rooftops to allow wide area coverage, and mobile stations are outdoors at street level. Buildings are typically low residential detached houses with one or two floors, or blocks of flats with a few floors. Occasional open areas such as parks or playgrounds between the houses make the environment rather open. Streets do not form urban-like regular strict grid structure. Vegetation is modest.

3. **Urban microcell (optional)**: This scenario is characterized by small cell radius (approximately 0.3 – 0.5 km BS to BS distance) BS antenna positions at rooftop heights or lower (typically 12.5m), high angle spread and moderate delay spread, and medium range of mobility (0 – 120 km/h). This model is sensitive to antenna height and scattering environment (such as street layout, LOS). In the urban microcell scenario, the heights of both the antenna at the BS and that at the MS

are assumed to be well below the tops of surrounding buildings. Both antennas are assumed to be outdoors in an area where streets are laid out in a Manhattan-like grid. The streets in the coverage area are classified as "the main street", where there is LOS from all locations to the BS, with the possible exception of cases in which LOS is temporarily blocked by traffic (e.g. trucks and busses) on the street. Streets that intersect the main street are referred to as perpendicular streets, and those that run parallel to it are referred to as parallel streets. This scenario is defined for both LOS and NLOS cases. Cell shapes are defined by the surrounding buildings, and energy reaches NLOS streets as a result of propagation around corners, through buildings, and between them. The *optional* **Bad urban microcell** scenarios are identical in layout to Urban Microcell scenarios. However, propagation characteristics are such that multipath energy from distant objects can be received at some locations. This energy can be clustered or distinct, has significant power (up to within a few dB of the earliest received energy), and exhibits long excess delays. Such situations typically occur when there are clear radio paths across open areas, such as large squares, parks or bodies of water.

4. **Indoor Small Office (optional)**: This scenario investigates isolated cells for home or small office coverage. In a typical small office environment, there are multiple floors and multiple rooms or areas.

5. **Outdoor to indoor (optional):** This scenario is the combination of an outdoor and an indoor scenario such as **urban microcell** and **indoor small office**. In this particular combination, the MS antenna height is assumed to be at 1 – 2 m (plus the floor height), and the BS antenna height below roof-top, at 5 - 15 m depending on the height of surrounding buildings (typically over four floors high).

6. **Indoor hotspot (optional)**: This scenario concentrates on the propagation conditions in a hotspot in the urban scenario with much higher traffic as in conference halls, shopping malls and teaching halls. The indoor hotspot scenario is also different from the indoor office scenario due to building structures.

7. **Open rural macrocell (optional)**: This scenario is characterized by large cell radius (approximately 1-10 km BS to BS distance), high BS antenna positions (above rooftop heights, between 10-75 m, typically 50 m), low delay spreads and low angle spreads and high range of mobility (0 – 350 km/h). In rural open area, there is low building density; the height of the BS antenna is much higher than the average building height. Depending on terrain, morphology and vegetation, LOS conditions might exist in most of the coverage area.

3.2.3. Path loss

The path loss model depends on the propagation scenario. For example, in a macrocell environment, the COST-231 modified Hata model [18] is well known and widely used for systems with a carrier frequency less than or equal to 2.5 GHz. The Erceg-Greenstein model [3] was proposed in IEEE 802.16d for carrier frequencies up to 3.5 GHz. Extensions to these path loss models to carrier frequencies above 3.5 GHz are also proposed in the WINNER model [13].

For the evaluation of IEEE 802.16m systems, the following path loss models are specified:

### 3.2.3.1.		Urban Macrocell

With default BS and MS heights of 32m and 1.5m respectively, and as derived in Appendix H, the modified COST 231 Hata path loss model for the urban macrocell at carrier frequency f [GHz] ($2 < f < 6$) is given by

$$PL_{urban\_macro}[dB] = 35.2 + 35\log_{10}(d) + 26\log_{10}(f/2) \tag{6}$$

where d in meters is the distance from the transmitter to the receiver.

### 3.2.3.2.		Suburban Macrocell

With default BS and MS heights of 32m and 1.5m respectively, and as shown in Appendix H, the modified COST 231 Hata path loss model for the suburban microcell at carrier frequency f [GHz] ($2 < f < 6$) is given by

$$PL_{suburban\_macro}[dB] = PL_{urban\_macro} - 2[1.5528 + \log_{10}(f)]^2 - 5.4 \tag{7}$$

### 3.2.3.3.		Urban Microcell

LOS case:

With default BS and MS heights of 12.5m and 1.5m respectively, and as shown in Appendix H the path loss model for the urban microcell with LOS [20] at carrier frequency f [GHz] is given by

$$PL_{urban\_micro\_LOS}[dB] = 32.4418 + 20\log_{10}(f) + 20\log_{10}(d) + 0.0174d + 20\log_{10}(\max(0.013d/f,1)) \tag{8}$$

where d in meters is the distance from the transmitter to the receiver.

NLOS Case:

With default BS and MS heights of 12.5m and 1.5m respectively, and as shown in Appendix H, the path loss model for the urban microcell with NLOS [20] at carrier frequency f in GHz is given by

$$PL_{urban\_micro\_NLOS}[dB] = \min\left(PL_{over\_the\_rooftop}, PL_{Berg}\right) \tag{9}$$

Where

$$PL_{over\_the\_rooftop} = 24 + 45\log_{10}(r_{Eu} + 20) \tag{10}$$

$$PL_{Berg} = 32.4418 + 20\log_{10}(f) + 20\log_{10}(d_n) + 20\log_{10}(\max(R/r_{bp},1)) + 20\log_{10}(R) + 0.0174R \tag{11}$$

$$r_{bp} = \min\{76.67f, r_0\},$$

and

$R = \sum_{j=1}^{n} r_{j-1}$ is the distance along streets between transmitter and receiver.

The distance r_j is the length of the street between nodes j and $j+1$ (there are $n+1$ nodes in total) and r_{Eu} is the Euclidean distance in meters from the transmitter to the receiver.

1   The distance d_n is the illusory distance and it is defined by the recursive expression:

$$k_j = k_{j-1} + d_j q_{j-1}$$

2   (12)

$$d_j = k_j r_{j-1} + d_{j-1}$$

3   with $k_0 = 1$, $d_0 = 0$ and $q_j(\theta_j) = \left(\dfrac{|\theta_j|}{90} \right)^{1.5}$

4   where θ_j is the angle between streets at junction *j*.
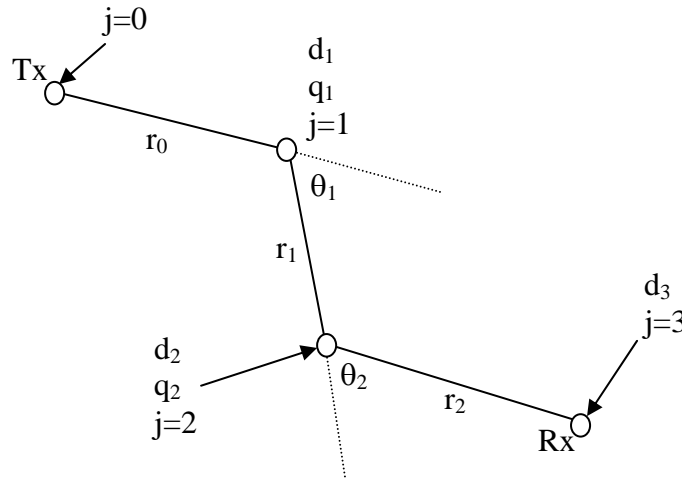
5
6   **Figure 4: Geometry of street sections used for microcellular NLOS path loss model**
7

8   Since the path loss defined above requires additional street layout information in
9   addition to just the BS-MS distance as typically specified in system simulation, in order
10 to make it possible to derive the path loss based on the BS-MS distance, the following
11 assumption on street layout should be used:
12   • Street intersection angle: 90 degree
13   • Segment length: 50m
14   • Number of street segments: round[d/[(SQRT(2)*segment_length)]], where d is
15   the distance between transmitter and receiver
16

17 For propagation scenarios that describe both LOS and NLOS situations, simulations
18 should use a random mix of LOS and NLOS scenarios with the probability of selecting a
19 LOS scenario given in Table 7.
20

Propagation Scenario	Probability of LOS as a function of distance d (m)
Urban Microcell	$P_{LOS} = 1 \qquad\qquad\qquad\qquad d \leq 15m$ $1 - \left[1 - \left(1 - \left(1.56 - 0.48\log_{10}(d)\right)^3 \right) \right]^{1/3} \quad d > 15m$
Indoor Hotspot	$P_{LOS} = 1 \quad d \leq 10m$ $e^{[-(d-10)/45]} \quad d > 10m$
Rural	$P_{LOS} = e^{(-d/1000)}$

21   **Table 7: LOS Probabilities for mixed LOS/NLOS scenario**

3.2.3.4.   Indoor Small Office

The WINNER model [13] defines the following model for NLOS case under the condition of 3 m < d < 100 m, $h_{BS} = h_{MS} = 1 \sim 2.5$m,

NLOS (Room to Corridor):

$$PL(dB) = 43.8 + 36.8 \log_{10}(d[m]) + 20 \log_{10}(f[GHz]/5.0) \tag{13}$$

NLOS (through-wall):

$$PL(dB) = 46.4 + 20 \log_{10}(d[m]) + 5n_w + 20 \log_{10}(f[GHz]/5.0) \quad \text{(Light Wall)} \tag{14}$$

$$PL(dB) = 46.4 + 20 \log_{10}(d[m]) + 12n_w + 20 \log_{10}(f[GHz]/5.0) \quad \text{(Heavy Wall)} \tag{15}$$

where n_w is the number of walls between BS and MS. It is assumed that there is one light wall every 3m and one heavy wall every 30 m.

< Notes: The above model (including the parameters in respective CDL models defined later) are currently aligned with IMT-Advanced, but will be adjusted if needed in order to fully align with the final model adopted in IMT-Advanced once available. Also all values need to be defined for simulation (e.g., n_w).>

3.2.3.5.   Indoor Hot Spot

LOS case (20 m < d < 60 m, $h_{BS} = h_{MS} = 1 \sim 2.5$m)

$$PL(dB) = 49.3 + 11.8 \log_{10}(d[m]) + 20 \log_{10}(f[GHz]/5.0) \tag{16}$$

NLOS case (20 m < d < 80 m, , $h_{BS} = h_{MS} = 1 \sim 2.5$m)

$$PL(dB) = 25.5 + 43.3 \log_{10}(d[m]) + 20 \log_{10}(f[GHz]/5.0) \tag{17}$$

The probability of selecting a LOS scenario is given in Table 7.

< Notes: The above model (including the parameters in respective CDL models defined later) are currently aligned with IMT-Advanced, but will be adjusted if needed in order to fully align with the final model adopted in IMT-Advanced once available. Also all values need to be defined for simulation.>

3.2.3.6.   Outdoor to Indoor

The WINNER model [13] defines the following path loss model for the NLOS case.

$$PL(dB) = PL_b + PL_{tw} + PL_{in} \tag{18}$$

Where $PL_b = PL_{B1}(d_{out} + d_{in})$, $PL_{tw} = 14 + 15(1 - \cos(\theta))^2$, $PL_{in} = 0.5 d_{in}$
3 m < $d_{out} + d_{in}$ < 1000 m, $h_{BS} = 12.5$ m, $h_{MS} = 2n_{Fl} + 2$ m, $n_{Fl} = 2$.

PL_{B1} is path-loss of urban-micro cell (a function with the input distance of $d_{out} + d_{in}$), d_{out} is the distance between the outside terminal and closest point of the wall to the inside terminal, d_{in} is the distance from wall to the inside terminal , θ is the angle between the

outdoor path and the normal of the wall. n_{Fl} is the number of the floor (the ground floor is assigned the number 1).

For simulation purposes, the default value of θ =45 degree can be used. Additionally, the path loss of the outdoor portion follows the NLOS case. n_{Fl} for BS is TBD.

< Notes: The above model (including the parameters in respective CDL models defined later) are currently aligned with IMT-Advanced, but will be adjusted if needed in order to fully align with the final model adopted in IMT-Advanced once available. Also all values need to be defined for simulation.>

3.2.3.7.   Open Rural Macrocell

According to the recent experimental result of the WINNER model [13], the path loss is

LOS:

$$PL(dB) = 44.2 + 21.5\log_{10}(d[m]) + 20*\log_{10}(f[GHz]/5.0) \quad 20m < d < d_{BP} \qquad (19)$$

$$PL(dB) = 8.7 + 40.0\log_{10}(d[m]) - 19.5\log_{10}(h_{BS}[m]) - 19.5\log_{10}(h_{ms}[m]) + 0.5\log_{10}(f[GHz]/5.0) \quad d > d_{BP}$$
$$(20)$$

NLOS:

$$PL(dB) = 55.4 + 25.1*\log_{10}(d[m]) + 21.3*\log_{10}(f[GHz]/5.0) - 0.13(h_{BS}[m]-25)\log_{10}(\tfrac{d}{d_0}) - 0.9(h_{ms}[m]-1.5) \quad (21)$$

Where d = distance
   d_{BP} = $4 \cdot h_{ms} \cdot h_{BS} \cdot f / c$
   h_{BS} = the height of the base station
   h_{ms} = the height of the mobile station
   f = the centre-frequency (GHz)
   c = the velocity of light in vacuum (m/s)
   σ = standard deviation
   d_0 =100 meter (the reference distance)

The probability of selecting a LOS scenario is given in Table 7.

< Notes: The above model (including the parameters in respective CDL models defined later) are currently aligned with IMT-Advanced, but will be adjusted if needed in order to fully align with the final model adopted in IMT-Advanced once available. Also all values need to be defined for simulation.>

3.2.3.8.   Path Loss Model for Baseline Test Scenario

This model is applicable for the test scenarios in urban and suburban areas outside the high rise core where the buildings are of nearly uniform height.

1
$$PL(dB) = 40(1 - 4x10^{-3}h_{BS})\log_{10}(R) - \log_{10}(h_{BS}) + 21\log_{10}(f) + 80 \qquad (22)$$
2

3 where R in kilometers is the distance from the transmitter to the receiver, f is the
4 carrier frequency in GHz and h_{BS} is the base station antenna height above rooftop
5
6 If the base station antenna height is fixed at 15 meters above the average rooftop and a
7 carrier frequency of 2 GHz, the path loss formula reduces to
8
9
$$PL(dB) = 128.1 + 37.6\log_{10}(R) \qquad (23)$$
10

11 Applying a frequency correction factor $21\log_{10}(2.5/2)$ for operation at 2.5 GHz, the path
12 loss can be calculated as
13
$$PL(dB) = 130.18 + 37.6\log_{10}(R) \qquad (24)$$

14 **3.2.4.   Shadowing Factor**
15 The shadowing factor (SF) has a log-normal distribution and a standard deviation
16 defined in the following table based on the WINNER parameters [13], for different
17 scenarios.
18
19 <*Notes: The values chosen for the shadowing factor are currently aligned with IMT-*
20 *Advanced, but will be adjusted if needed to completely align with the final model*
21 *adopted in IMT-Advanced once available>*
22

Propagation Scenario	Shadowing Factor
Urban macrocell	8 dB
Suburban macrocell	8 dB
Urban microcell	NLOS: 4 dB, LOS 3 dB
Indoor Small Office	NLOS (Room to Corridor) 4 dB, NLOS (through-wall) 6 dB (light wall), 8 dB (heavy-wall)
Indoor Hot Spot	LOS 1.5 dB, NLOS 1.1 dB
Outdoor to indoor	7 dB
Open Rural Macrocell	NLOS: 8 dB, LOS: 6 dB

23
24   **Table 8: Standard Deviation of Shadow Fading Distribution**
25

26 The site-to-site shadowing correlation is 0.5. The SF of closely positioned MSs is
27 typically observed similar or correlated. Therefore, the SF can be obtained via
28 interpolation in the following way.

29 For each base station, a uniformly spaced grid is generated using the pre-defined de-
30 correlation distance as shown in Figure 5. Each node $S_{n,l}$ on the grid represents the
31 shadowing factor corresponding to base station l at the geographic location n with (x, y)
32 coordinate. All nodes $\{S_{n,0},\cdots,S_{n,L}\}$, where L represents the set of base stations in the

1 simulation, correspond to a single geographical location n in a simulated system. The
2 distance between closest nodes, D_{cor}, in the grid is the pre-defined de-correlation
3 distance (e.g. 50 meters).

4 For a mobile location, either from a random drop or a result of mobility, the shadowing
5 factor from the mobile to a base station l should be calculated by interpolating the
6 shadowing factors of the closest four nodes, $S_{0,l}$-$S_{3,l}$ for the corresponding base station l
7 in Figure 5. Specifically, the shadowing factor $g_{k,l}$ at a location corresponding to base
8 station l is determined by

9
$$SF(g_{k,l}) = \left(\sqrt{1 - \frac{x_{pos}}{D_{cor}}} \right) \left[S_{0,l} \sqrt{\frac{y_{pos}}{D_{cor}}} + S_{3,l} \left(\sqrt{1 - \frac{y_{pos}}{D_{cor}}} \right) \right] + \left[S_{1,l} \sqrt{\frac{y_{pos}}{D_{cor}}} + S_{2,l} \left(\sqrt{1 - \frac{y_{pos}}{D_{cor}}} \right) \right] \sqrt{\frac{x_{pos}}{D_{cor}}} \quad (25)$$

10 Note that the linear interpolation above guarantees smooth change of shadowing
11 factors around the nodes on the grid, and moving from one square to another square.
12 Additionally, the linear interpolation above guarantees the same standard deviation of
13 shadowing factors at all points in the simulated system.
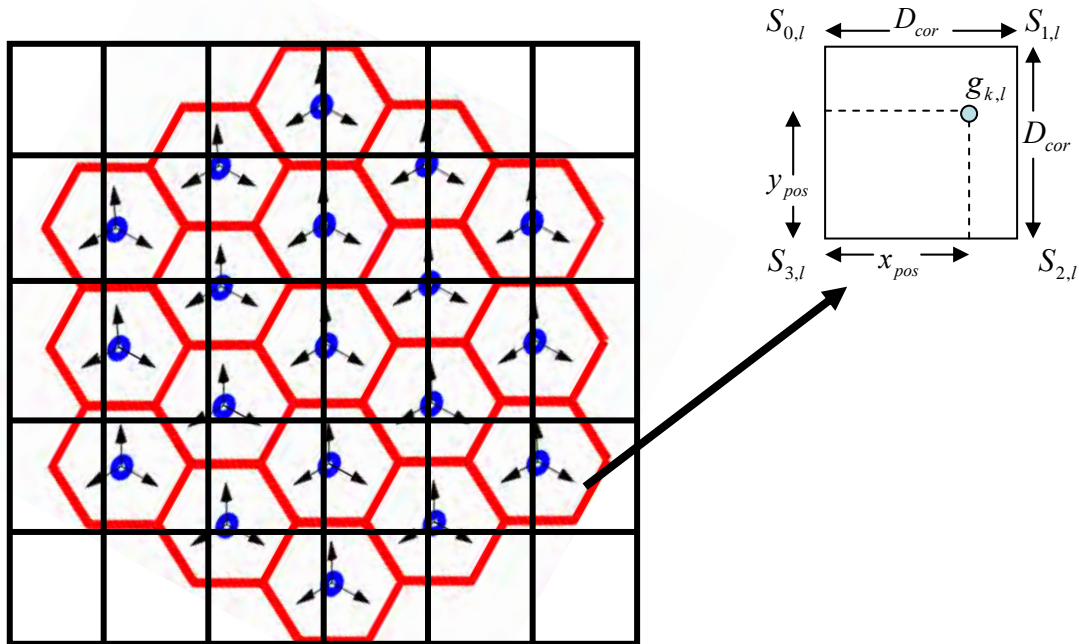
14
15   **Figure 5: Shadowing factor grid example showing interpolation**

16
17 The shadow fading $SB_{n,lB}$ at the nodes is modeled as a Gaussian distributed random
18 variable with zero mean and standard deviation σ as defined in Table 8. The shadow
19 fading component is expressed as the weighted sum of a common component, Z_n, to all
20 cell sites, and an independent component, Z_l, from each cell site. In other words, Z_n is
21 generated based on local shadowing point at the node coordinates (e.g. related to a

mobile station location), and Z_l is generated based on local shadowing point for a given base station. The shadow fading value between node n and base station l is $SB_{n,lB} = aZ_n + bZ_l$. Typical values for a and b are $a^2 + b^2 = 1/2$. That is, the correlation is 0.5 between sectors from different cells and 1.0 between sectors of the same cell. Once the shadow fading values at the grid nodes have been determined according to the preceding procedure, the interpolation of equation (25) can be carried out according to each mobile location or along the mobile trajectory for handoff simulations during one drop.

3.2.5.   Cluster-Delay-Line Models

The CDL models as referred in the WINNER report define tap delayed line models for the power delay profile with additional spatial information such as per-tap mean AoA, AoD, and per-tap angular spread (thus the power angular profile). The CDL models can be deemed as a spatial extension of the TDL model with the number of taps (clusters), their delays and powers, the mean AoA and AoD of each cluster, and the arrival and departure angular spread (AS). So they offer well-defined radio channels with fixed parameters to obtain comparable simulation results with relatively non-complicated channel models. Note that the word "cluster" is used in "clustered delay lines" in a way that deviates from its commonly accepted definition in the scientific literature. Clusters are either defined as (i) groups of multipath components (MPCs) whose large-scale characteristics change in a similar way (e.g., as the MS moves over large distances, the relative AoAs, AoDs, and delays of the MPCs within one cluster do not change, or (ii) as groups of MPCs with similar delays, AoAs, and AoDs. For the latter definition, it is important to notice the difference between clusters and multipath groups. i.e., a number of MPCs that are indistinguishable to a RX because of limited resolution are different from a cluster. A cluster consists usually of several multipath groups with similar delays and angles, and is surrounded (in the delay-angle plane) by areas of no "significant "power. For a receiver with very low angular/delay resolution, it might happen that each cluster contains only a single multipath group, or even that a multipath group contains several clusters. Consequently, the MPCs belonging to a cluster do not change, even as the resolution of the measurement device becomes finer and finer; while the MPCs belonging to a multipath group change as the resolution becomes finer.

As discussed in Section 3.1, the use of fixed values for delay and mean AoA/AoD makes the CDL model a simplification, as it does not account for the (experimentally observed) random variations of delay spread, angular spread, etc. This might have significant consequences for the absolute and even relative performance of various systems. While the model is suitable for the purposes of standardization, it is not recommended for scholarly investigations.

For each propagation scenario, the corresponding CDL is given as follows that includes a power delay profile and the corresponding per-tap power angular profile. Note that the AoA and AoD values given in the following tables are the mean AoA/AoD of each cluster (i.e., tap or path). The mean power of each tap and its delay is also given. The ray power is 1/20 of the mean tap power (i.e., -13 dB).

In a CDL model, each tap may be simulated via generating 20 equal-power rays with fixed offset angles, as suggested in WINNER. The offset angles are the same as those

defined in SCM and they are specified in a way such that by adjusting the interval between these equal-power rays a Laplacian power angular profile can be approximated. Note that the offset angles are the deviation from the mean AoA/AoD (see Table 47 in Appendix A for the offset). In the case when a ray of dominant power exists, the cluster has 20+1 rays. This dominant ray has a zero angle offset. The departure and arrival rays are coupled randomly.

CDL models also allow for the generation of spatial correlation mathematically, which can be used directly to generate the matrix channel coefficients. The spatial correlation for each tap can be derived from the mean AoA/AoD and the Laplacian power angular profile with the specified angular spread. Per-tap correlation can also be derived numerically based on the 20 equal-power rays used to approximate the Laplacian power angular profile.

Most of the taps have a single delay. In case a tap has three delays values, these correspond to sub-clusters as defined in the table below:

Sub-cluster #	Mapping to Rays	Fractional Power	Delay Offset (ns)
1	1,2,3,4,5,6,7,8,19,20	10/20	0
2	9,10,11,12,17,18	6/20	5
3	13,14,15,16	4/20	10

Table 9: Sub-cluster model used for some taps in Spatial TDL or CDL model

The sub-cluster can be easily simulated with a ray-based model. But when a spatial correlation is computed in the correlation-based implementation, the three sub-taps should be approximated to have the same correlation.

The cross polarization ratio XPR_V is the power ratio of vertical-to-vertical polarized component to vertical-to-horizontal polarized component, XPR_H is the power ratio of horizontal-to-horizontal polarized component to horizontal-to-vertical polarized component. It is assumed that $XPR_V = XPR_H = XPR$ and the cross polarization ratios are assumed the same for all clusters (i.e., taps). A reference cross polarized antenna configuration is also defined in order to derive spatial correlation, in which case the BS antenna element is assumed to be 45-deg cross-polarized and the MS antenna element is 90-deg cross-polarized, as assumed in Appendix B.

3.2.5.1.   Urban Macrocell

Cluster #	Delay [ns]			Power [dB]			AoD [º]	AoA [º]	Ray power [dB]	Cluster ASD = 2º	Cluster ASA = 15º
1	0			-6.4			11	61	-19.5		
2	60			-3.4			-8	44	-16.4		
3	75			-2.0			-6	-34	-15.0		
4	145	150	155	-3.0	-5.2	-7.0	0	0	-13.0		
5	150			-1.9			6	33	-14.9		

Cluster #	Delay [ns]			Power [dB]			AoD [º]	AoA [º]	Ray power [dB]
6	190			-3.4			8	-44	-16.4
7	220	225	230	-3.4	-5.6	-7.4	-12	-67	-13.4
8	335			-4.6			-9	52	-17.7
9	370			-7.8			-12	-67	-20.8
10	430			-7.8			-12	-67	-20.8
11	510			-9.3			13	-73	-22.3
12	685			-12.0			15	-83	-25.0
13	725			-8.5			-12	-70	-21.5
14	735			-13.2			-15	87	-26.2
15	800			-11.2			-14	80	-24.2
16	960			-20.8			19	109	-33.8
17	1020			-14.5			-16	91	-27.5
18	1100			-11.7			15	-82	-24.7
19	1210			-17.2			18	99	-30.2
20	1845			-16.7			17	98	-29.7

Table 10: Urban macrocell CDL (XPR = 5 dB)

Cluster #	Delay [ns]			Power [dB]			AoD [º]	AoA [º]	Ray power [dB]		
1	0			-4.7			-10	61	-17.7	Cluster ASD = 2º	Cluster ASA = 15º
2	0	5	10	-3	-5.2	-7	0	0	-13		
3	10			-7.2			12	-75	-20.2		
4	10			-6.3			-11	-70	-19.3		
5	30	35	40	-4.8	-7	-8.8	-12	76	-14.8		
6	50			-3.7			-9	53	-16.7		
7	80			-7.4			-12	76	-20.4		
8	110			-7.2			12	-75	-20.2		
9	155			-9.6			14	-87	-22.7		
10	165			-5.2			-10	64	-18.3		
11	165			-6.3			11	70	-19.3		
12	250			-8.9			14	83	-21.9		
13	280			-8.5			13	-81	-21.5		
14	440			-8.4			13	-81	-21.4		
15	490			-8.5			-13	81	-21.5		
16	525			-5			10	62	-18		
17	665			-10.9			15	92	-23.9		
18	685			-10.9			15	92	-24		
19	4800			-9.7			-135	25	-22.7		
20	7100			-13			80	40	-26		

Table 11: Bad urban macrocell CDL (XPR = 5 dB)

3.2.5.2. Suburban Macrocell

Cluster #	Delay [ns]			Power [dB]			AoD [º]	AoA [º]	Ray power [dB]	Cluster ASD = 2º	Cluster ASA = 10º
1	0	5	10	-3.0	-5.2	-7.0	0	0	-13.0		
2	25			-7.5			13	-71	-20.5		
3	35			-10.5			-15	-84	-23.5		
4	35			-3.2			-8	46	-16.2		
5	45	50	55	-6.1	-8.3	-10.1	12	-66	-16.1		
6	65			-14.0			-17	-97	-27.0		
7	65			-6.4			12	-66	-19.4		
8	75			-3.1			-8	-46	-16.1		
9	145			-4.6			-10	-56	-17.6		
10	160			-8.0			-13	73	-21.0		
11	195			-7.2			12	70	-20.2		
12	200			-3.1			8	-46	-16.1		
13	205			-9.5			14	-80	-22.5		
14	770			-22.4			22	123	-35.4		

Table 12: Suburban Macrocell CDL (XPR = 5.5 dB)

3.2.5.3. Urban Microcell

In the LOS model Ricean K-factor is 3.3 dB, which corresponds to 20m distance between Tx and Rx.

Cluster #	Delay [ns]			Power [dB]			AoD [º]	AoA [º]	Ray power [dB]		Cluster ASD = 3º	Cluster ASA = 18º
1	0			0.0			0	0	-0.31[*]	-24.7[**]		
2	30	35	40	-10.5	-12.7	-14.5	5	45	-20.5			
3	55			-14.8			8	63	-27.8			
4	60	65	70	-13.6	-15.8	-17.6	8	-69	-23.6			
5	105			-13.9			7	61	-26.9			
6	115			-17.8			8	-69	-30.8			
7	250			-19.6			-9	-73	-32.6			
8	460			-31.4			11	92	-44.4			

Table 13: Urban Microcell CDL (LOS) (XPR = 9.5 dB)

[*]   Power of dominant ray,
[**]   Power of each other ray

Cluster #	Delay [ns]			Power [dB]			AoD [º]	AoA [º]	Ray power [dB]	Cluster ASD =10º	Cluster ASA = 22º
1	0			-1.0			8	-20	-14.0		
2	90	95	100	-3.0	-5.2	-7.0	0	0	-13.0		
3	100	105	110	-3.9	-6.1	-7.9	-24	57	-13.9		
4	115			-8.1			-24	-55	-21.1		
5	230			-8.6			-24	57	-21.6		

6	240	-11.7	29	67	-24.7		
7	245	-12.0	29	-68	-25.0		
8	285	-12.9	30	70	-25.9		
9	390	-19.6	-37	-86	-32.6		
10	430	-23.9	41	-95	-36.9		
11	460	-22.1	-39	-92	-35.1		
12	505	-25.6	-42	-99	-38.6		
13	515	-23.3	-40	94	-36.4		
14	595	-32.2	47	111	-45.2		
15	600	-31.7	47	110	-44.7		
16	615	-29.9	46	-107	-42.9		

Table 14: Urban Microcell CDL (NLOS) (XPR = 7.5 dB)

Bad Urban Microcell

Cluster #	Delay [ns]			Power [dB]			AoD [º]	AoA [º]	Ray power [dB]	Cluster ASD = 3º	Cluster ASA = 5º
1	0	5	10	-3.0	-5.2	-7.0	0	0	-13.0		
2	25	30	35	-3.4	-5.6	-7.3	-14	31	-13.4		
3	25			-1.7			-13	30	-14.7		
4	35			-1.9			-14	31	-14.9		
5	45			-2.2			15	-34	-15.2		
6	70			-5.0			22	51	-18.0		
7	70			-3.6			19	44	-16.6		
8	90			-3.8			-19	-45	-16.8		
9	155			-6.4			-25	-58	-19.4		
10	170			-2.7			-17	-38	-15.7		
11	180			-7.5			-27	-63	-20.5		
12	395			-16.5			-41	93	-29.5		
13	1600			-5.7			-110	15	-18.7		
14	2800			-7.7			75	-25	-20.7		

Table 15: Bad urban Microcell CDL (NLOS) (XPR = 7.5 dB)

3.2.5.4.   Indoor Small Office

Only NLOS condition is given below.

Cluster #	Delay [ns]			Power [dB]			AoD [º]	AoA [º]	Ray power [dB]	Cluster ASD = 5º	Cluster ASA = 5º
1	0	5	10	-3.0	-5.2	-7.0	0	0	-13.0		
2	5			-4.0			59	-55	-17.0		
3	20			-4.7			-64	-59	-17.7		
4	25			-9.0			89	-82	-22.0		
5	30			-8.0			83	-77	-21.0		
6	30	35	40	-4.0	-6.2	-8.0	-67	62	-14.0		
7	35			-1.1			32	29	-14.2		
8	45			-5.2			-67	62	-18.2		

9	55	-9.5	-91	-84	-22.5			
10	65	-7.9	-83	77	-20.9			
11	75	-6.8	-77	-71	-19.8			
12	90	-14.8	-113	105	-27.8			
13	110	-12.8	-106	98	-25.8			
14	140	-14.1	111	-103	-27.2			
15	210	-26.7	-152	141	-39.7			
16	250	-32.5	-168	-156	-45.5			

Table 16: Indoor Small Office (NLOS) (XPR = 10 dB)

3.2.5.5.   Indoor Hotspot

The CDL parameters of LOS and NLOS condition are given below. In the LOS model Ricean K factor are 15.3 dB and 10.4 dB, respectively for the first and second clusters.

Cluster #	Delay [ns]	Power [dB]	AoD [º]	AoA [º]	Ray power [dB]			
1	0	0	0	0	-0.1[*]	-28.4[**]	Cluster ASD = 5º	Cluster ASA = 8º
2	5	-3.4	64	-73	-3.7[*]	-27.1[**]		
3	10	-9.2	115	80	-22.2			
4	20	-18.9	7	13	-31.9			
5	30	-17.1	11	16	-30.1			
6	40	-16.3	-7	-34	-29.3			
7	50	-13.7	-60	-12	-26.7			
8	60	-16.3	-43	-17	-29.3			
9	70	-16.8	11	-59	-29.8			
10	80	-17.9	8	-78	-30.9			
11	90	-15.9	14	-65	-28.9			
12	100	-17.4	-1	-56	-30.4			
13	110	-25.8	-11	-57	-38.8			
14	120	-31.0	-129	-22	-44.0			
15	130	-33.4	-123	-12	-46.4			

Table 17: Indoor Hotspot CDL (LOS) (XPR = 11dB)

[*] Power of dominant ray,
[**] Power of each other ray

Cluster #	Delay [ns]	Power [dB]	AoD [º]	AoA [º]	Ray power [dB]		
1	0	-6.9	2	2	-19.9	Cluster ASD = 5º	Cluster ASA = 11º
2	5	0	-2	9	-13.0		
3	10	-0.7	-7	14	-13.7		
4	15	-1.0	87	-111	-14.0		
5	20	-1.4	-88	126	-14.4		
6	25	-3.8	-15	-18	-16.8		
7	30	-2.6	0	-3	-15.6		

8	35	-0.2	-26	-3	-13.2
9	45	-3.6	-29	14	-16.6
10	55	-5.7	1	44	-18.7
11	65	-11.6	4	13	-24.6
12	75	-8.9	-5	65	-21.9
13	95	-7.3	-11	46	-20.3
14	115	-11.2	-4	35	-24.2
15	135	-13.5	-3	48	-26.5
16	155	-13.4	-7	41	-26.4
17	175	-12.2	8	7	-25.2
18	195	-14.7	4	69	-27.7
19	215	-15.8	-11	133	-28.8

Table 18: Indoor Hotspot CDL (NLOS) (XPR = 11dB)

3.2.5.6.   Outdoor to Indoor

Cluster #	Delay [ns]			Power [dB]			AoD [º]	AoA [º]	Ray power [dB]	Cluster ASD = 5º	Cluster ASA = 8º
1	0			-7.7			29	102	-20.8		
2	10	15	20	-3.0	-5.2	-7.0	0	0	-13.0		
3	20			-3.7			20	70	-16.7		
4	35			-3.0			-18	-64	-16.0		
5	35			-3.0			18	-63	-16.0		
6	50			-3.7			20	70	-16.7		
7	55	60	65	-5.4	-7.6	-9.4	29	100	-15.4		
8	140			-5.3			24	84	-18.3		
9	175			-7.6			29	100	-20.6		
10	190			-4.3			-21	76	-17.3		
11	220			-12.0			36	-126	-25.0		
12	585			-20.0			46	163	-33.0		

Table 19: Outdoor to indoor CDL (NLOS) (XPR = 8 dB)

3.2.5.7.   Rural Macrocell

The CDL parameters of LOS and NLOS condition are given below. In the LOS model Ricean K-factor is 13.7 dB.

Cluster #	Delay [ns]			Power [dB]			AoD [º]	AoA [º]	Ray power [dB]		Cluster ASD = 2º	Cluster ASD = 3º
1	0			0.0			0	0	-0.02[*]	-35.9[**]		
2	40			-22.3			-95	189	-35.3			
3	40			-25.6			102	203	-38.6			
4	40	45	50	-23.1	-25.3	-27.1	-90	-179	-33.1			
5	40	45	50	-23.7	-25.9	-27.7	104	-208	-33.7			

6	60	-27.4	-105	210	-40.4		
7	115	-27.0	104	-208	-40.0		
8	135	-25.2	-101	-201	-38.2		
9	175	-30.1	110	-219	-43.1		
10	195	-32.5	114	228	-45.5		
11	215	-31.7	-113	-225	-44.7		
12	235	-33.9	-117	-233	-46.9		
13	235	-31.0	-112	223	-44.0		

Table 20: Rural macrocell CDL (LOS) (XPR = 7dB)

* Power of dominant ray,
** Power of each other ray

Cluster #	Delay [ns]			Power [dB]			AoD [º]	AoA [º]	Ray power [dB]	Cluster ASD = 2º	Cluster ASD = 3º
1	0	5	10	-3.0	-5.2	-7.0	0	0	-13.0		
2	0			-1.8			-8	28	-14.8		
3	5			-3.3			-10	38	-16.3		
4	10	15	20	-4.8	-7.0	-8.8	15	-55	-14.8		
5	20			-5.3			13	48	-18.3		
6	25			-7.1			15	-55	-20.1		
7	55			-9.0			-17	62	-22.0		
8	100			-4.2			-12	42	-17.2		
9	170			-12.4			20	-73	-25.4		
10	420			-26.5			29	107	-39.5		

Table 21: Rural macrocell CDL (NLOS) (XPR = 7dB)

3.2.6. Channel Type and Velocity Mix

In system level simulations, users may be associated with a set of different channel types and velocities. In such cases, a mix of user speeds and channel types is evaluated.

The channel types and mobility mixes corresponding to the required test scenarios are defined in Table 3.

3.2.7. Doppler Spectrum for Stationary Users

If the TX and the RX are stationary, and the channel at time t is to be computed, then each cluster is made of a number of coherent (fixed) rays N_c and a number of scattered (variable) rays N_s ($N_c + N_s$ = total number of rays per clusters).

1 The variable rays are ascribed a bell-shaped Doppler spectrum as described in [3]:

2 $$S(f) = \begin{cases} 1 - 1.72 f_0^2 + 0.785 f_0^4 & f_0 \leq 1 \\ 0 & f_0 > 1 \end{cases} \quad where \quad f_0 = \frac{f}{f_m} \qquad (26)$$

3

4 where f_m is the maximum Doppler rate (suggested value: 2 Hz in [3]). The fixed rays
5 within a cluster share the same amplitude and phase, and their Doppler spectrum is a
6 Dirac impulse at $f = 0$ Hz.

7

8 An alternative is to simply model the Doppler spectrum as a Jakes spectrum with 2 Hz
9 Doppler frequency.

10 ### 3.2.8.   Generation of Spatial Channels

11 The following procedure describes the simulation procedure based on the spatial TDL
12 or CDL models. In the correlation based implementation, the spatial and temporal
13 correlation need to be derived first before generating the channel coefficients. In the
14 ray-based approach, the time-variant matrix channels are constructed from all the rays.
15

16 **Step 1:** *Choose a propagation scenario (e.g. Urban Macro, Suburban Macro etc.). After*
17   *dropping a user, determine the various distance and orientation parameters.*
18

19 The placement of the MS with respect to each BS is to be determined according to the
20 cell layout. From this placement, the distance between the MS and the BS (d) and the
21 LOS directions with respect to the BS and MS (θ_{BS} and θ_{MS} respectively) can be
22 determined. Note that θ_{BS} and θ_{MS} are defined relative to the broadside directions. The
23 MS antenna array orientations (Ω_{MS}), are i.i.d., drawn from a uniform 0 to 360 degree
24 distribution.
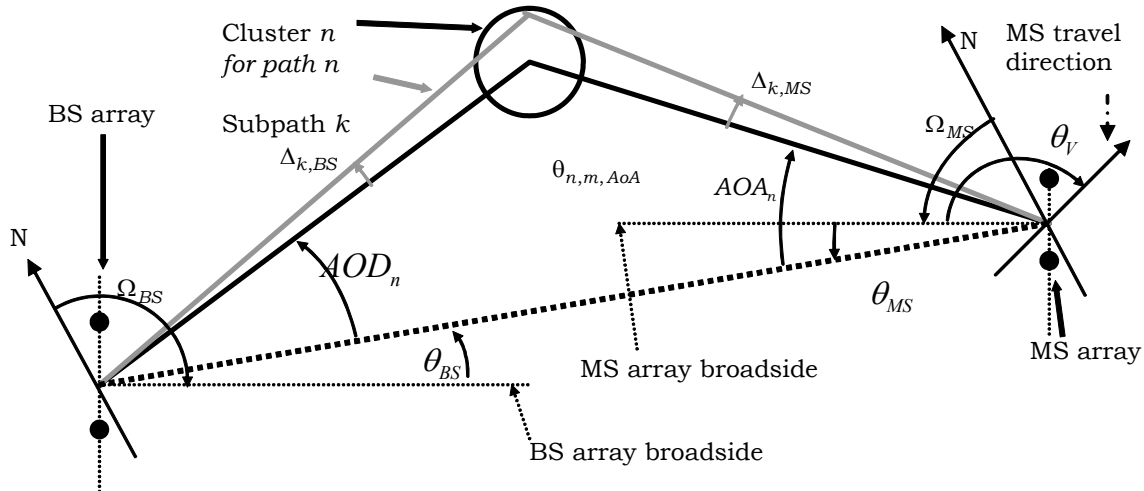
Figure 6: The MIMO channel model angle parameters

30 **Step 2:** *Calculate the bulk path loss associated with the BS to MS distance.*

Step 3: *Determine the Shadowing Factor (SF).*

The SF is randomly generated from a log-normal distribution with a pre-specified standard deviation. Generate the SF according to Section 3.2.4

If a ray-based implementation is being used, skip steps 4, 6 and 7.

Step 4: *Calculate the per-tap spatial correlation matrix based on per-tap $AS_{BS, path}$ at the BS and the per-tap $AS_{MS, path}$ at the MS, both of which are specified in the reduced complexity models specified in 3.2.5 (denoted as "cluster ASD" and "cluster ASA" respectively). The spatial correlation also depends on the BS/MS antenna configurations (a random broadside direction, number and spacing of antennas, polarization, etc.)*

Once the per-tap AS, mean AoA, and mean AoD are defined, the theoretical spatial correlation at both BS and MS can be derived, assuming Laplacian power angular distribution. Assuming omni directional antennas at the BS and MS the antenna spatial correlations, the antenna spatial correlations between the p-th and q-th antenna at the BS and MS respectively, are

$$r_{n,BS}(p,q) = \int_{-\infty}^{\infty} f(\alpha) \exp\left\{ j \frac{2\pi d_{BS}}{\lambda}(p-q)\sin(AOD_n + \alpha) \right\} d\alpha$$

$$r_{n,MS}(p,q) = \int_{-\infty}^{\infty} f(\beta) \exp\left\{ j \frac{2\pi d_{MS}}{\lambda}(p-q)\sin(AOA_n + \beta) \right\} d\beta$$

(27)

where d_{BS} (d_{MS}) is the antenna spacing at BS (MS) and λ is the wavelength. α is the angular offset around the mean AoD at BS, and β is the angular offset around the mean AoA at MS. The PDF of angular offsets is

$$f(\alpha) = \frac{1}{\sqrt{2} AS_{BS,Path}} \exp\left\{ -\frac{\sqrt{2}|\alpha|}{AS_{BS,Path}} \right\}$$

$$f(\beta) = \frac{1}{\sqrt{2} AS_{MS,Path}} \exp\left\{ -\frac{\sqrt{2}|\beta|}{AS_{MS,Path}} \right\}$$

(28)

Note that $AS_{BS, path}$ and $AS_{MS, path}$ are specified in the reduced complexity models specified in 3.2.5 where they are denoted as "cluster ASD" and "cluster ASA" respectively. The above integration can be computed with two approaches (other alternatives may also exist). See Appendix A for details. In summary, the first approach is to approximate the Laplacian PDF with 20 rays, after which the integration is reduced to a summation. The second approach is to compute the integration using a numerical method. The second approach is to compute the integration using the exact expression given in the Appendix A. Either using 20-ray approximation or exact expression, it is possible to quantize the AoA or AoD and then pre-compute the spatial correlation for each quantized AoA and AoD values. Using pre-stored correlation matrices may reduce the simulation run-time.

Denoting the spatial correlation matrix at BS and MS as $\mathbf{R}_{BS,n}$ and $\mathbf{R}_{MS,n}$, the per-tap spatial correlation is determined as

$$\mathbf{R}_n = \mathbf{R}_{BS,n} \otimes \mathbf{R}_{MS,n} \, (\text{Kronecker product}) \tag{29}$$

In the case that the antenna elements are cross-polarization antennas, the per-tap channel correlation is determined as

$$\mathbf{R}_n = \mathbf{R}_{BS,n} \otimes \mathbf{\Gamma} \otimes \mathbf{R}_{MS,n} \tag{30}$$

where $\mathbf{\Gamma}$ is a cross-polarization matrix based on the cross polarization defined in the CDL models. An example of how to derive $\mathbf{\Gamma}$ is given in Appendix B based on the assumption of a default antenna configuration.

Step 5: *Determine the antenna gains of the BS and MS paths as a function of their respective AoDs and AoAs. Calculate the per-tap average power with BS/MS antenna gain as*

$$P_n^{''} = P_n \bullet G_{BS}(AOD_n + \theta_{BS}) \bullet G_{MS}(AOA_n + \theta_{MS}) \tag{31}$$

<Editor's notes: The BS antenna pattern will in theory make the power angular profile not Laplacian any more. Also the Doppler spectrum in step-6 will be affected. In contribution 07/140r1, Von Mises distribution, rather than Laplacian, was proposed to approximate the power angular spectrum and the BS antenna pattern. A decision was deferred for future study and to be resolved by TGm. However, the current draft is built upon Laplacian assumption.>

Step 6: Determine Doppler spectrum using one of two approaches:

<u>Approach #1</u>: *Determine the Doppler spectrum of each tap, based on the traveling direction chosen in Step 1, the array broadside direction defined in step 4, a Laplacian power angular profile with the RMS angular spread AS defined in the CDL models.*

From the Doppler spectrum defined for any arbitrary Doppler spectrum in [22], the Doppler spectrum at tap-n for the case of Laplacian power angular profile is:

$$S_n(f) \propto \begin{cases} \dfrac{1}{\sqrt{f_{\max}^2 - f^2}} \exp\left\{ -\dfrac{\sqrt{2}\left|\cos^{-1}(f/f_{\max}) + \vartheta_n\right|}{AS_{MS,Path}} \right\}, & |f| \le f_{\max} = f_c v / c \\ 0, & \text{otherwise} \end{cases} \tag{32}$$

where ϑ_n is the angle between the traveling direction and the mean AoA for tap-n.

<u>Approach #2</u>: *Jakes spectrum is used.* It is recognized that the use of a Jakes spectrum is self-inconsistent when a non-uniform power angular spectrum occurs at the mobile station. However, it is used in simulations to trade off between simulation

complexity and model accuracy. Generating the time-varying fading process from a Doppler spectrum based on the traveling direction and mean AoA can be computationally expensive. The impact on the overall system level performance with this more accurate method may be small. This method will facilitate easy generation of such a time-varying process (e.g. offline generation).

<Notes: Only one of the options will be adopted as the final method after some system level studies>

Step 7: *Generate time-variant MIMO channels with above-defined per-tap spatial correlations.*

For each tap, generate NxM i.i.d. channels first that satisfies the specified Doppler spectrum H_{iid} (each tap is a NxM matrix) where N is the number of receive antennas and M is the number of transmit antennas.

To generate temporally correlated Gaussian process that satisfies a specific Doppler spectrum, one implementation method is to use the summation of equal-power sinusoids where their frequencies are calculated numerically using either Method of Exact Doppler Spread (MEDS) or L_2-Norm Method (LNPM) [23]. Pre-computing the sinusoid frequencies for a set of quantized angle ϑ_n can be considered as a means to reduce simulation run time, comparing with computing the sinusoid frequencies on the fly. As an example, the non-Jakes Doppler spectrum as specified in Approach #1 of the previous step can be simulated using the summation of 10 equal-power sinusoids with random phases, but their frequencies are defined as

$$f_{n,i} = f_{\max} \cos(\phi_{n,i}) \tag{33}$$

where

$$\phi_{n,i} = \vartheta_n + AS_{MS,Path} *[-1.8157,-1.0775,-0.6456,-0.3392,-0.1015, 0.1015, 0.3392, 0.6456, 1.0775, 1.8157]$$

It is also possible to use more than 10 sinusoids where the angle spacing between equal power sub-rays is chosen to make sure that area under the Laplacian PDF (i.e., separated by the sub-rays) equal to 1/(N+1) where N is the number of sub-rays, i.e., for the positive side

$$\frac{1}{2}\left[\exp\left\{-\frac{\sqrt{2}|\alpha_1|}{AS}\right\} - \exp\left\{-\frac{\sqrt{2}|\alpha_2|}{AS}\right\}\right] = \frac{1}{N+1} \tag{34}$$

where α_1 and α_2 are two adjacent angles with an increasing order and for the first angle on the positive side assuming an even N is

$$\frac{1}{2}\left[1-\exp\left\{-\frac{\sqrt{2}|\alpha_1|}{AS}\right\}\right] = \frac{0.5}{N+1} \tag{35}$$

1   For N=10 and AS=1, the angles are [±1.2054   ±0.7153   ±0.4286   ±0.2252   ±0.0674].
2   Note that due to finite quantization, the standard deviation of all the ten angles is not "1"
3   any more, it is C=0.6639 instead. So scaling of 1/C must be used to compensate for the
4   finite quantization.
5
6   Compute the correlated channel at each tap as

$$\mathbf{H}_n = unvec\left\{ R_n^{1/2} vec(H_{iid}) \right\} \tag{36}$$

8
9   where *vec(H)* denotes the column-wise stacking of matrix H and *unvec* is the reverse
10 operation. $R_n^{1/2}$ denotes the square-root of matrix R_n.
11
12 **Step 8 (Ray-based method only, Skip for correlation-based implementation):**
13   *Generate time-variant MIMO channels*.
14
15 For an *N* element linear BS array and a *M* element linear MS array, the channel
16 coefficients for one of *L* multipath components are given by a *NxM* matrix of complex
17 amplitudes. We denote the channel matrix for the *n*th multipath component (*n* = 1,…,*L*)
18 as $\mathbf{H}_n(t)$. The (*u,s*)th component (*s* = 1,…,*N, u* = 1,…,*M*) of $\mathbf{H}_n(t)$ is given in the
19 following, assuming   polarized arrays (If polarization is not considered, the 2x2
20 polarization matrix can be replaced by scalar $\exp(\Phi_{n,m})$ and only vertically polarized field
21 patterns applied)

$$h_{u,s,n}(t) = \sqrt{\frac{P_n \sigma_{SF}}{M}} \sum_{m=1}^{M} \left(\begin{bmatrix} \chi_{BS}^{(v)}(\theta_{n,m,AoD}) \\ \chi_{BS}^{(h)}(\theta_{n,m,AoD}) \end{bmatrix}^T \begin{bmatrix} \exp\left(j\Phi_{n,m}^{(v,v)}\right) & \sqrt{r_{n1}}\exp\left(j\Phi_{n,m}^{(v,h)}\right) \\ \sqrt{r_{n2}}\exp\left(j\Phi_{n,m}^{(h,v)}\right) & \exp\left(j\Phi_{n,m}^{(h,h)}\right) \end{bmatrix} \begin{bmatrix} \chi_{MS}^{(v)}(\theta_{n,m,AoA}) \\ \chi_{MS}^{(h)}(\theta_{n,m,AoA}) \end{bmatrix} \times \right.$$
$$\left. \exp\left(jkd_s \sin(\theta_{n,m,AoD})\right) \times \exp\left(jkd_u \sin(\theta_{n,m,AoA})\right) \times \exp\left(jk\|\mathbf{v}\|\cos(\theta_{n,m,AoA} - \theta_v)t\right) \right) \tag{37}$$

23
24

25   where

26   P_n is the power of the nth path

27   σ_{SF} is the lognormal shadow factor
28   *M*   is the number of subpaths per-path.

29              $\theta_{n,m,AoD}$ is equal to (AoD$_n$ + α + θ_{BS}), where α is the angular offset around the
30   mean AoD$_n$ at BS (See angular offsets in Appendix A).

31              $\theta_{n,m,AoA}$ is equal to (AoA$_n$ + β + θ_{MS}), where β is the angular offset around the mean
32   AoA$_n$ at MS (See angular offsets in Appendix A).
33   j   is the square root of -1.
34   k   is the wave number $2\pi/\lambda$ where λ is the carrier wavelength in meters.
35   d_s is the distance in meters from BS antenna element s from the reference (s

36   = 1) antenna. For the reference antenna s = 1, d_1=0.
37   d_u is the distance in meters from MS antenna element u from the reference (u

38   = 1) antenna. For the reference antenna u = 1, d_1=0.
39              $\Phi_{n,m}$ is the phase of the mth subpath of the nth path.

$\|\mathbf{v}\|$ is the magnitude of the MS velocity vector.

θ_v is the angle of the MS velocity vector.

$\chi_{BS}^{(v)}(\theta_{n,m,AoD})$ is the BS antenna complex response for the V-pol component.

$\chi_{BS}^{(h)}(\theta_{n,m,AoD})$ is the BS antenna complex response for the H-pol component.

$\chi_{MS}^{(v)}(\theta_{n,m,AoA})$ is the MS antenna complex response for the V-pol component.

$\chi_{MS}^{(h)}(\theta_{n,m,AoA})$ is the MS antenna complex response for the H-pol component.

r_{n1} is the random variable representing the power ratio of waves of the nth path leaving the BS in the vertical direction and arriving at the MS in the horizontal direction (v-h) to those leaving in the vertical direction and arriving in the vertical direction (v-v).

r_{n2} is the random variable representing the power ratio of waves of the nth path leaving the BS in the horizontal direction and arriving at the MS in the vertical direction (h-v) to those leaving in the vertical direction and arriving in the vertical direction (v-v).

$\Phi_{n,m}^{(x,y)}$ phase offset of the mth subpath of the nth path between the x component (either the horizontal h or vertical v) of the BS element and the y component (either the horizontal h or vertical v) of the MS element.]

Step 9: *If a non-zero K-factor is to be enforced (i.e., K≠0), adjust the LOS path power.* See Appendix C for details.

Step 10: *Introduce receive antenna gain imbalance or coupling, if needed.* See Appendix D for details.

3.2.9.   Channel Model for Baseline Test Scenario

In section 2.3, a baseline test scenario with a 2x2 antenna configuration is defined for calibrating system level simulators. A similar test scenario is also defined for liaisoning with NGMN.

A simplified correlation-based approach is used to implement the channel model for these test scenarios by determining a spatial correlation matrix for each user and applying the same correlation matrix for all the taps of the ITU TDL model [4].

Two types of spatial correlation are defined, assuming the Jakes Doppler spectrum for both cases:

  Case 1: Uncorrelated antennas at both BS and MS

  Case 2: Uncorrelated antennas at MS, correlated antennas at BS with the correlation (identical for all taps) derived as in Appendix-A according to the following assumptions:

        a. Mean AoD determined according to the MS-BS LOS direction, relative to the BS antenna array bore sight.

        b. Uniform linear antenna array at the BS with any number of elements and an inter-element spacing of 4 wavelengths.

c. Laplacian angular power profile at the BS with an angular spread of 3 degrees for baseline test scenario corresponding to 1.5 km site-to-site distance, and 15 degrees for the NGMN configuration with 0.5 km site-to-site distance (15 degrees is the same as the mean angular spread specified in 3GPP/3GPP2 SCM urban macrocell environment).

The two test scenarios and the methodology described in this section are also suitable to optionally simulate larger antenna configurations with any number of antennas at the BS and MS, different antenna spacing and angular spreads.

The default ITU channel models are described by their power delay profiles as they appear in Table 22.

Path Index	Pedestrian B		Vehicular A	
	Power (dB)	Delay (ns)	Power (dB)	Delay (ns)
1	0.4057	0	0.4850	0
2	0.3298	200	0.3853	310
3	0.1313	800	0.0611	710
4	0.0643	1200	0.0485	1090
5	0.0673	2300	0.0153	1730
6	0.0017	3700	0.0049	2510

Table 22: ITU Power Delay Profiles

The modified power delay profiles [72] for the ITU channel models are specified in Table 23. Baseline channel models for a 10MHz system bandwidth as defined in Table 3 shall use these profiles. Table 23 provides the delays relative to the first path in nanoseconds and the relative power of each path compared to the strongest (similar to the default ITU models). The modified ITU Pedestrian B and Vehicular A channel models use 24 paths.

Path Index	Modified Pedestrian B		Modified Vehicular A	
	Power (dB)	Delay (ns)	Power (dB)	Delay (ns)
1	-1.175	0	-3.1031	0
2	0	40	-0.4166	50
3	-0.1729	70	0	90
4	-0.2113	120	-1.0065	130
5	-0.2661	210	-1.4083	270
6	-0.3963	250	-1.4436	300
7	-4.32	290	-1.5443	390
8	-1.1608	350	-4.0437	420
9	-10.4232	780	-16.6369	670
10	-5.7198	830	-14.3955	750
11	-3.4798	880	-4.9259	770
12	-4.1745	920	-16.516	800
13	-10.1101	1200	-9.2222	1040
14	-5.646	1250	-11.9058	1060
15	-10.0817	1310	-10.1378	1070
16	-9.4109	1350	-14.1861	1190

17	-13.9434	2290	-16.9901	1670
18	-9.1845	2350	-13.2515	1710
19	-5.5766	2380	-14.8881	1820
20	-7.6455	2400	-30.348	1840
21	-38.1923	3700	-19.5257	2480
22	-22.3097	3730	-19.0286	2500
23	-26.0472	3730	-38.1504	2540
24	-21.6155	3870	-20.7436	2620

Table 23: Modified ITU Profiles for Wideband Systems

3.3.   Link Level Channel Model

The link level channel model should be the same as the CDL channel model described in Section 3.2.

For various propagation scenarios, the corresponding CDL model can be directly used for link simulation, assuming the AoA and AoD are relative to the broadside direction of the receiver array, instead of assuming random orientation of the array in system simulations.

In the case of correlation-based implementation, the spatial correlation can be easily derived once the AoA/AoD is well defined based on either 20-ray approximation or numerical integration. The antenna configuration is assumed to either a linear array with a spacing of TBD-λ or a polarized antenna with XPD values defined in the CDL models. The Doppler spectrum depends on traveling direction relative to the AoA. Instead of setting a random traveling direction which can vary from simulation to simulation, a worst case Jakes spectrum should be used.

4. Link-to-System Mapping

4.1.   Background of PHY Abstraction

The objective of the physical layer (PHY) abstraction is to accurately predict link layer performance in a computationally simple way. The requirement for an abstraction stems from the fact that simulating the physical layer links between multiples BSs and MSs in a network/system simulator can be computationally prohibitive. The abstraction should be accurate, computationally simple, relatively independent of channel models, and extensible to interference models and multi-antenna processing.

In the past, system level simulations characterized the average system performance, which was useful in providing guidelines for system layout, frequency planning etc. For such simulations, the average performance of a system was quantified by using the topology and macro channel characteristics to compute a geometric (or average) SINR distribution across the cell. Each subscriber's geometric SINR was then mapped to the highest modulation and coding scheme (MCS), which could be supported based on link level SINR tables that capture fast fading statistics.   The link level SINR-PER look-up tables served as the PHY abstraction for predicting average link layer performance. Examples of this static methodology may be found in [26], [27].

Current cellular systems designs are based on exploiting instantaneous channel conditions for performance enhancement. Channel dependent scheduling and adaptive coding and modulation are examples of channel-adaptive schemes employed to improve system performance.   Therefore, current system level evaluation methodologies are based on explicitly modeling the dynamic system behavior by including fast fading models within the system level simulation. Here the system level simulation must support a PHY abstraction capability to accurately predict the instantaneous performance of the PHY link layer.

4.2.   Dynamic PHY Abstraction Methodology

In system level simulations, an encoder packet may be transmitted over a time-frequency selective channel. For example, OFDM systems may experience frequency selective fading, and hence the channel gain of each sub-carrier may not be equal. In OFDM, the coded block is transmitted over several sub-carriers and the post-processing SINR values of the pre-decoded streams are thus non-uniform. Additionally, the channel gains of sub-carriers can be time selective, i.e. change in time due to the fading process and possible delays involved in H-ARQ re-transmissions. The result on a transmission of a large encoder packet is encoded symbols of unequal SINR ratios at the input of the decoder due to the selective channel response over the encoder packet transmission.

PHY abstraction methodology for predicting instantaneous link performance for OFDM systems has been an active area of research and has received considerable attention in the literature [28]-[37]. The role of a PHY abstraction method is to predict the coded block error rate (BLER) for given a received channel realization across the OFDM sub-carriers used to transmit the coded FEC block. In order to predict the coded performance, the post-processing SINR values at the input to the FEC decoder are considered as input to the PHY abstraction mapping. As the link level curves are generated assuming a frequency flat channel response at given SINR, an effective SINR, $SINR_{eff}$ is required to accurately map the system level SINR onto the link level curves to determine the resulting BLER. This mapping is termed *effective SINR mapping (ESM).* The ESM PHY abstraction is thus defined as compressing the vector of received SINR values to a single effective SINR value, which can then be further mapped to a BLER number as shown in Figure 7.

Several ESM PHY abstractions to predict the instantaneous link performance have been proposed in the literature. Examples include mean instantaneous capacity [28]-[30], exponential-effective SINR (EESM, [31], [33]-[35]) and Mutual information effective SINR (MIESM, [36], [37]). Within the class of MIESM there are two variants, one is based on the mutual information per received symbol normalized to yield the bit mutual information and the other directly computes the bit mutual information. Each of these PHY abstractions uses a different function to map the vector of SINR values to a single number. Given the instantaneous EESM SINR, mean capacity or mutual information effective SINR, the BLER for each MCS is calculated using a suitable mapping function.
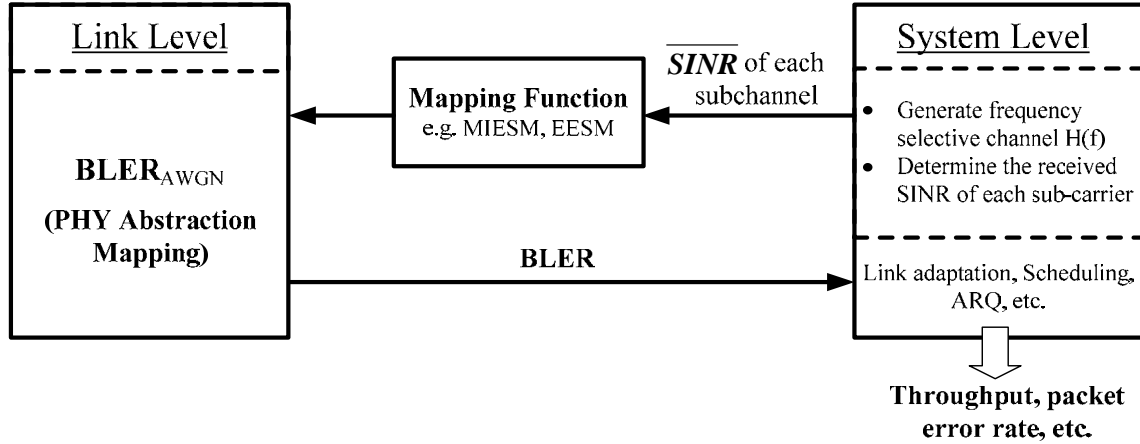
Figure 7: PHY link-to-system mapping procedure

In general, the ESM can be described as follows,

$$SINR_{eff} = \Phi^{-1}\left\{\frac{1}{N}\sum_{n=1}^{N}\Phi\left(SINR_{n}\right)\right\} \tag{38}$$

where N is the number of symbols in a coded block, and $\Phi(\bullet)$ is an invertible function.

In the case of the mutual information and capacity based ESM the function $\Phi(\bullet)$ is derived from the constrained capacity. While in the case of EESM, the function $\Phi(\bullet)$ is derived based on the Chernoff bound for the probability of error. In the next three sections, we describe in detail these ESM methods.

4.3.   Mutual Information Based Effective SINR Mapping

The accuracy of a mutual information-based metric depends on the equivalent channel over which this metric is defined. Capacity is the mutual information based on a Gaussian channel with Gaussian inputs. Modulation constrained capacity metric is the mutual information of a "symbol channel" (i.e. constrained by the input symbols from a complex set).

The computation of the mutual information per coded bit can be derived from the received symbol-level mutual information; this approach is termed received bit mutual information rate (RBIR). An alternative is a method that directly arrives at the bit-level mutual information; this method called mean mutual information per bit (MMIB).

4.3.1.   Received Bit Mutual Information Rate (RBIR) ESM

A block diagram for the MIESM approach is shown in Figure 8. Given a set of N received encoder symbol SINRs from the system level simulations, denoted as $SINR_1$, $SINR_2$, $SINR_3$, …, $SINR_N$, the mutual information per symbol (SI) is computed as a function of the M-ary modulation scheme, with $m = \log_2 M$ bits/symbol, as follows:

1
$$SI\left(SINR_n, m(n)\right) = I(X;Y) = E_{XY}\left(\log_2\left(\frac{P(Y\mid X, SINR_n)}{\sum_X P(X)P(Y\mid X, SINR_n)}\right)\right) \tag{39}$$

2   In Equation (39), $Y = X + U$ is the received symbol and $P(Y\mid X, SINR)$ is the channel
3   transition probability density conditioned on the input symbol X for a given $SINR$. It is
4   assumed that the transmitted symbols are equally likely, thus $P(X) = 1/M$, where M is
5   the size of the modulation alphabet and that U is modeled as zero mean complex
6   Gaussian with variance $1/(2SINR_n)$ per component.

7
8   Equation (39) can be re-written as

9
$$SI\left(SINR_n, m(n)\right) = \log_2 M - \frac{1}{M}\sum_{m=1}^{M} E_U\left\{\log_2\left(1 + \sum_{k=1, k\neq m}^{M} \exp\left[-\frac{|X_k - X_m + U|^2 - |U|^2}{(1/SINR_n)}\right]\right)\right\} \tag{40}$$

10
11   The mutual information curves $SI(SINR, m)$ are generated, and stored once in the
12   system simulator, for each of the modulation and coding formats.
13
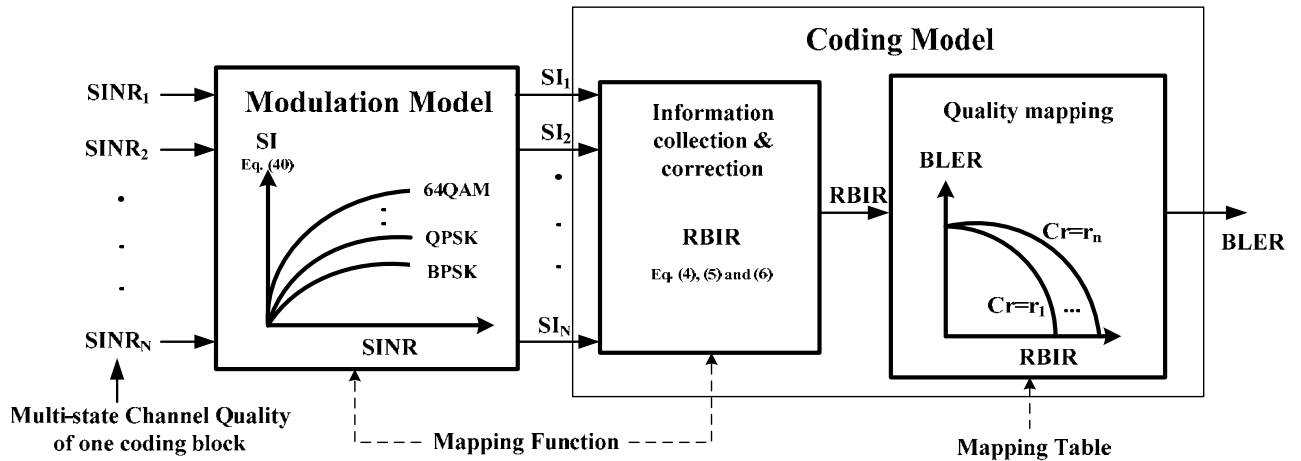
14
15
16   **Figure 8: Computational procedure for RBIR ESM method**
17
18   Assuming N sub-carriers are used to transmit a coded block, the received mutual
19   information over a coded block (*RBI*) is computed as

20
$$RBI = \sum_{n=1}^{N} SI\left(SINR_n, m(n)\right) \tag{41}$$

21   We note that even though we refer to the coded block being carried over a set of sub-
22   carriers, in general, the coded block may be carried over multiple dimensions, including
23   the spatial dimensions available with MIMO. Also, note that in the above, the mutual

1   information may be computed even with non-uniform modulation across the coded
2   block. Next we compute the normalized mutual information per received bit (*RBIR*)
3   which is given by

$$RBIR = \frac{\sum_{n=1}^{N} SI\left(SINR_n, m(n)\right)}{\sum_{n=1}^{N} m(n)} \tag{42}$$

5   The advantage of computing the *RBIR* is that the relationship between the *RBIR* and
6   the BLER is dependent only on the AWGN curves for the code rate and is independent
7   of the modulation scheme. This feature is very useful in computing the PHY abstraction
8   for cases where the coded block is comprised of mixed modulation symbols.
9
10   We further note that an adjustment parameter, $SINR_{adjust}$, may be specified with the
11   RBIR metric that can account for deviations of the *RBIR* mapping with respect to the
12   AWGN curves. This adjustment parameter is given by

$$RBIR = \frac{\sum_{n=1}^{N} SI\left(SINR_n / SINR_{adjust}, m(n)\right)}{\sum_{n=1}^{N} m(n)} \tag{43}$$

14   The exact specification of this adjustment parameter is determined through simulations
15   and shall be specified along with the PHY abstraction tables, once the 802.16m
16   numerology is specified.

17   **4.3.1.1.   RIBIR ML Receiver Abstraction for SISO/MIMO**
18   **1) RBIR Mapping**
19   The symbol-level log-likelihood ratio (LLR) for the ML receiver can be computed as

$$LLR_i = \log_e \left(\frac{P(y \mid x = x_i)}{\sum_{\substack{k=1 \\ k \neq i}}^{M} P(y \mid x = x_k)} \right) = \log_e \left(\frac{e^{-\frac{d_i^2}{\sigma^2}}}{\sum_{\substack{k=1 \\ k \neq i}}^{N} e^{-\frac{d_k^2}{\sigma^2}}} \right) \qquad i = 1, 2, ..., N \tag{44}$$

21
22   d_i, *i=1, 2, …, M*, indicates the ith distances for the current received symbol which is

23   output from MLD detector, so there is $d_k = \left| y - Hx_k \right| = \sqrt{(y - Hx_k)(y - Hx_k)^H}$.

24
25   Due to the different QAM mappings, the RBIR over one constellation can be
26   represented as

$$I(x, LLR) = \frac{1}{m} \sum_{i=1}^{m} I(x_i, LLR(x_i))$$

where $I(x_i, LLR(x_i))$ is the RBIR metric of the transmission symbol x_i over the whole constellation.

For a WiMAX system, the mutual information – RBIR metric will be considered for all N-subcarriers as

$$RBIR = \frac{1}{mN} \sum_{n=1}^{N} \sum_{i=1}^{m} I_n(x_i, LLR(x_i)) \tag{45}$$

2) Generalized Symbol LLR PDF Model – Gaussian Approximation

The conditional PDF of symbol LLR can be approximated as a single Gaussian curve for SISO under the three modulations; for SISO, the distribution of LLR for an ML receiver can be written as $p(LLR_{SISO}) = N(AVE, VAR)$.

For a MIMO Matrix B 2x2 system, the conditional PDF of symbol LLR output can be approximated as two Gaussian curves for the two streams for each of three modulations for the 'horizontal' encoding system. The distribution of LLR for one stream from ML receiver can be written as $p(LLR_{MIMO,stream}) = N(AVE_{stream}, VAR_{stream})$.

For a MIMO Matrix B 2x2 and 'vertical' encoding system, the probability distribution function of the LLR from the ML receiver can be written as a weighted sum

$$p(LLR_{MIMO}) = p_1 \cdot N(AVE_{stream1}, VAR_{stream1}) + p_2 \cdot N(AVE_{stream2}, VAR_{stream2})$$

3) Procedure for RBIR PHY Mapping for SISO/MIMO System under ML Receiver

The principle of RBIR PHY Mapping in an ML Receiver is the fixed relationship between the LLR distribution and BLER. Given the channel matrix 'H' and SNR, the system has a fixed symbol LLR distribution. This implies that we can have a fixed predicted PER/BLER, which is the principle for RBIR PHY mapping for an ML Receiver. RBIR MLD metric requires a numerical integration to compute the average over all the LLR values for one resource block and for each sub-carrier to compute the PER/BLER for one block.

Given channel matrix 'H' and SNR, the real symbol LLR distribution $p(AVE, VAR)$ can be approximated by the formula provided in the procedure below. This enables us to set up the fixed mapping function between the parameter-bin (H, SNR) and PER/BLER (from real LLR distribution) which is our RBIR PHY Mapping function for ML symbol-level detection.

Procedure for RBIR PHY Mapping on symbol-level ML detection:

    1. Given the channel matrix 'H' and SNR for each sub-carrier, the fixed LLR

distribution parameter pair (AVE, VAR) can be obtained as specified below. Here in the LLR calculation, we used the given constellation point (1,1) for QPSK, (1,1,1,1) for 16QAM and (1,1,1,1,1,1) for 64QAM. Also, in the LLR distribution calculation we only considered the impact from the neighboring dominant constellation points so that all modulations will have the same theoretical formulation as below. For example, for all modulations, the neighboring 3 constellation points are considered.

1) For SISO system

The average of LLR is given as

$$AVE = E\{LLR\} = \frac{d^2 |h|^2}{\sigma^2} - E\{K\} \tag{46}$$

and the variance of LLR is given as

$$VAR = E\{|LLR - E(LLR)|^2\} = E\{K^2\} - E^2\{K\}$$

where

$$E\{K\} = \int_{-3\frac{|h|}{\sigma}}^{3\frac{|h|}{\sigma}} \frac{1}{\sqrt{2\pi} \frac{|h|}{\sigma}} e^{-\frac{x^2}{2\frac{|h|^2}{\sigma^2}}} \log_e(2e^{-2dx} + e^{-\frac{d^2|h|^2}{\sigma^2}} e^{-4dx}) dx$$

$$E\{K^2\} = \int_{-3\frac{|h|}{\sigma}}^{3\frac{|h|}{\sigma}} \frac{1}{\sqrt{2\pi} \frac{|h|}{\sigma}} e^{-\frac{x^2}{2\frac{|h|^2}{\sigma^2}}} [\log_e(2e^{-2dx} + e^{-\frac{d^2|h|^2}{\sigma^2}} e^{-4dx})]^2 dx \tag{47}$$

Here the simplified numerical integration can be applied for the above calculation of the mean and variance of symbol level LLR as [73]:

$$E\{K\} = \log_e(2) + [\frac{2}{3} f_2(0) + \frac{f_2(\sqrt{3VAR_t})}{6} + \frac{f_2(\sqrt{3VAR_t})}{6}]$$

$$f_2(x) = \log_e(1 + a_k e^{-2x}) \qquad a_k = \frac{1}{2} e^{-\frac{d^2|h|^2}{\sigma^2}} \qquad VAR_t = \frac{d^2 |h|^2}{\sigma^2} \tag{48}$$

And

$$E\{K^2\} \approx 4VAR_t + 2\log_e(2)E\{K\} - \log_e^2(2)$$

$$+ \left[\frac{2}{3} f_3(0) + \frac{f_3(\sqrt{3VAR_t})}{6} + \frac{f_3(\sqrt{3VAR_t})}{6}\right] - 4\left[\frac{2}{3} f_4(0) + \frac{f_4(\sqrt{3VAR_t})}{6} + \frac{f_4(\sqrt{3VAR_t})}{6}\right] \tag{49}$$

where the function $f_3(\cdot)$ and $f_4(\cdot)$ has the following definition

$$f_3(x) = \log_e^2(1 + a_k e^{-2x})$$

$$f_4(x) = x\log_e(1 + a_k e^{-2x})$$

The three modulations will have the same formula for the real LLR distribution $p(AVE, VAR)$. The only difference is the minimum distance '*d*'. Here for QPSK: $d = \sqrt{2}$; 16QAM: $d = 2/\sqrt{10}$; 64QAM: $d = 2/\sqrt{42}$. '*d*' indicates the minimum distance in QAM constellation.

1. For MIMO Matrix B 2x2 System

   The mean and variance for 1st stream are

$$AVE_1 = \frac{d^2(|h_{11}|^2 + |h_{21}|^2)}{\sigma^2} - E\{K_1\}$$

$$VAR = E\{K_1^2\} - E^2[K_1]$$

where

$$E\{K_1\} = \int_{-3\frac{d|H_1|}{\sigma}}^{3\frac{d|H_1|}{\sigma}} \frac{1}{\sqrt{2\pi}\frac{d|H_1|}{\sigma}} e^{-\frac{x^2}{2d^2\frac{|H_1|^2}{\sigma^2}}} \log_e(2e^{-x} + e^{-\frac{d^2|H_1|^2}{\sigma^2}}e^{-2x})dx$$

$$E\{K_1^2\} = \int_{-3\frac{d|H_1|}{\sigma}}^{3\frac{d|H_1|}{\sigma}} \frac{1}{\sqrt{2\pi}\frac{d|H_1|}{\sigma}} e^{-\frac{x^2}{2d^2\frac{|H_1|^2}{\sigma^2}}} [\log_e(2e^{-x} + e^{-\frac{d^2|H_1|^2}{\sigma^2}}e^{-2x})]^2 dx$$

and $\quad H = [H_1 \quad H_2] = \begin{bmatrix} h_{11} & h_{12} \\ h_{21} & h_{22} \end{bmatrix}, \ |H_1| = \sqrt{|h_{11}|^2 + |h_{21}|^2}$

The same simplified function as in SISO section can be used for above integration for the expectation over the K_1 and K_1^2. A similar formula could be used for the second stream of 'horizontal' encoding system of WiMAX.

2. Calculate the RBIR metric based on RBIR definition as below and LLR distribution as Step 1.

   Introducing some approximation in the previous derivation, the distribution of 'LLR' can be modified as ' $p(LLR) = N(a \times AVE, VAR)$ ', The RBIR can then be computed as:

$$RBIR = \frac{1}{\log_2 N} \frac{1}{N} \sum_{i=1}^{N} \int_{LLR_i} \frac{1}{\sqrt{2\pi \cdot VAR}} e^{-\frac{(LLR_i - AVE_i)^2}{2VAR_i}} \log_2 \frac{N}{1+\exp(-LLR_i)} dLLR_i$$

$$= \frac{1}{\log_2 N} \int_{LLR} \frac{1}{\sqrt{2\pi \cdot VAR}} e^{-\frac{(LLR - a \times AVE)^2}{2VAR}} \log_2 \frac{N}{1+\exp(-LLR)} dLLR$$

The simplified numerical integration for the above RBIR can be written as [73]

$$RBIR \approx 1 - \frac{1}{\log_2 N \log_e 2} \left[\begin{array}{l} \frac{2}{3} f_1(a \cdot AVE) + \dfrac{f_1(a \cdot AVE + \sqrt{3VAR})}{6} \\ + \dfrac{f_1(a \cdot AVE - \sqrt{3VAR})}{6} \end{array} \right] \qquad (50)$$

where the function $f_1(\cdot)$ has the following definition

$$f_1(x) = \log_e(1 + e^{-x}).$$

The parameter 'a' is used to close the gap between measured PER and RBIR MLD PHY.

For QPSK, 16QAM and 64QAM, the LLR mean value will be optimized as $AVE = a \cdot AVE_{computed}$ for the RBIR calculation.

The LLR variance will be optimized for 64QAM as, $VAR = 2 \cdot VAR_{computed}$.

Here only 64QAM modulation needs to be tuned because in the LLR calculation, the 3 dominant constellation points are not enough for 64QAM from the simulation results on the LLR variance. For 64QAM, the 8 constellation points need to be considered for the LLR variance, which can use the variance tune parameter '2' to realize the impact from 8 constellation point from the simulation.

The 'a' values will be presented in next sub-section for the different H ranges.

3. Average the RBIR values over the multiple sub-carriers for OFDM system
4. Convert the averaged RBIR for one resource block to one single 'effective SINR' from the SNR-to-MI Table.
5. Lookup the static AWGN table to get the predicted PER/BLER.

4) Parameter 'a' for RBIR MLD PHY Mapping for ML Receiver

In the WiMAX 2x2 system simulation, it is not easy to divide 'H' into several classes based on independent h_{ij} for the different qualities of 'H' as shown in the Symbol LLR

1 calculation for the mean and variance. Since the 'H' separated into independent h_{ij}

2 terms will result in many scenarios, it is not reasonable for practical implementation. We
3 therefore rely on the eigen value decomposition method to divide 'H' into several ranges
4 for the different qualities of 'H' as shown in Table 24 to Table 29. From simulations, it is
5 concluded that 'H' can be classified into scenarios by the following eigenvalue
6 decomposition

7
$$H^H H = V \begin{bmatrix} \lambda_{max} & \\ & \lambda_{min} \end{bmatrix} V^H \quad \text{and} \quad k = \frac{\lambda_{max}}{\lambda_{min}}$$
(51)
$$\lambda_{min} dB = 10 \log 10(\lambda_{min} / \sigma^2)$$

8 According to the simulation, the optimized parameters 'a' for a certain channel model
9 (Ped-B channel model at 3 km/hr is used.) are searched in the following Tables.
10

Parameters 'a'	$\lambda_{min} dB <= -10$	$-10 <= \lambda_{min} dB < 8$	$\lambda_{min} dB => 8$
1<=k<10	0.9000	2.8372	1.2000
10<=k<100	1.9264	0.8833	1.1000
k=>100	0.8000	0.9736	0.9000

11 **Table 24: QPSK 1/2 case for the 1st stream**
12

Parameters 'a'	$\lambda_{min} dB <= -10$	$-10 <= \lambda_{min} dB < 8$	$\lambda_{min} dB => 8$
1<=k<10	0.9000	1.4801	1.2000
10<=k<100	1.6172	0.8857	1.1000
k=>100	0.8111	2.6241	0.9000

13 **Table 25: QPSK 1/2 case for the 2nd stream**
14

Parameters 'a'	$\lambda_{min} dB <= -10$	$-10 <= \lambda_{min} dB < 8$	$\lambda_{min} dB => 8$
1<=k<10	1.0000	0.4343	0.6000
10<=k<100	1.0000	0.5000	0.5500
k=>100	0.4000	1.7303	0.4500

15 **Table 26: 16 QAM 1/2 case for the 1st stream**
16
17

Parameters 'a'	$\lambda_{min} dB <= -10$	$-10 <= \lambda_{min} dB < 8$	$\lambda_{min} dB => 8$
1<=k<10	1.0000	0.6389	0.6000
10<=k<100	1.0000	0.5000	0.5500
k=>100	0.4000	0.4667	0.4500

18 **Table 27: 16 QAM 1/2 case for the 2nd stream**
19

Parameters 'a'	$\lambda_{min} dB <= -10$	$-10 <= \lambda_{min} dB < 8$	$\lambda_{min} dB => 8$
1<=k<10	1.0000	0.7872	0.4965
10<=k<100	2.0000	0.6611	0.7310
k=>100	10.0000	1.4895	0.9000

20 **Table 28: 64 QAM 1/2 case for the 1st stream**
21

Parameters 'a'	$\lambda_{min} dB <= -10$	$-10 <= \lambda_{min} dB < 8$	$\lambda_{min} dB => 8$

1<=k<10	1.0000	1.1000	0.3111
10<=k<100	2.0000	0.6500	0.9111
k=>100	8.9000	0.6444	0.9000

Table 29: 64 QAM 1/2 case for the 2nd stream

Then RBIR can be computed from numerical integration.

5) Optimized Parameter '*a*' Searching

These parameters are optimized to minimize the difference between effective SNR and static AWGN SNR for every definite PER. The searching procedure can be described as follows:

$$SNR_{AWGN} = Static\_AWGN\_PER\_to\_SNR(PER)$$

$$SNR_{eff} = AWGN\_RBIR\_to\_SNR(RBIR(H, SNR, a)) \qquad (52)$$

$$a = \min_{a} \left| SNR_{AWGN} - SNR_{eff} \right|$$

Since there are 9 parameters, if the search is based on combined optimization, it will be too complex to achieve. The practical suboptimal searching program can be used here to get the optimal parameter '*a*'.

4.3.2.   Mean Mutual Information per Bit (MMIB) ESM

It is possible to obtain the mutual information per bit metric from the symbol channel by simply normalizing this constrained capacity (i.e. by dividing by the modulation order) as done in the RBIR method. Note, however that the symbol channel does not account for the constellation mapping, i.e. the mapping of bits to symbols in the constellation, thus it is invariable to different bit-to-symbol mappings. An alternative metric is to define the mutual information on the bit channel itself, which we will refer to as Mutual Information per coded Bit or MIB (or MMIB when a mean of multiple MIBs is involved). It is however possible that for certain constellation mappings (say Gray encoding) MMIB and RBIR functions may be similar.

More generally, given that our goal is to abstract the performance of the underlying binary code, the closest approximation to the actual decoder performance is obtained by defining an information channel at the coder-decoder level, i.e. defining the mutual information between bit input (into the QAM mapping) and LLR output (out of the LLR computing engine at the receiver), as shown in Figure 9. The concept of "bit channel" encompasses SIMO/MIMO channels and receivers. We will demonstrate that this definition will greatly simplify the PHY abstraction by moving away from an empirically adjusted model and introducing instead MIB functions of equivalent bit channels.
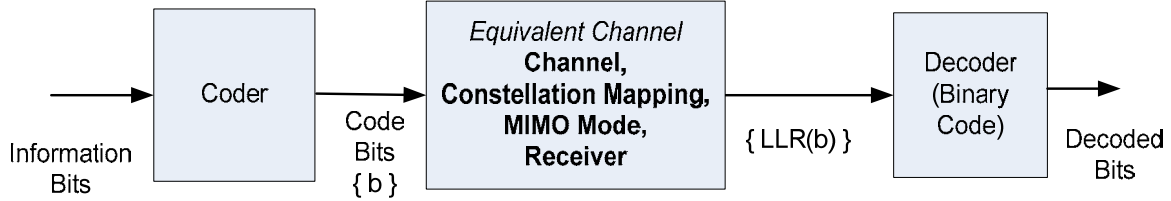
Figure 9: Bit Interleaved Coded Modulation System

In the bit channel of Figure 9, the task now is to define functions that capture the mutual information per bit. The following sections further develop an efficient approach for MIB computation by approximating the LLR PDF with a Gaussian mixture PDFs. We will begin with the development of explicit functions for MIBs in SISO and later extend it to MIMO.

The concept of deriving mutual information between coded bits and their LLR values was also well known from work in MIESM for BPSK [41]. For BPSK, however, bit-level capacity is the same as symbol-level capacity.

4.3.2.1.   MIB Mapping for SISO Systems

The mutual information of the coded bit is dependent on the actual constellation mapping. The MI of each bit-channel is obtained and averaged across the bits in a QAM symbol. After encoding (e.g. Turbo or CTC), a binary coded bit stream c_k is generated before QAM mapping. The QAM modulation can be represented as a labeling map $\mu : A \rightarrow X$, where A is the set of m-tuples, $m \in \{2,4,6\}$ to represent QPSK, 16 and 64-QAM, of binary bits and X is the constellation. Given the observation y_n corresponding to the nth QAM symbol in a codeword, the demodulator computes the log-likelihood ratio (LLR) $LLR(b_{i,n})$ of the ith bit comprising the symbol via the following expression (where the symbol index n is dropped for convenience)

$$LLR(b_i) = \ln\left(\frac{P(y \mid b_i = 1)}{P(y \mid b_i = 0)}\right) \tag{53}$$

When the coded block sizes are very large in a bit-interleaved coded modulation (BICM) system, the bit interleaver effectively breaks up the memory of the modulator, and the system can be represented as a set of parallel independent bit-channels [39]. Conceptually, the entire encoding process can be represented as shown in Figure 9.

Due to the asymmetry of the modulation map, each bit location in the modulated symbol experiences a different 'equivalent' bit-channel. In the above model, each coded bit is randomly mapped (with probability $1/m$) to one of the m bit-channels. The mutual information of the equivalent channel can be expressed as:

$$I(b, LLR) = \frac{1}{m}\sum_{i=1}^{m} I(b_i, LLR(b_i)) \tag{54}$$

where $I(b_i, LLR(b_i))$ is the mutual information between input bit and output LLR for i^{th} bit in the modulation map. As can be seen, the bit LLR reflects the demodulation process to compute LLR, which was not reflected in the symbol-level MI and the RBIR defined above. This is the main difference between the bit- and symbol-level MI definitions.

More generally, however, the mean mutual information – computed by considering the observations over N symbols (or channel uses) – over the codeword may be computed as

$$M_I = \frac{1}{mN} \sum_{n=1}^{N} \sum_{i=1}^{m} I(b_i^{(n)}, LLR(b_i^{(n)})) \tag{55}$$

The mutual information function $I(b_i^{(n)}, LLR(b_i^{(n)}))$ is, of course, a function of the QAM symbol SINR, and so the mean mutual information M_I (MMIB) may be alternatively written as

$$M_I = \frac{1}{mN} \sum_{n=1}^{N} \sum_{i=1}^{m} I_{m,b_i^{(n)}}(SINR_n) = \frac{1}{N} \sum_{n=1}^{N} I_m\left(SINR_n\right) \tag{56}$$

The mean mutual information is dependent on the SINR on each modulation symbol (index n) and the code bit index i (or i-th bit channel), and varies with the constellation order m. Accordingly, the relationship $I_{m,b_i^{(n)}}(SINR)$ is required for each modulation type and component bit index in order to construct $I_m(SINR)$.[2]

For BPSK/QPSK, a closed form expression is given in[39]-[40], which is a non-linear function that can be approximated in polynomial form. For the particular case of BPSK/QPSK, the function would be the same as that obtained by defining the mutual information of a symbol channel (symbol channel is just a bit channel for BPSK).

For BPSK, conditional LLR PDF is Gaussian and the MIB can be expressed as

$$J(x) \approx \begin{cases} a_1 x^3 + b_1 x^2 + c_1 x, & \text{if } x \leq 1.6363 \\ 1 - \exp(a_2 x^3 + b_2 x^2 + c_2 x + d_2) & \text{if } 1.6363 \leq x \leq \infty \end{cases} \tag{57}$$

where $a_1 = -0.04210661, b_1 = 0.209252$ and $c_1 = -0.00640081$ for the first approximation, and where $a_2 = -0.00181492, b_2 = -0.142675, c_2 = -0.0822054$ and $d_2 = 0.0549608$ for the second approximation.

The inverse function needed for the effective SINR computation is given by

---

[2] *Note that in the 802.16e specification, bit indexing typically proceeds from 0.*

1
$$J^{-1}(y) \approx \begin{cases} a_3 y^2 + b_3 y + c_3 \sqrt{y}, & \text{if } 0 \le y \le 0.3646 \\ a_4 \log_e \left[b_4 (y-1) \right] + c_4 y & \text{if } 0.3645 \le y \le 1 \end{cases} \tag{58}$$

2

3   where $a_3 = 1.09542$, $b_3 = 0.214217$, $c_3 = 2.33727$, $a_4 = -0.706692$, $b_4 = -0.386013$,

4    $c_4 = 1.75017$.

5

6   It can be shown that the LLR PDFs for any other modulation can be approximated as a
7   mixture of Gaussian distributions. Further they are non-overlapping at asymptotically
8   high SINR.

9

10   If the LLR distribution can be approximated by a mixture of Gaussian distributions
11   (which are nonoverlapping), then it follows that the corresponding MIB can be
12   expressed as a sum of $J(\bullet)$ functions, i.e.

13
$$I_m(x) = \sum_{k=1}^{K} a_k J(c_k x) \text{ and } \sum_{k=1}^{K} a_k = 1$$

14

15   We will use this parameterized function for expressing all non-linear MIB functions. The
16   corresponding parameters themselves would be a function of the modulation.

17

18   The optimized functions for QPSK, 16-QAM and 64-QAM are given by

19

MI Function	Numerical Approximation
$I_2(\gamma)$ (QPSK)	$M_I = J(2\sqrt{\gamma})$ (*Exact*)
$I_4(\gamma)$ (16-QAM)	$M_I = \frac{1}{2} J\left(0.8\sqrt{\gamma}\right) + \frac{1}{4} J\left(2.17\sqrt{\gamma}\right) + \frac{1}{4} J\left(0.965\sqrt{\gamma}\right)$
$I_6(\gamma)$ (64-QAM)	$M_I = \frac{1}{3} J\left(1.47\sqrt{\gamma}\right) + \frac{1}{3} J\left(0.529\sqrt{\gamma}\right) + \frac{1}{3} J\left(0.366\sqrt{\gamma}\right)$

20
21   **Table 30: Numerical approximations for MMIB mappings**
22

23   Once the MMIB is computed over a set of sub-carriers corresponding to coded symbols,
24   a direct MMIB to BLER relationship can be used to obtain block error rate, without
25   necessarily defining an effective SINR.

26

27   The BS can store the lookup tables for the AWGN reference curves for different MCS
28   levels in order to map the MMIB to BLER. Another alternative is to approximate the
29   reference curve with a parametric function. For example, we consider a Gaussian
30   cumulative model with 3 parameters which provides a close fit to the AWGN
31   performance curve, parameterized as

32
$$y = \frac{a}{2}\left[1 - erf\left(\frac{x-b}{\sqrt{2}c} \right) \right], \quad c \ne 0 \tag{59}$$

1　where a is the "transition height" of the error rate curve, b is the "transition center" and
2　c is related to the "transition width" (transition width = $1.349c$) of the Gaussian
3　cumulative distribution. In the linear BLER domain, the parameter a can be set to 1,
4　and the mapping requires only two parameters, which are given for each MCS index in
5　the table below. The accuracy of the curve fit with this model is verified with MCS
6　modes supported in 802.16e as shown in Figure 10. This parameterization of AWGN
7　reference considerably simplifies the storage and simulation requirements.
8
9　So, for each MCS the BLER is obtained as

10
$$BLER_{MCS} = \frac{1}{2}\left[1 - erf\left(\frac{x - b_{MCS}}{\sqrt{2}c_{MCS}}\right)\right], \quad c \neq 0 \tag{60}$$

11
12　Figure 10 plots MMIB versus BLER for parameters based on the 802.16e system using
13　6 different MCS's with rates 1/2 and 3/4 on an AWGN channel. It can be seen from
14　Figure 10 that, to a first-order approximation, the mapping from MMIB to BLER can be
15　assumed independent of the QAM modulation type. However, since code performance
16　is strongly dependent on code sizes and code rates, $BLER_{MCS}$ will not be independent of
17　these parameters. Further, we can achieve an additional simplification.
18
19　With the above result, we can achieve the following simplification: We generalize the
20　AWGN reference curves to be a function of the block size and coding rate (BCR) only,
21　thus

22
$$BLER_{BCR} = \frac{1}{2}\left[1 - erf\left(\frac{x - b_{BCR}}{\sqrt{2}c_{BCR}}\right)\right], \quad c \neq 0 \tag{61}$$

23　With this simplification, only two parameters need to be stored for each supported BCR.
24
25　Note: The choice of this particular MMIB to BLER mapping is due to the underlying
26　physical interpretation. The parameter b is closely related to the binary code rate and
27　will be equal to the code rate for an ideally designed code. Similarly, parameter c
28　represented the rate of fall of the curve and is also related to the block size.
29
30　Table 31 shows the parameters based on the performance in a static AWGN channel.
31

BCR Index	Code Rate	Information Word Length(bits)	Code Word Length (bits)	b_{BCR}	c_{BCR}
1	1/2	432	864	0.5512	0.0307
2	1/2	480	960	0.5512	0.0307
3	3/4	432	576	0.7863	0.03375
4	2/3	384	576	0.7082	0.0300
5	5/6	480	576	0.8565	0.02622

32　**Table 31: Parameters for Gaussian cumulative approximation**

1
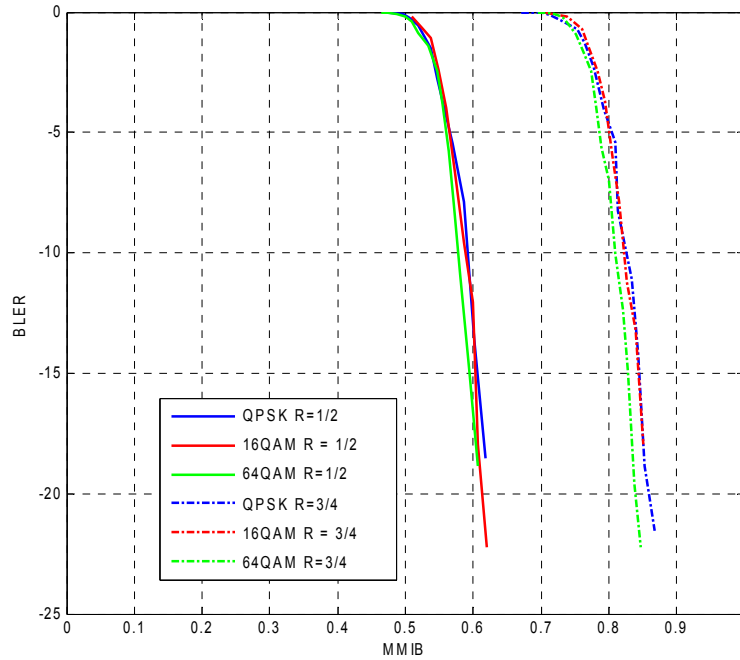
2
3   **Figure 10: BLER mappings for MMIB from AWGN performance results**
4

4.3.2.2.   MIMO Receiver Abstraction

With linear receivers like MMSE, each one of the N_T MIMO streams is treated as an equivalent SISO channel with SINRs given by post combining SINRs of the linear receiver. For vertically encoded SM, the MIB can be obtained as

$$M_I = \frac{1}{NN_T} \sum_{n=1}^{N} \sum_{k=1}^{N_T} I_m(\gamma_{nk})$$

and   (62)

$$BLER = B_{BCR}(M_I)$$

where γ_{nk} is the post combining SINR of the k-th layer on the n-th sub-carrier, N_T is the number of transmit antennas, N is the total number of coded sub-carriers, and the mapping functions $I_m(.)$ and $B_{BCR}(.)$ are defined in sections on SISO for each BCR. Note that the block size should correspond to the total codeword size of the N_T streams.

4.3.2.3.   MIMO ML Receiver Abstraction

MMIB can be evaluated for an ML receiver. In this section, we summarize the ML receiver abstraction to optimally compute MIB with the ML receiver using mixture Gaussian models for LLR PDFs.

1

2   With vertical encoding, a codeword is transmitted on both the streams. In this case, for
3   the purpose of code performance prediction, a single MIB metric is sufficient, which is
4   the average MIB of the two streams. This section describes the computation of this
5   metric for each modulation.

6

7   1) Obtain the Eigen value decomposition of the equivalent channel matrix

8
$$H^H H = VDV^H \tag{63}$$

9   such that D is in the format

10
$$D = \begin{pmatrix} \lambda_{\max} & 0 \\ 0 & \lambda_{\min} \end{pmatrix} \tag{64}$$

11 where

12
$$\begin{aligned} \lambda_{\min} &= \text{Minimum Eigen Value} \\ \lambda_{\max} &= \text{Maximum Eigen Value} \end{aligned} \tag{65}$$

13 2) From the decomposition obtain the 3$^{\text{rd}}$ parameter

14
$$p_a = \text{Eigen mode subspace power distribution} = \min\{p, 1-p\}$$
$$\text{where } |\mathbf{V}| . |\mathbf{V}| = \begin{pmatrix} p & 1-p \\ 1-p & p \end{pmatrix}, \ 0 \le p \le 1 \tag{66}$$

15 3) Obtain the following array of conditional means sorted in ascending order

16
$$\begin{aligned} \gamma = sort_{asc}\{ & \lambda_{\max} p_a + \lambda_{\min}(1-p_a), \lambda_{\min} p_a + \lambda_{\max}(1-p_a), \\ & \lambda_{\max}(1-2\sqrt{p_a(1-p_a)}) + \lambda_{\min}(1+2\sqrt{p_a(1-p_a)})\} \end{aligned} \tag{67}$$

17 4)

18 i) For QPSK, the MMIB of the MIMO symbol is

19
$$I_2^{(2\times2)}(\lambda_{\min}, \lambda_{\max}, P_a) = \frac{1}{2} J(a\sqrt{\gamma(1)}) + \frac{1}{2} J(b\sqrt{\gamma(2)}), \ a = 0.85, b = 1.19 \tag{68}$$

20 where $I_m^{(2\times2)}(.)$ is the 2x2 SM MI function for modulation level m.

21 ii) For 16QAM and 64QAM, the 2x2 SM MI mapping is modeled as

22
$$I_m^{(2\times2)}(\lambda_{\min}, \lambda_{\max}, p_a) = \frac{1}{3}\left[J\left(a_m \sqrt{\gamma(1)}\right) + J\left(b_m \sqrt{\gamma(2)}\right) + J\left(c_m \sqrt{\gamma(3)}\right) \right] \tag{69}$$

23 Where a_m, b_m and c_m are the parameters which are listed in Table 32 and Table 33 for
24 each SNR and condition number ($\kappa = \lambda_{\max}/\lambda_{\min}$) partition.

16 QAM	$1 < \kappa \le 10$	$10 < \kappa \le 100$	$\kappa > 100$
$-10dB < \lambda_{\min,dB} < 8dB$	$a = 0.48, \ b = 0.27$ $c = 0.69$	$a = 0.40, \ b = 0.21$ $c = 0.56$	$a = 0.32, \ b = 0.13$ $c = 0.37$
$\lambda_{\min,dB} > 8dB$	$a = 0.35, \ b = 0.43$ $c = 0.59$	$a = 0.37, \ b = 0.33$ $c = 100$	$a = 0.42, \ b = 0.11$ $c = 100$

Table 32: Numerical Approximation for 16QAM 2x2 SM

64 QAM	$1 < \kappa \le 10$	$10 < \kappa \le 100$	$\kappa > 100$
$-10dB < \lambda_{\min,dB} < 8dB$	$a = 0.23, \ b = 0.16$ $c = 0.59$	$a = 0.12, \ b = 0.12$ $c = 0.38$	$a = 0.08, \ b = 0.07$ $c = 0.17$
$\lambda_{\min} > 8dB$	$a = 0.20, \ b = 0.21$ $c = 0.62$	$a = 0.22, \ b = 0.13$ $c = 100$	$a = 0.24, \ b = 0.08$ $c = 100$

Table 33: Numerical Approximation for 64 QAM 2x2 SM

where $\lambda_{\min,dB} = 10\log_{10}\left(\lambda_{\min}\right)$.

The MMIB of the channel realization is given by

$$M_I^{(2\times2)} = \frac{1}{N}\sum_{i=1}^{N} I_m^{(2\times2)}\left(\lambda_{\min}\left(\mathbf{H}_i\right), \lambda_{\max}\left(\mathbf{H}_i\right), p_a\left(\mathbf{H}_i\right)\right) \tag{70}$$

where $\mathbf{H}_i$ is the $N_R \times 2$ channel matrix on the i-th sub-carrier.

The MMIB to BLER mapping is similar to that of SISO as in section 4.3.2.2. The code size should correspond to the total codeword size on the two streams.

4.3.3.   Exponential ESM (EESM)

The EESM abstraction method is given by

$$SINR_{eff} = -\beta\ln\left(\frac{1}{N}\sum_{n=1}^{N}\exp\left(-\frac{SINR_n}{\beta}\right)\right) \tag{71}$$

where β is a value for optimization/adjustment that depends on the MCS and the encoding block length. A table of these β values shall be provided once the numerology has been decided.

4.4.   Remarks on PHY Abstraction

The decision on which of the ESM PHY abstraction methods used in the final evaluation report shall be decided based on a rigorous set of comparisons using simulations and analyses.

4.5.   Per-tone SINR Computation

All PHY abstraction metrics are computed as a function of post-processing per-tone SINR values across the coded block at the input to the decoder. The post-processing

1 per-tone SINR is therefore dependent on the transmitter/receiver algorithm used to
2 modulate/demodulate the symbols.

3 ### 4.5.1.   Per-tone Post Processing SINR for SISO

4 As an illustration of how the post-processing per-tone SINR values can be computed,
5 we first consider the simple case of a single-input-single output (SISO) system with a
6 matched filter receiver.   Without loss of generality, let the target user/sector be denoted
7 by the index 0. The received signal at the *n-th* sub-carrier for the target user is
8 calculated as:

9
$$Y^{(0)}(n) = \sqrt{P_{tx}^{(0)} P_{loss}^{(0)}} H^{(0)}(n) X^{(0)}(n) + \sum_{j=1}^{N_I} \sqrt{P_{tx}^{(j)} P_{loss}^{(j)}} H^{(j)}(n) X^{(j)}(n) + U^{(0)}(n) \tag{72}$$

10 where
11 N_I is the number of interferers,
12 $P_{tx}^{(j)}$ is the total transmit power from j -*th* BS (per sector) or MS,
13 $P_{loss}^{(j)}$ is the distance dependent path loss including shadowing and antenna gain/loss and
14 cable losses from the j -*th* sector or MS, $P_{loss}^{(j)}$ (is a linear term) that is smaller or equal
15 to unity,
16 $H^{(j)}(n)$ is the channel gain for the desired MS for the *n*-th sub-carrier and j -*th*
17 user/sector,
18 $X^{(j)}(n)$ is the transmitted symbols by the j -*th* user/sector on the *n*-th sub-carrier,
19 $U^{(0)}(n)$ is the receiver thermal noise, modeled as AWGN noise with zero mean and
20 variance σ^2.
21
22 Using a matched filter receiver, given by $H^{(0)}(n)^* Y^{(0)}(n)$, the post-processing SINR
23 may be expressed as

24
$$SINR^{(0)}(n) = \frac{P_{tx}^{(0)} P_{loss}^{(0)} \left| H^{(0)}(n) \right|^2}{\sigma^2 + \sum_{j=1}^{N_I} P_{tx}^{(j)} P_{loss}^{(j)} \left| H^{(j)}(n) \right|^2} \tag{73}$$

25 ### 4.5.2.   Per-tone Post Processing SINR for SIMO with MRC

26 In order to obtain the per tone post processing SINR for the SIMO with MRC, we
27 consider a 1 transmit and N_R receive antennas system. The received signal at the *n*-th
28 sub-carrier in the *r*-th receive antenna is expressed as

29
$$Y_r^{(0)}(n) = \sqrt{P_{tx}^{(0)} P_{loss}^{(0)}} H_r^{(0)}(n) X^{(0)}(n) + \sum_{j=1}^{N_I} \sqrt{P_{tx}^{(j)} P_{loss}^{(j)}} H_r^{(j)}(n) X^{(j)}(n) + U_r^{(0)}(n) \tag{74}$$

1   After MRC process, the post-processing SINR of the desired user for the n-th sub-
2   carrier is given as

$$SINR^{(0)}(n) = \frac{P_{tx}^{(0)} P_{loss}^{(0)} \left(\sum_{r=0}^{N_R-1} \left| H_r^{(0)}(n) \right|^2 \right)^2}{\left(\sum_{r=0}^{N_R-1} \left| H_r^{(0)}(n) \right|^2 \right) \sigma^2 + \sum_{j=1}^{N_I} P_{tx}^{(j)} P_{loss}^{(j)} \left| \sum_{r=0}^{N_R-1} H_r^{(0)}(n)^* H_r^{(j)}(n) \right|^2}$$

(75)

4.5.3.   Per-tone Post Processing SINR for MIMO STBC with MRC

5   In order to obtain the per tone post processing SINR for the MIMO STBC (matrix A), we
6   consider a 2 transmit and N_R receive antennas system. The interferers are divided into
7   the set with STBC and the set with non-STBC because interference statistics are
8   different from each other. The received signal at the n-th sub-carrier in the 1st and the
9   2nd STBC symbol interval are expressed as

$$Y_r^{(0)}(n,0) = \sum_{j \in STBCset} \sqrt{\frac{P_{tx}^{(j)} P_{loss}^{(j)}}{2}} \left(H_{0,r}^{(j)}(n) X_0^{(j)}(n,0) - H_{1,r}^{(j)}(n) X_1^{(j)}(n,0)^* \right) +$$

$$\sum_{j \notin STBCset} \sum_{t=0}^{N_T^{(j)}-1} \sqrt{\frac{P_{tx}^{(j)} P_{loss}^{(j)}}{N_T^{(j)}}} H_{t,r}^{(j)}(n) X_t^{(j)}(n,0) + U_r^{(0)}(n,0),$$

(76)

$$Y_r^{(0)}(n,1) = \sum_{j \in STBCset} \sqrt{\frac{P_{tx}^{(j)} P_{loss}^{(j)}}{2}} \left(H_{0,r}^{(j)}(n) X_0^{(j)}(n,1) + H_{1,r}^{(j)}(n) X_1^{(j)}(n,1)^* \right) +$$

$$\sum_{j \notin STBCset} \sum_{t=0}^{N_T^{(j)}-1} \sqrt{\frac{P_{tx}^{(j)} P_{loss}^{(j)}}{N_T^{(j)}}} H_{t,r}^{(j)}(n) X_t^{(j)}(n,1) + U_r^{(0)}(n,1),$$

11   where

12   $STBCset$, is a set for transmit with MIMO STBC. The index 0 is for the desired user and
13   others are for interferers that transmit with MIMO STBC, and includes the interferers
14   who transmit with MIMO STBC,

15   r is the received antenna index,

16   t is the transmit antenna index,

17   $N_T^{(j)}$ is the number of transmitting antennas for the j-th interferer with non-STBC
18   transmission,

19   $Y_r^{(0)}(n,i)$ is the received signal in the i-th STBC symbol interval for the target user,
20   $i = 0,1$,

21   $X_t^{(j)}(n,i)$ is the transmitted symbol in the i-th STBC symbol interval, $i = 0,1$,

1   In the case of non-STBC, if we define transmitted symbol vector

2    $X^{(j)}(n) \triangleq [X^{(j)}(n,0)^T, X^{(j)}(n,1)^T]^T$ (where $X^{(j)}(n,i) \triangleq [X_0^{(j)}(n,i),...,X_{N_T^{(j)}-1}^{(j)}(n,i)]^T$), covariance

3   of vectors $X^{(j)}(n)$ are $\sigma_j^2 I_{2N_T^{(j)} \times 2N_T^{(j)}}$ $j \notin STBCset$

4   In the case of STBC, $X_0^{(j)}(n,0) = X_1^{(j)}(n,1)^*$, $X_1^{(j)}(n,0) = -X_0^{(j)}(n,1)^*$ and the covariance of

5   symbol vector $X^{(j)}(n,0)$ is $\sigma_j^2 I_{2 \times 2}$ $j \in STBCset$,

6    $H_{t,r}^{(j)}(n)$ is the channel gain between the *t*-th transmit and the *r*-th receive antenna, and

7   is assumed to be static for two STBC symbols,

8    $U_r^{(0)}(n,i)$ is the receiver thermal noise in the *i*-th STBC symbol interval, $i = 0,1$, and

9   modeled as AWGN noise with zero mean and variance σ^2.

10

11   The 1st and the 2nd STBC symbols are obtained through the following processes as

12

13
$$\hat{X}^{(0)}(n,0) = \sum_{r=0}^{N_R-1} \left(H_{0,r}^{(0)*}(n)Y_r^{(0)}(n,0) + H_{1,r}^{(0)}(n)Y_r^{(0)}(n,1)^* \right)$$

$$\hat{X}^{(0)}(n,1) = \sum_{r=0}^{N_R-1} \left(H_{1,r}^{(0)}(n)^* Y_r^{(0)}(n,0) - H_{0,r}^{(0)}(n)Y_r^{(0)}(n,1)^* \right)$$

(77)

14   After decoding process of STBC, the post-processing SINR of the desired user for the

15   *n*-th sub-carrier SINR is given as

16
$$SINR^{(0)}(n) = \frac{P_S}{P_N + P_{I\_NonSTBC} + P_{I\_STBC}}$$

(78)

17   where

$$P_s = P_{tx}^{(0)} P_{loss}^{(0)} \sigma_0^2 \left(\sum_{t=0}^{1} \sum_{r=0}^{N_R-1} \left| H_{t,r}^{(0)}(n) \right|^2 \right)^2 ,$$

18
$$P_N = \left(\sum_{t=0}^{1} \sum_{r=0}^{N_R-1} \left| H_{t,r}^{(0)}(n) \right|^2 \right)^2 \sigma^2 ,$$

19
$$P_{I\_NonSTBC} = \sum_{\substack{j \neq 0, \\ j \notin STBCset}} P_{tx}^{(j)} P_{loss}^{(j)} \sigma_j^2 \left(\sum_{t=0}^{N_T^{(j)}-1} \left| \sum_{r=0}^{N_R-1} H_{0,r}^{(0)}(n)^* H_{t,r}^{(j)}(n) \right|^2 + \sum_{t=0}^{N_T^{(j)}-1} \left| \sum_{r=0}^{N_R-1} H_{1,r}^{(0)}(n) H_{t,r}^{(j)}(n)^* \right|^2 \right),$$

20   and

$$P_{I\_STBC} = \sum_{\substack{j \neq 0, \\ j \in STBCset}} P_{tx}^{(j)} P_{loss}^{(j)} \sigma_j^2 \left(\frac{\left| \sum_{r=0}^{N_R-1} H_{0,r}^{(0)}(n)^* H_{0,r}^{(j)}(n) + H_{1,r}^{(0)}(n) H_{1,r}^{(j)}(n)^* \right|^2}{+ \left| \sum_{r=0}^{N_R-1} H_{1,r}^{(0)}(n) H_{0,r}^{(j)}(n)^* - H_{0,r}^{(0)}(n)^* H_{1,r}^{(j)}(n) \right|^2} \right).$$

4.5.4.   Per-Tone Post Processing SINR Calculation for Spatial Multiplexing

A linear minimum mean square error (MMSE) receiver will be used as baseline receiver for the matrix B in the system level simulation methodology.

To illustrate the per-tone post processing SINR calculation for a MIMO system based on a linear MMSE receiver, we assume an N_T transmit and N_R receive antennas. Since these calculations are illustrative, for the sake of simplicity, we assume that N_T spatial streams are transmitted and $N_R \geq N_T$. We also assume that interferers and the desired signal use the same MIMO scheme for transmission. The simplified signal model is described as follows:

$$\underline{Y}^{(0)}(n) = \sqrt{P_{tx}^{(0)} P_{loss}^{(0)}} \underline{H}^{(0)}(n) \underline{X}^{(0)}(n) + \sum_{j=1}^{N_I} \sqrt{P_{tx}^{(j)} P_{loss}^{(j)}} \underline{H}^{(j)}(n) \underline{X}^{(j)}(n) + \underline{U}^{(0)} \tag{79}$$

where

$\underline{Y}^{(0)}(n)$ is a $N_R \times 1$ dimensional received signal vector at the desired MS for the *n*-th sub-carrier,

$\underline{H}^{(j)}(n)$ is the $N_R \times N_T$ channel gain matrix between the desired user and the interfering BS for the *n*-th sub-carrier,

$\underline{X}^{(0)}(n)$ and $\underline{X}^{(j)}(n)$ are the data modulation vectors ($N_T \times 1$) of the desired MS and the *j*-th interfering MS, with covariances $\sigma_0^2 \underline{I}$ and $\sigma_j^2 \underline{I}$ $j = 1, 2, \cdots, N_I$, respectively, and

$\underline{U}^{(0)}$ is modeled as zero mean AWGN noise vector with covariance $\sigma^2 \underline{I}$, $\underline{I}$ is the $N_R \times N_R$ identity matrix.

A linear MMSE receiver is used to demodulate the transmitted signal vector, thus

$$\underline{X}^{(0)}(n) = W^*(n) \underline{Y}^{(0)}(n) \tag{80}$$

Here, the MMSE weights $W(n)$ ($N_R \times N_T$ matrix) are specified as

$$W(n) = \left(P_{tx}^{(0)} P_{loss}^{(0)} \underline{H}^{(0)}(n) \underline{H}^{(0)^*}(n) + \tilde{\sigma}^2 I \right)^{-1} \sqrt{P_{tx}^{(0)} P_{loss}^{(0)}} \underline{H}^{(0)}(n) \tag{81}$$

where (.)* is the Hermitian operator and $\tilde{\sigma}^2 = \sigma^2 I + \sum_{j=1}^{N_I} P_{tx}^{(j)} P_{loss}^{(j)} \underline{H}^{(j)}(n) \underline{H}^{(j)^*}(n)$

The post-processing SINR can be computed by defining the following two expressions:

$$D(n) = diag\left[W^*(n)\sqrt{P_{tx}^{(0)}P_{loss}^{(0)}}\,\underline{H}^{(0)}(n) \right]$$ which denotes the desired signal component

and $I_{self}(n) = W^*(n)\sqrt{P_{tx}^{(0)}P_{loss}^{(0)}}\,\underline{H}^{(0)}(n) - D(n)$ which is the self interference between MIMO streams.

The post-processing SINR of the desired MS for *n-th* sub-carrier and the *k-th* MIMO stream is thus given as:

$$SINR_k^{(0)}(n) = \frac{diag\left[\sigma_0^2 D(n)D^*(n) \right]_{kk}}{diag\left[\sigma^2 W^*(n)W(n) + \sigma_0^2 I_{self}I_{self}^* + \sum_{j=1}^{N_I} P_{tx}^{(j)}P_{loss}^{(j)}\sigma_j^2 W^*(n)\underline{H}^{(j)}(n)\underline{H}^{(j)}(n)^* W(n) \right]_{kk}} \quad (82)$$

4.5.5.   Interference Aware PHY Abstraction

Proponents should provide justification of assumptions related to knowledge of interference statistics used in system level simulations.

4.5.6.   Practical Transmitter/Receiver Impairments

The evaluation should account for practical transmitter and receiver impairments and implementation losses.

4.5.7.   Channel Estimation Errors

The per-tone post processing SINR for SIMO on the n-th subcarrier during the k-th OFDM symbol, including the effect of imperfect channel estimation and pilot weighted do-product operation is given by

$$SINR_1^{(0)}(n,k) = E_H\left[SINR^{(0)}(n,k), SINR_{Pilot}^{(0)}(n,k), SINR^{(0)}(n,k)\cdot SINR_{Pilot}^{(0)}(n,k) \right] \quad (83)$$

where $E_H[x,y] = \dfrac{1}{x^{-1}+y^{-1}}$ denotes the harmonic sum of *x* and *y*. $SINR_{Pilot}^{(0)}(n,k)$ is the SINR of channel estimation used to demodulate the n-th sub-carrier during the k-th OFDM symbol.

The SINR of channel estimate $SINR_{Pilot}^{(0)}(n)$ is computed as follows: Assuming white noise, equal power on data and pilot tones, and least-squares channel estimation, the SINR of channel estimate is given by

$$SINR_{Pilot}^{(0)}(n,k) = E_H\left[\varsigma \cdot SINR_{PA}^{(0)}(n,k)\cdot \alpha[k], \frac{1}{\beta[k]} \right] \quad (84)$$

1 where $\alpha[k]$ is the gain from averaging the channel estimate across multiple OFDM

2 symbols and $\beta[k]$ models the inter-symbol coherence loss due to Doppler. ζ is the

3 averaged number of used pilot tones per subcarrier for channel estimation in frequency

4 domain and could be changeable according to the channel estimation schemes.

5 $SINR_{PA}^{(0)}(n,k)$, the SINR before diversity combining across the receive antennas, is given

6 by

7
$$SINR_{PA}^{(0)}(n,k) = \text{Max.}\left\{SINR^{(0)}(0,n,k),\cdots,SINR^{(0)}(N_{Rx}-1,n,k)\right\} \tag{85}$$

8 where $SINR^{(0)}(i,n,k)$ is the SINR on the *i*-th receive antenna and *n*-th subcarrier during

9 the *k*-th OFDM symbol, and N_{Rx} is the number of receive antennas. $\text{Max.}\{x,y,z\}$

10 denotes the maximum value among *x*, *y* and *z*.

11

12 Suppose the channel estimate used to demodulate the data symbols in the k-th OFDM
13 symbol is obtained by combining/averaging pilot tones from adjacent OFDM symbols.
14 Prior to inter-symbol averaging, the pilot tones are assumed to be normalized by the
15 relative pilot gains on the adjacent OFDM symbols. If the channel estimate averaging
16 weights are $\left[c_{0,k},c_{1,k},\cdots,c_{J-1,k}\right]$, and the relative pilot gains are $\left[\gamma_{0,k},\gamma_{1,k},\cdots,\gamma_{J-1,k}\right]$ the

17 averaging gain $\alpha[k]$ and the inter-symbol coherence loss $\beta[k]$ are given by

18
$$\alpha[n] = \frac{\left|\displaystyle\sum_{j=0}^{J-1}\frac{c_{j,k}}{\sqrt{\gamma_{j,k}}}\right|^2}{\displaystyle\sum_{j=0}^{J-1}\frac{\left|c_{j,k}\right|^2}{\gamma_{j,k}}}, \qquad \beta[n] = \left|1-\sum_{j=0}^{J-1}c_{j,k}\exp\left(2\pi f_d\tau_{j,k}\right)\right|^2 \tag{86}$$

19

20 where $\tau_{j,k}$ is the time offset between the OFDM symbol associated with the averaging

21 weight $c_{j,k}$, and the k-th OFDM symbol containing the data sub-carrier to be

22 demodulated. f_d is the Doppler frequency.

23 ### 4.5.8.   Interference Aware Modeling
24 In the previous sections we assumed that the receiver has knowledge of interference
25 power per sub-carrier when computing the post-processing SINR. In practice, the per-
26 sub-carrier interference power is unknown at the decoder. Therefore, the per-sub-carrier
27 SINR is modified by averaging the interference power across the set of sub-carriers
28 used.
29
30
31
32
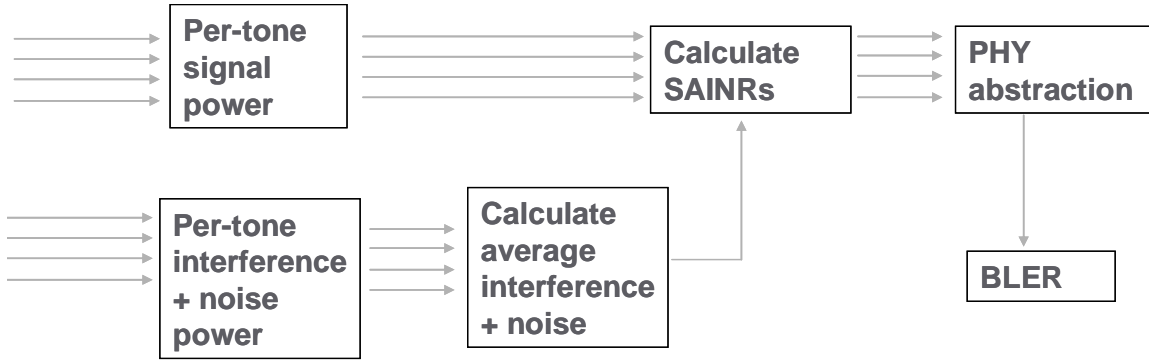
Figure 11: PHY abstraction simulation procedure for average interference knowledge.

As seen from Figure 11, the interference plus noise in the post processing SINR equation are averaged over all the occupied sub-carriers. Thus, the per-tone signal-to-average interference plus noise (SAINR) is calculated and used as input to the PHY abstraction. This method of accounting for the effect of practical interference knowledge applies to all transmitter/receiver configurations.

4.5.9. Error Vector Magnitude

The model of the received signal in Equation (72) ignored the non-idealities of the transmitted waveform. Appendix K includes a discussion on the typical effects of peak-to-average power reduction (PAPR) methods and their impact on the transmitted waveform quality, captured in terms of a quantity termed error vector magnitude (EVM). Thus, in the case of evaluating PAPR reduction methods, the EVM component should be included in the per-tone SINR computation. The transmitted waveform is thus composed of the desired signal plus an error signal whose power is proportional to the transmitted signal power. Thus, an EVM term should be added by including an additional interferer using the same channel matrix as the target user and transmit power lower by EVM than the user's transmit power, i.e. $10^{-EVM/10} P_{tx}^{(0)}$.

Taking into account the effect of EVM, the per-tone SINR for the SISIO case as an example becomes

$$SINR^0\left(n\right)=\frac{P_{tx}^{(0)}P_{loss}^{(0)}\left|H^{(0)}\left(n\right)\right|^2}{\sigma^2+\sum_{j=1}^{N_i}P_{tx}^{(j)}P_{loss}^{(j)}\left|H^{(j)}\left(n\right)\right|^2+10^{-EVM/10}\cdot P_{tx}^{(0)}P_{loss}^{(0)}\left|H^{(0)}\left(n\right)\right|^2} \tag{87}$$

where EVM value is defined in Table 3.

4.6. Deriving Packet Error Rate from Block Error Rate

A packet comprises several FEC blocks. The packet error rate (PER) is the probability that an error occurs in at least one of FEC blocks comprising the packet. The PHY

abstraction predicts the link performance, in terms of BLER, for a coded FEC block. Here we need to extrapolate the PER given the predicted BLER. If a packet is comprised of J blocks and the predicted BLERs are given by $BLER_1$, $BLER_2$, …, $BLER_J$, then the PER is derived as

$$PER = 1 - \prod_{j=1}^{J} \left(1 - BLER_j\right) \tag{88}$$

4.7.   PHY Abstraction for H-ARQ

PHY abstraction of H-ARQ depends on the H-ARQ method. Similar to the non-HARQ PHY abstraction, proponents should provide the additional parameters required for the H-ARQ coding and retransmission schemes. This section summarizes the methods that are generally applicable to all PHY abstraction approaches with H-ARQ. Specifically, the approaches are similar for all bit-based mutual information-based abstraction techniques (MMIB, RBIR). For convenience, we will just refer to these metrics as MI in this section.

4.7.1.   Baseline Modeling

The following abstraction is proposed as baseline:

- For Chase combining (CC): The SINR values of the corresponding sub-carriers are summed across retransmissions, and these combined SINR values will be fed into the PHY abstraction.
- For Incremental redundancy (IR): The transmission and retransmissions are regarded as a single codeword, and all the SINR values are fed into the PHY abstraction. In practice, some partial repetition occurs, when part of the coded information is repeated in subsequent retransmissions.

For methods combining CC and IR the second approach is preferred but should be justified by link level simulations.

4.7.2.   Chase Combining

The post-processing SINR in this case can be obtained as the sum of the SINRs from the first transmission and subsequent retransmissions, and thus the post-combining mutual information metric is given by

$$M_I = \frac{1}{N} \sum_{n=1}^{N} I_m \left(\sum_{j=1}^{q} \gamma_{nj} \right) \tag{89}$$

where q is the number of transmissions, $I_m(.)$ is the MI function for modulation order 'm' and γ_{nj} is the n-th symbol SINR during j-th retransmission. The mutual information metric can then be input to the AWGN reference characterized by the 'b' and 'c' parameters (as used in section 4.3.2).

Similarly, the effective SINR for EESM in the case of Chase combining is given by

$$\gamma_{eff} = -\beta \ln\left(\frac{1}{N} \sum_{n=1}^{N} \exp\left(-\frac{\sum_{j=1}^{q} \gamma_{nj}}{\beta} \right) \right) \tag{90}$$

where γ_{eff} is the effective SINR after q transmissions that is input to the AWGN reference to compute the BLER.

4.7.3. Incremental Redundancy (IR)

With no repetition of coded bits, the performance of the decoder at each stage is that corresponding to a binary code with the modified equivalent code rate and code size as illustrated in Figure 12 for MI based approaches.

X Information Bits
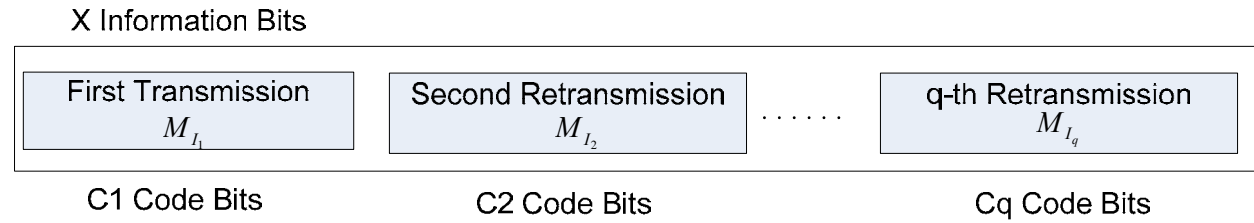
Figure 12: MI-based parameter update after transmission

The required input parameters for AWGN mapping function are given below

$$R_{eff} = \frac{X}{\sum_{i=1}^{q} C_i}$$

$$L_{eff} = \sum_{i=1}^{q} C_i \tag{91}$$

$$M_{I_{IR,q}} = \frac{\sum_{i=1}^{q} C_i M_{I_i}}{\sum_{i=1}^{q} C_i}$$

where R_{eff}, L_{eff} and $M_{I_{IR,q}}$ are the effective code rate, block size and mutual information after q retransmissions, respectively.

In practice, due to finite granularity in IR implementation, partial repetition of coded bits is possible. Depending on the rate matching algorithm used, every H-ARQ transmission could have a set of new parity bits and other bits that are repeated. Accumulating the mutual information is appropriate as long as new parity bits are transmitted in every symbol. Otherwise, the receiver combines the demodulation symbols or, more typically, the LLRs. In this section, we consider a rate-matching approach that does pure IR transmissions and involves coded bit repetitions once all the coded bits from a base code rate are exhausted.

1   To handle this general case, we consider a retransmission including a set of N_{NR} new
2   coded bits and a set of N_R coded bits repeated from pervious transmissions. Further,
3   we assume that there are N_{pre} coded bits that are not re-transmitted in this re-
4   transmission. The averaged mutual information per bit from previous transmissions is
5   $M_{I_{old}}$. The averaged mutual information per bit in this re-transmissions is $\overline{I}_b$.

6
7   We can then compute an updated mutual information metric after this retransmission as
8   follows

9
$$M_{I_{new}} = \frac{N_{pre} \cdot M_{I_{old}} + N_{NR} \cdot \overline{I}_b + N_R \cdot f_1\left(f_1^{-1}\left(M_{I_{old}}\right) + f_1^{-1}\left(\overline{I}_b\right)\right)}{N_{pre} + N_{NR} + N_R} \tag{92}$$

10
11   where $f_1(\cdot)$ is a mapping from bit SINR to MI. If the modulation is constant across
12   retransmissions, $f_1(.)$ should be the MI function corresponding to that modulation.
13   Otherwise, it is recommended to use the MI function corresponding QPSK. When the
14   number of retransmissions is greater than one, Equation (92) is used recursively.
15

16   The BLER can be obtained by looking up the AWGN MI to BLER relationship
17   corresponding to the modified effective code rate and code size, which are given by

18
$$R_{eff} = \frac{X}{N_{Pre} + N_{NR} + N_R}$$
$$L_{eff} = N_{Pre} + N_{NR} + N_R \tag{93}$$

19   A code rate-code size parameterized relationship for *b* and *c* parameters in the AWGN
20   reference (see Section 4.3.2), is recommended to cover the new and many possible
21   BCR combinations with IR. Such a relationship can be obtained by expressing the *b* and
22   *c* parameters as simple 2-dimensional parameterized functions of block size and code
23   rate as follows, which could further reduce storage requirements and streamline
24   simulation methodology,

25
$$b = f(R, L) = R + f'(R, L)$$
$$c = g(R, L) \tag{94}$$

26
27   where *R* is the code rate (e.g.1/2) and *L* is the block size (e.g. 500 bits).
28
29   For EESM, if the modulation does not change in retransmission, the effective SINR for
30   *k*-th transmission can be calculated as follows:

$$SINR_{eff}^1 = -\beta \ln\left(\frac{1}{|U_1|}\sum_{n\in U_1}\exp\left(-\frac{SINR_{n,1}}{\beta}\right)\right)$$

and   (95)

$$SINR_{eff}^k = -\beta \ln\left(\frac{1}{|U_k|}\left(\sum_{n\in U_{k-1}}\exp\left(-\frac{1}{\beta}\left(SINR_{eff}^{k-1}+I_{n,k}SINR_{n,k}\right)\right) + \sum_{n\in V_k, n\notin U_{k-1}}\exp\left(-\frac{SINR_{n,k}}{\beta}\right)\right)\right)$$

where $SINR_{eff}^k$ is k-th transmission's effective SINR, $SINR_{n,k}$ is k-th transmission's post processed SINR for bit index n, V_k is the set of indices where a coded bit was transmitted on k-th transmission, $I_{i,k}$ is an indicator function for codeword bit index i for the set V_k, ($I_{i,k}$ = 0 for $i\notin V_k$., and $I_{i,k}$ = 1 for $i\in V_k$), and U_k is the unique bit indices transmitted up to transmission k, $U_k = \bigcup_{j=1}^{k} V_j$. The choice of β's is TBD.

4.8.   PHY Abstraction for Repetition Coding

The SINR values of the sub-carriers are summed across repetition number, and these combined SINR values will be fed into the PHY abstraction.

5. Link Adaptation

Link adaptation can enhance system performance by optimizing resource allocation in varying channel conditions. System level simulations should include adaptation of the modulation and coding schemes, according to link conditions.

The purpose of this section is to provide guidelines for link adaptation in system evaluations. The use of link adaptation is left to the proponent as it may not pertain to all system configurations. The link adaptation algorithms implemented in system level simulations are left to Individual proponents for each proposal. Proponents should specify link adaptation algorithms including power, MIMO rank, and MCS adaptation per resource block.

5.1.   Adaptive Modulation and Coding

The evaluation methodology assumes that adaptive modulation and coding with various modulation schemes and channel coding rates is applied to packet data transmissions. In the case of MIMO, different modulation schemes and coding rates may be applied to different streams.

5.1.1.   Link Adaptation with HARQ

The link adaptation algorithm should be optimized to maximize the performance at the end of the HARQ process (e.g. maximize the average throughput under constraint on the delay and PER, or maximize number of users per service).

5.2.   Channel Quality Feedback

A Channel Quality Indicator (CQI) channel is utilized to provide channel-state information from the user terminals to the base station scheduler. Relevant channel-state information can be fed back. For example, Physical CINR, effective CINR, MIMO mode selection and frequency selective sub-channel selection may be included in CQI feedback. Some implementations may use other methods, such as channel sounding, to provide accurate channel measurements. CQI feedback granularity and its impact may also be considered. Proponents should describe the CQI feedback type and assumptions of how the information is obtained.

5.2.1.   Channel Quality Feedback Delay and Availability

Channel quality feedback delay accounts for the latency associated with the measurement of channel at the receiver, the decoding of the feedback channel, and the lead-time between the scheduling decision and actual transmission. The delay in reception of the channel quality feedback shall be modeled to accurately predict system performance.

Channel quality feedback may not be available every frame due to system constraints such as limited feedback overhead or intermittent bursts. The availability of the channel quality feedback shall be modeled in the system simulations.

The proponents should indicate the assumptions of channel quality feedback delay and availability for system proposals.

5.2.2.   Channel Quality Feedback Error

System simulation performance should include channel quality feedback error by modeling appropriate consequences, such as misinterpretation of feedback or erasure.

The proposals shall describe if CQI estimation errors are taken into account and how those errors are modeled.

6. HARQ

The Hybrid ARQ (HARQ) protocol should be implemented in system simulations. Multiple parallel HARQ streams may be present in each frame, and each stream may be associated with a different packet transmission, where a HARQ stream is an encoder packet transaction pending, i.e., a HARQ packet has been transmitted but has not been acknowledged. Different MIMO configurations may also have an impact on the HARQ implementation.

Each HARQ transmission results in one of the following outcomes: successful decoding of the packet, unsuccessful decoding of the packet transmission requiring further re-transmission, or unsuccessful decoding of the packet transmission after maximum number of re-transmissions resulting in packet error. The effective SINR for packet transmissions after one or more HARQ transmissions used in system simulations is determined according to the PHY abstraction in Section 4.7.

1   When HARQ is enabled, retransmissions are modeled based on the HARQ option
2   chosen. For example, HARQ can be configured as synchronous/asynchronous with
3   adaptive/non-adaptive modulation and coding schemes for Chase combining or
4   incremental redundancy operation. Synchronous HARQ may include synchronous
5   HARQ acknowledgement and/or synchronous HARQ retransmissions. Synchronous
6   HARQ acknowledgement means that the HARQ transmitter side expects the HARQ
7   acknowledgments at a known delay after the HARQ transmission. Synchronous HARQ
8   retransmission means that the HARQ receiver side expects the HARQ retransmissions
9   at known times. In the case of asynchronous HARQ, the acknowledgement and/or
10 retransmission may not occur at known times. Adaptive H-ARQ, in which the
11 parameters of the retransmission (e.g. power, MCS) are changed according to channel
12 conditions reported by the MS may be considered. In the case of non-adaptive HARQ,
13 the parameters of the retransmission are not changed according to channel conditions.
14
15 The HARQ model and type shall be specified with chosen parameters, such as
16 maximum number of retransmissions, minimum retransmission delay, incremental
17 redundancy, chase combining, etc. HARQ overhead (associated control) should be
18 accounted for in the system simulations on both the uplink and downlink

19 ## 6.1.   HARQ Acknowledgement
20 The HARQ acknowledgment is used to indicate whether or not a packet transmission
21 was successfully received.
22
23 Modeling of HARQ requires waiting for HARQ acknowledgment after each transmission,
24 prior to proceeding to the next HARQ transmission. The HARQ acknowledgment delay
25 should include the processing time which includes, decoding of the traffic packet, CRC
26 check, and preparation of acknowledgment transmissions. The amount of delay is
27 determined by the system proposal.
28
29 Misinterpretation, missed detection, or false detection of the HARQ acknowledgment
30 message results in transmission (frame or encoder packet) error or duplicate
31 transmission. Proponents of each system proposal shall justify the system performance
32 in the presence of error of the HARQ acknowledgment.

33 ## 7. Scheduling
34
35 The scheduler allocates system resources for different packet transmissions according
36 to a set of scheduling metrics, which can be different for different traffic types. The same
37 scheduling algorithm shall be used for all simulation runs. Various scheduling
38 approaches will have different performance and overhead impacts and will need to be
39 aligned. System performance evaluation and comparison require that fairness be
40 preserved or at least known in order to promote comparisons. The owner(s) of any
41 proposal is also to specify the scheduling algorithm, along with assumptions on
42 feedback. The scheduling will be done with consideration of the reported metric where
43 the reported metric may include CQI and other information. The scheduler shall

calculate the available resources after accounting for all control channel overhead and protocol overhead.

7.1. DL scheduler

For the baseline simulation, a generic proportionally fair scheduler shall be used for the full-buffer traffic model. The generic proportionally fair scheduler is defined in Appendix F.

In the general deployment case, the MAC scheduler should be capable of handling a traffic mix of different QoS service classes that are enabled by the air interface. The proponent may present additional results with a more sophisticated scheduler other than proportionally fair scheduler and shall specify the scheduler algorithm in detail.

7.2. UL scheduler

The UL scheduler is very similar to DL Scheduler. The UL scheduler maintains the request-grant status of various uplink service flows. Bandwidth requests arriving from various uplink service flows at the BS will be granted in a similar fashion as the downlink traffic.

8. Handover

The system simulation defined elsewhere in the document deals with throughput, spectral efficiency, and latency. User experience in a mobile broadband wireless system is also influenced by the performance of handover. This section focuses on the methods to study the performance of handover which affects the end-users experience. Proponents of system proposals specifically relating to handover should provide performance evaluations according to this section.

For parameters such as cell size, DL&UL transmit powers, number of users in a cell, traffic models, and channel models; the simulation follows the simulation methodology defined elsewhere in the document. In this document, only intra-radio access technology handover is considered; inter-radio access technology handover is not considered.

The handover procedure consists of cell reselection via scanning, handover decision and initiation, and network entry including synchronization and ranging with a target BS.

Latency is a key metric to evaluate and compare various handover schemes as it has direct impact on application performance perceived by a user. Total handover latency is decomposed into several latency elements. Further, data loss rate and unsuccessful handover rate are important metrics.

8.1. System Simulation with Mobility

Two possible simulation models for mobility related performance are given in this section. The first is a reduced complexity model that considers a single MS moving along one of three trajectories with all other users at fixed locations, and a second

simulation model that considers all mobiles in the system moving along random trajectories.

8.1.1. Single Moving MS Model

For simplicity, one moving MS and multiple fixed MSs can be modeled as a baseline for the mobility simulations. The mobility related performance metrics shall be computed only for this moving terminal. The mobility mix for MSs is specified in the test scenarios of Section 2.3. The speed of the single moving MS is selected from the speed(s) specified in the mobility mix of the test scenario.

The trajectory of the moving MS can be chosen from the trajectories given in following section.

8.1.1.1. Trajectories

The movement of the single moving MS is constrained to one of the trajectories defined in this section. More detailed and realistic mobility models may be considered.

8.1.1.1.1. Trajectory 1

In this trajectory, the MS moves from Cell 1 to Cell 2 along the arrow shown in Figure 13. The trajectory starts from the center of Cell 1 to the center of Cell 2 while passing through the midpoint of the sector boundaries as shown in Figure 13. The purpose of this trajectory is to evaluate handover performance in a scenario where the signal strength from the serving sector continuously decreases whereas the signal strength from the target sector continuously increases.
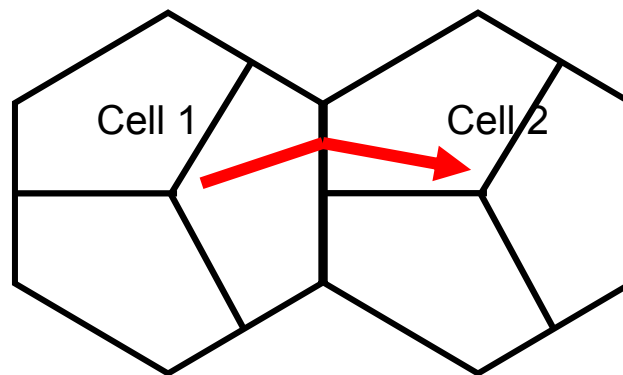
Figure 13: Trajectory 1

8.1.1.1.2. Trajectory 2

In this trajectory, the single moving MS moves from Cell 1 to Cell 2 along the arrow shown in Figure 14. The MS moves along the sector boundary between Cell 1 and Cell 2 until the midpoint of the cell boundary between Cell 1 and Cell 2. The purpose of this trajectory is to evaluate handover performance when the MS moves along the boundary of two adjacent sectors.
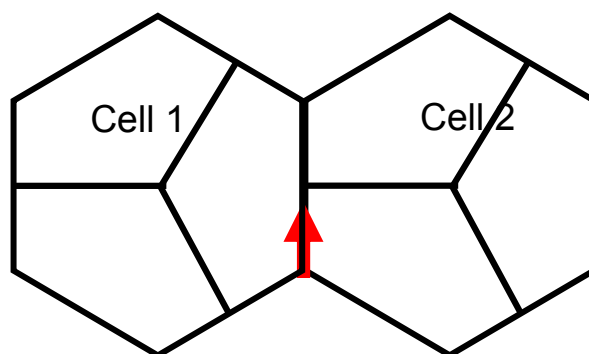
Figure 14: Trajectory 2

8.1.1.1.3. Trajectory 3

In this trajectory, the single moving MS moves from Cell 2 to Cell 1 along the arrow shown in Figure 15. The MS starts from the center of Cell 2, moves along the boundary of two adjacent sectors of Cell 2 and towards the center of the Cell 1. The purpose of this trajectory is to evaluate a handover performance in the scenario where the MS traverses multiple sector boundaries.
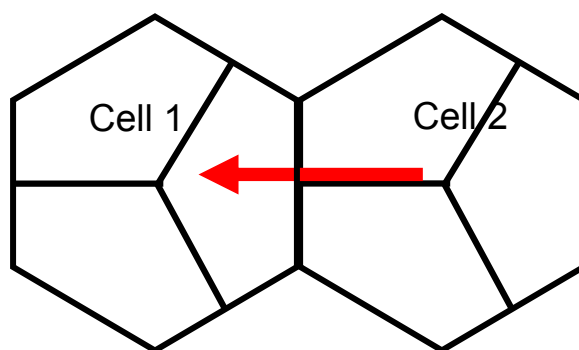
Figure 15: Trajectory 3

8.1.1.2. 10 Cell Topology

As a reduced complexity option, a 10 cell topology may be used for handover evaluation with a single moving MS. In the 10 cell topology, both serving and target cells should have one tier of neighboring cells as interferers shown in Figure 16.
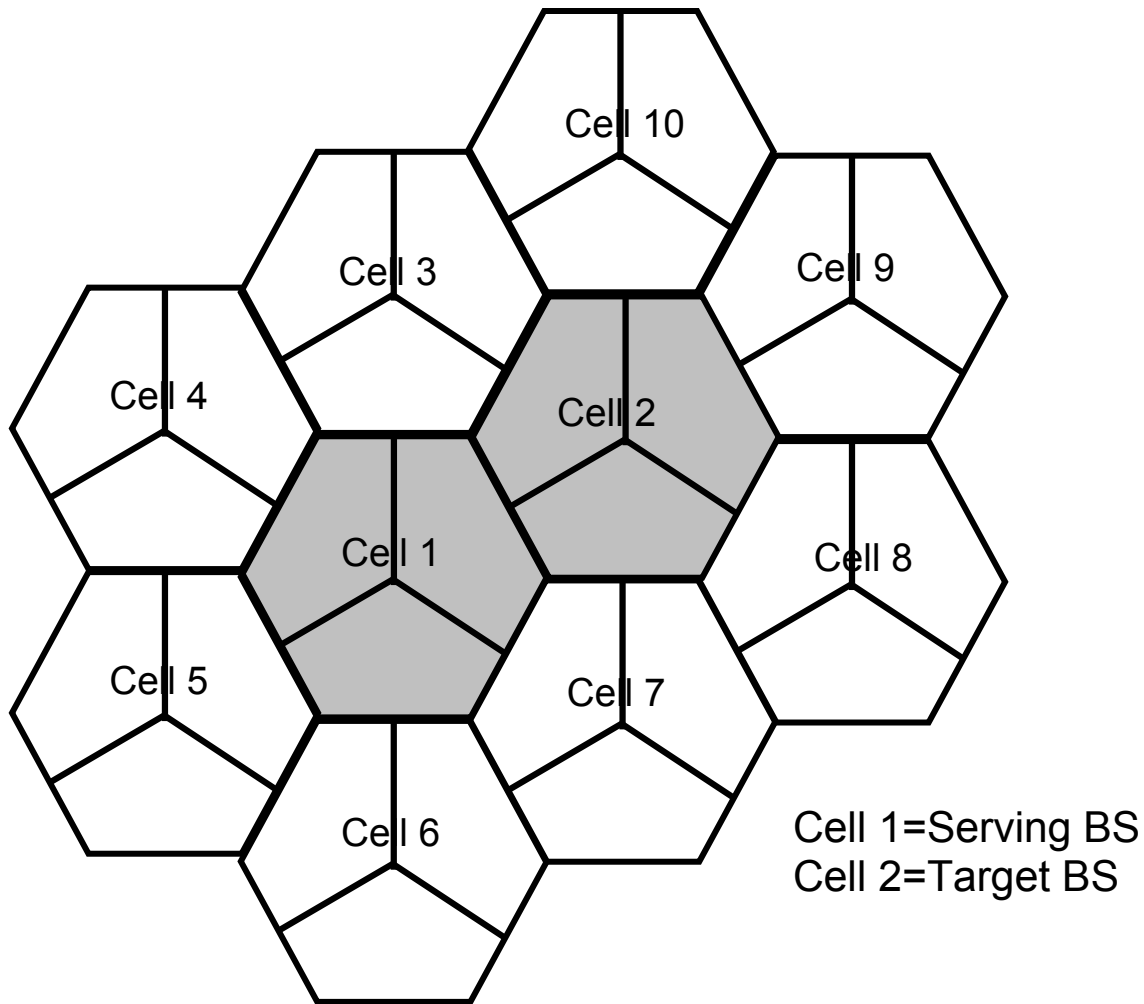
Figure 16: 10 Cell Topology

8.1.1.3.   Handover Evaluation Procedure

1. The system may be modeled using the 10 cell topology as illustrated in Figure 16 for the evaluation of handover performance. Each cell has three sectors and frequency reuse is modeled by planning frequency allocations in different sectors in the network.

2. N MSs are dropped independently with uniform distribution across the cell area. Different load levels in the network are simulated by changing the number of MSs and the traffic generated.

3. Path loss, shadow fading and fast fading models for each MS should be consistent with the models defined in Section 3. Fading signal and fading interference are computed from each mobile station into each sector and from each sector to each mobile for each simulation interval.

4. In the single MS model, the trajectories defined in Section 8.1.1.1 should be used to model the movement of a single MS associated with the center cell. The locations of all other MSs are assumed to be fixed and the serving sector for the fixed MSs does not change for the duration of the drop.

5. Path loss, shadow fading and fast fading are updated based on location and velocity of a moving MS. As the MS moves along the specified trajectory, the target sector is chosen according to the metric used to perform handover.

6. Traffic generated by the MSs should be according to the mixes specified in Table 44 in Section 10.7. The moving MS may be assigned one of the traffic types in the chosen traffic mix to analyze the effect of handover on the performance of the assigned traffic application. Traffic from the fixed MSs constitutes background load. Start times for each traffic type for each user should be randomized as specified in the traffic model being simulated.

7. Statistics related to handover metrics are collected for the moving MS only.

8. Packets are not blocked when they arrive into the system (i.e. queue depths are infinite). Packets are scheduled with a packet scheduler using the required fairness metric. Channel quality feedback delay, PDU errors are modeled and packets are retransmitted as necessary. The HARQ process is modeled by explicitly rescheduling a packet as part of the current packet call after a specified HARQ feedback delay period.

9. Sequences of simulation are run, each with a different random seed. For a given drop the simulation is run for this duration, and then the process is repeated with the MSs dropped at new random locations. A sufficient number of drops are simulated to ensure convergence in the system performance metrics.

8.1.2. Multiple Moving MS Model

In this model, multiple moving MSs are uniformly placed over the simulation environment and given a random trajectory and speed. The parameters selected remain in effect until a drop is completed.

8.1.2.1. Trajectories

Each MS is assigned an angle of trajectory at the beginning of a call. The assigned angle is picked from a uniform distribution across the range of 0-359 degrees in one degree increments. The angle of zero degrees points directly North in the simulation environment. Movement of the MS is established by selecting a random speed for the users according to profiles in Section 2.3 such that the population of MS users meets the desired percentages. The MS remains at the selected random speed and direction for the duration of the simulation drop. When a MS crosses a wrap around boundary point within the simulation space, the MS will wrap around to the associated segment

1   identified within Appendix G, continuing to keep the same speed and trajectory. Figure
2   17 depicts an example of the movement process for a 19-cell system.
3
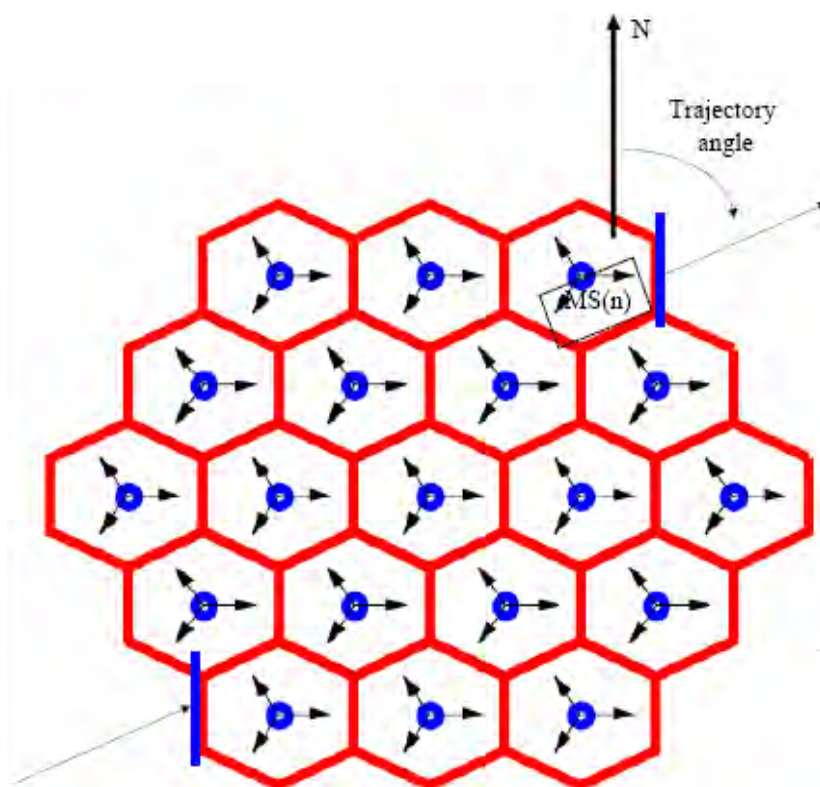
4
5
6   **Figure 17: 19 cell abbreviated example of MS movement in a wrap around topology ***
7
8   * Blue lines denote paired wrap around boundary segments

9   **8.1.2.2.   19 Cell Topology**
10   The 19 cell topology with wrap around can be used for handover evaluation with
11   multiple moving MSs. The details of this topology can be found in Appendix G.

12   **8.1.2.3.   Handover Evaluation Procedure**
13   For the 19 cell topology with wrap around defined for the multiple moving MS model, the
14   simulation procedure outlined in Section 11 should be followed. In step 7 of this
15   procedure, for the purposes of simulating handover performance, it may additionally be
16   assumed that an MS is initially connected to a specific serving sector. As the MS moves
17   along the trajectory described in Section 8.1.2.1, the target sector is chosen according
18   to the metric used to perform handover.

19   **8.2.   Handover Performance Metrics**
20   The following parameters should be collected in order to evaluate the performance of
21   different handover schemes. These statistics defined in this section should be collected

in relation to the occurrence of handovers. A CDF of each metric may be generated to evaluate a probability that the corresponding metric exceeds a certain value.

For a simulation run, we assume:

- The total number of successful handovers occurred during the simulation time = $N_{HO\_success}$
- The total number of failed handover during the simulation time = N_{HO_fail}
- The total number of handover attempts during the simulation time = $N_{attempt}$, where $N_{attempt} = N_{HO\_success} + N_{HO\_fail}$

8.2.1.   Radio Layer Latency

This value measures the delay between the time instance $T_{1,i}$ that an MS transmits a serving BS its commitment to HO (for a hard handover (HHO), this is the time that the MS disconnects from the serving BS) and the time instance $T_{2,i}$ that the MS successfully achieves PHY layer synchronization at the target BS (i.e., frequency and DL timing synchronization) due to handover occurrence i. The exact thresholds for successful PHY synchronization are for further study. For this metric, the average radio latency will be measured as

$$\text{Average Radio Layer Latency} = \frac{\sum_{i=1}^{N_{HO\_success}} (T_{2,i} - T_{1,i})}{N_{HO\_success}} \tag{96}$$

8.2.2.   Network Entry and Connection Setup Time

This value represents the delay between an MS's radio layer synchronization at $T_{2,i}$, and the start of transmission of first data packet from the target BS at $T_{3,i}$ due to handover occurrence i. In the case of the reference system, this consists of ranging, UL resource request processes (contention or non-contention based), negotiation of capabilities, registration, DL packet coordination and a path switching time. The transmission error rate of MAC messages associated with network entry can be modeled dynamically or with a fixed value (e.g., 1%). A path switching time, as a simulation input parameter, may vary depending on network architecture.

$$\text{Average Network Entry and Connection Setup Time} = \frac{\sum_{i=1}^{N_{HO\_success}} (T_{3,i} - T_{2,i})}{N_{HO\_success}} \tag{97}$$

8.2.3.   Service Disruption Time

This value represents time duration that a user can not receive any service from any BS. It is defined as the sum of Radio Layer Latency, Network Entry Time and Connection Setup Time due to handover occurrence i.

8.2.4.   Data Loss

This value represents the number of lost bits during the handover processes. This document uses DL data loss to evaluate the data loss performance of the air link. $D_{RX,i}$

and $D_{TX,i}$ denotes the number of received bits by the MS and the number of total bits transmitted by the serving and the target BSs during the MS performs handover occurrence *i*, respectively. Traffic profiles used for the simulation experiments to compare different handover schemes need to be identical.

$$\text{Data Loss} = \frac{\sum_{i=1}^{N_{HO\_success}} (D_{TX,i} - D_{RX,i})}{N_{HO\_success}} \qquad (98)$$

8.2.5.   Handover Failure Rate

This value represents the ratio of failed handover to total handover attempts. Handover failure occurs if handover is executed while the reception conditions are inadequate on either the DL or the UL such that the mobile would have to go to a network entry state.

$$\text{Handover Failure Rate} = \frac{N_{HO\_fail}}{N_{attempt}} \qquad (99)$$

9. Power Management (informative)

The implementation of an idle state is proposed to be used in the IEEE 802.16m broadband wireless system to conserve battery power of mobile devices when a call session is not active. A mobile device returns to active state whenever required, e.g., when there is incoming data for the said device. IDLE to ACTIVE_STATE transition latency is a key metric to evaluate and compare various proposals related to IDLE to ACTIVE_STATE transition schemes as this latency has direct impact on application performance experienced by a user.

The IDLE to ACTIVE_STATE transition latency requirement is specified in the IEEE 802.16m Requirements document. According to this document, the IDLE to ACTIVE_STATE transition latency is defined as the time it takes for a device to go from an idle state (fully authenticated/registered and monitoring the control channel) to when it begins exchanging data with the network on a traffic channel.

IDLE to ACTIVE_STATE transition latency has several components as formulated in Section 9.1. Section 9.2 provides a simulation procedure to evaluate IDLE to ACTIVE_STATE transition latency. Proponents of system proposals specifically relating to IDLE to ACTIVE_STATE transition should evaluate performance according to this section.

9.1.   Formulation for IDLE to ACTIVE_STATE transition latency

The IDLE to ACTIVE_STATE transition may be initiated either by the device or by the network. The first case is referred to as device-initiated IDLE to ACTIVE_STATE transition and the second case is referred to as network-initiated IDLE to ACTIVE_STATE transition. The components of the IDLE to ACTIVE_STATE transition latency are described in the following sub-sections.

9.1.1. Device-initiated IDLE to ACTIVE_STATE transition

The steps involved during device-initiated IDLE to ACTIVE_STATE transition are as follows:

1. Ranging
2. Network re-entry

During the ranging process the device adjusts its transmission parameters. During the network re-entry [61] service flows, CIDs, and other connection related states are established for the said device. The successful completion of the network re-entry process can be indicated by using appropriate network re-entry success message or other signaling mechanisms.

9.1.2. Network-initiated IDLE to ACTIVE_STATE transition

The steps involved during network-initiated IDLE to ACTIVE_STATE transition are as follows:

1. Transmission of paging indication
2. Ranging
3. Network re-entry

During the transmission of the paging indication, the BSs in the paging area of the said idle mode device transmit a paging indication message containing the identification information of the said idle mode device. This step is completed when the said idle mode device successfully receives the paging indication. The measurement of IDLE to ACTIVE_STATE transition latency starts from the time when the said device receives paging indication through a paging message (i.e., not including the paging period). The ranging and network re-entry procedures are as defined in Section 9.1.1.

The IDLE to ACTIVE_STATE transition, the latency, τ_d, is given by

9.1.3. IDLE to ACTIVE_STATE transition latency

$$\tau_d = T_r + T_e \tag{100}$$

where T_r and T_e are the times required to execute ranging and network re-entry, respectively.

9.2. Procedure for Evaluation of IDLE to ACTIVE_STATE transition latency

1. An idle mode device that is synchronized to the downlink channel, fully registered and authenticated with the network is considered as the candidate device to receive the paging indication using a paging message. In addition, it is considered that the said candidate device in idle mode is residing in the same paging group (PG) and IP subnet after entering into idle operation. This eliminates the need for evaluating the effect of backbone messages on the IDLE to ACTIVE_STATE transition latency.

   The IDLE to ACTIVE_STATE transition latency shall be evaluated for device-initiated IDLE to ACTIVE_STATE transition as well as network-initiated IDLE to ACTIVE_STATE transition.

2. The system is modeled using the cell topology as defined in Section 8.1.1.2 and each cell has three sectors. Frequency reuse is modeled by planning frequency allocations in different sectors in the network.

3. N MSs are dropped independently with uniform distribution across the cell area. Different load levels in the network are simulated by changing the number of MSs and the traffic generated.

4. Path loss, shadow fading and fast fading models for each MS should be consistent with the models defined in Section 3. Fading signal and fading interference are computed from each mobile station into each sector and from each sector to each mobile for each simulation interval.

5. It is considered that the device performing IDLE to ACTIVE_STATE transition is stationary and may be located anywhere in the center cell with uniform probability. The IDLE to ACTIVE_STATE transition is triggered by the MAC layer of the device in case of device-initiated IDLE to ACTIVE_STATE transition. In the case of network-initiated IDLE to ACTIVE_STATE transition, the IDLE to ACTIVE_STATE transition is triggered by the MAC layer of the BSs in the paging group of the device.

6. Traffic generated by the MSs in the fixed locations should be according to the mixes specified in Table 44 in Section 10.7 and this traffic constitutes background load.

7. Statistics of IDLE to ACTIVE_STATE transition latency are measured at different locations of the center cell. A weighted sum of these measurements is used to determine the mean value of the IDLE to ACTIVE_STATE transition latency.

8. Packets are not blocked when they arrive into the system (i.e. queue depths are infinite). Packets are scheduled with a packet scheduler using the required fairness metric.

Sequences of simulation are run, each with a different random seed. A sufficient number of runs are simulated to ensure convergence in the performance metrics.

10. Traffic Models

This section describes traffic models in detail. A major objective of system simulations is to provide an operator with a view of the maximum number of active users that can be supported for a given service under a specified configuration at a given coverage level.

Modeling of user arrival process: Typically all users are not active at a given time and even the active users might not register for the same service. In order to avoid different user registration and demand models, the objective of the proposed simulation model is restricted to evaluate the performance with the users that are maintaining a session with transmission activity. This model can be used to determine the number of such

registered users that can be supported. This document does not address the arrival process of such registered users, i.e. it does not address the statistics of subscribers that register and become active.

The traffic generated by a service should be accurately modeled in order to evaluate the performance of a system. This may be a time consuming exercise. Traffic modeling can be simplified, as explained below, by not modeling the user arrival process and assuming full queue traffic which is considered as the baseline. Modeling non-full-queue traffic is also discussed in the subsections that follow.

Full Queue model: In the full queue user traffic model, all the users in the system always have data to send or receive. In other words, there is always a constant amount of data that needs to be transferred, in contrast to bursts of data that follow an arrival process. This model allows the assessment of the spectral efficiency of the system independent of actual user traffic distribution type. A user is in outage if residual PER after HARQ retransmissions exceeds 1%.

In the following sections, we will concentrate on traffic generation only for the non-full queue case. In addition, the interaction of the generated traffic with the higher layer protocol stack such as TCP is not fully included here. Instead, we will provide references to documents which provide the detailed TCP transport layer implementation and its interaction with the various traffic models.

The models described in this section shall be used for evaluating 802.16m proposals. Optionally, for liaison with NGMN, statistical traffic models and associated parameters defined in [63] or its latest revision may be used for system performance evaluation.

10.1.   Web Browsing (HTTP) Traffic Model

HTTP traffic characteristics are governed by the structure of the web pages on the World Wide Web (WWW), and the nature of human interaction. The nature of human interaction with the WWW causes the HTTP traffic to have a bursty profile, where the HTTP traffic is characterized by ON/OFF periods as shown in Figure 18.
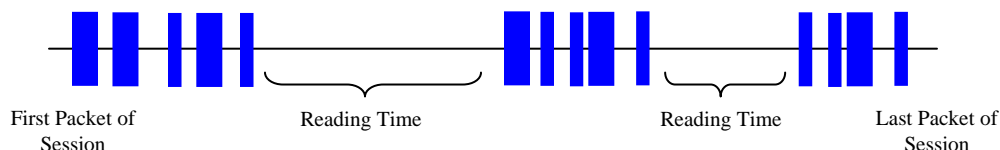
Figure 18: HTTP Traffic Pattern

The ON periods represent the sequence of packets in which the web page is being transferred from source to destination; while the OFF periods represent the time the user spends reading the webpage before transitioning to another page. This time is also known as Reading Time [43][44].

The amount of information passed from the source to destination during the ON period is governed by the web page structure. A webpage is usually composed of a main object and several embedded objects. The size of the main object, in addition to the number and size of the embedded objects define the amount of traffic passed from source to destination.

In summary, the HTTP traffic model is defined by the following parameters:
S_M: Size of main object in page
N_d: Number of embedded objects in a page
S_E: Size of an embedded object in page
D_{pc}: Reading time
T_p: Parsing time for the main page

In addition to the model parameters, HTTP traffic behavior is also dependent on the HTTP version used. Currently HTTP 1.0 and HTTP 1.1 are widely used by servers and browsers [45]-[48]. In HTTP 1.0, also known as burst mode transfer, a distinct TCP connection is used for each object in the page, thereby facilitating simultaneous transfer of objects. The maximum number of simultaneous TCP connections is configurable, with most browsers using a maximum of 4 simultaneous TCP connections. In HTTP/1.1, also known as persistent mode transfer, all objects are transferred serially over a single persistent TCP connection. Table 34 provides the model parameters for HTTP traffic.

Component	Distribution	Parameters	PDF
Main object size (SM)	Truncated Lognormal	Mean = 10710 bytes SD = 25032 bytes Min = 100 bytes Max = 2 Mbytes (before truncation)	$f_x = \dfrac{1}{\sqrt{2\pi}\sigma x}\exp\left[\dfrac{-(\ln x - \mu)^2}{2\sigma^2}\right], x \geq 0$ $\sigma = 1.37, \mu = 8.37$ if x>max or x<min, discard and generate a new value for x
Embedded object size (SE)	Truncated Lognormal	Mean = 7758 bytes SD = 126168 bytes Min = 50 bytes Max = 2 Mbytes (before truncation)	$f_x = \dfrac{1}{\sqrt{2\pi}\sigma x}\exp\left[\dfrac{-(\ln x - \mu)^2}{2\sigma^2}\right], x \geq 0$ $\sigma = 2.36, \mu = 6.17$ f x>max or x<min, discard and generate a new value for x
Number of embedded objects per page (Nd)	Truncated Pareto	Mean = 5.64 Max. = 53 (before truncation)	$f_x = \dfrac{\alpha k^{\alpha}}{x^{\alpha+1}}, k \leq x < m$ $f_x = \left(\dfrac{k}{m}\right)^{\alpha}, x = m$ $\alpha = 1.1, k = 2, m = 55$ Subtract k from the generated random

			value to obtain Nd if x>max, discard and regenerate a new value for x
Reading time (Dpc)	Exponential	Mean = 30 sec	$f_x = \lambda_e^{-\lambda x}, x \geq 0$ $\lambda = 0.033$
Parsing time (Tp)	Exponential	Mean = 0.13 sec	$f_x = \lambda_e^{-\lambda x}, x \geq 0$ $\lambda = 7.69$

Table 34: HTTP Traffic Parameters

To request an HTTP session, the client sends an HTTP request packet, which has a constant size of 350 bytes. From the statistics presented in the literature, a 50%-50% distribution of HTTP versions between HTTP 1.0 and HTTP 1.1 has been found to closely approximate web browsing traffic in the internet [49].

Further studies also showed that the maximum transmit unit (MTU) sizes most common to in the internet are 576 bytes and 1500 bytes (including the TCP header) with a distribution of 24% and 76% respectively. Thus, the web traffic generation process can be described as in Figure 19.
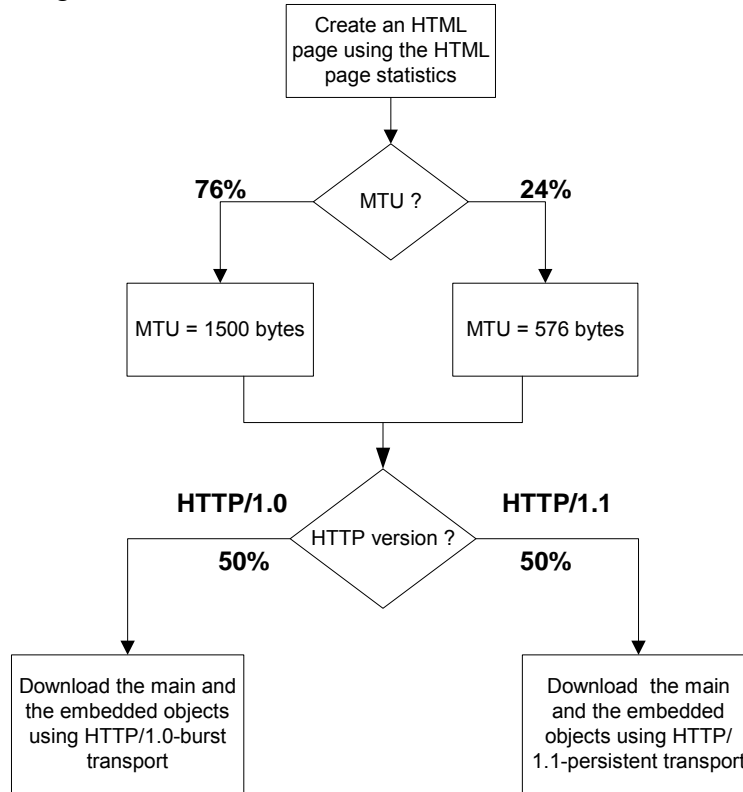
Figure 19: HTTP Traffic Profiles

A user is defined in outage for HTTP service if the average packet call throughput is less than the minimum average throughput requirement of 128 kbps. The system outage requirement is such that no more than 3% of users can be in outage. The air link PER of MAC SDUs for HTTP traffic should be not be greater than 1%.

10.1.1.   HTTP and TCP interactions for DL HTTP traffic

Two versions of the HTTP protocol, HTTP/1.0 and HTTP/1.1, are widely used by servers and browsers. Users shall specify 50% HTTP/1.0 and 50% HTTP/1.1 for HTTP traffic. For people who have to model the actual interaction between HTTP traffic and the underling TCP connection, refer to 4.1.3.2, 4.2.4.3 of [50] for details.

10.1.2.   HTTP and TCP interactions for UL HTTP traffic

HTTP/1.1 is used for UL HTTP traffic. For details regarding the modeling of the interaction between HTTP traffic and the underling TCP connection, refer to 4.2.4.1, 4.2.4.2 of [50].

10.2.   File Transfer Protocol Model

File transfer traffic is characterized by a session consisting of a sequence of file transfers, separated reading times. Reading time is defined as the time between end of transfer of the first file and the transfer request for the next file. The packet call size is therefore equivalent to the file size and the packet call inter-arrival time is the reading time. A typical FTP session is shown in Figure 20.
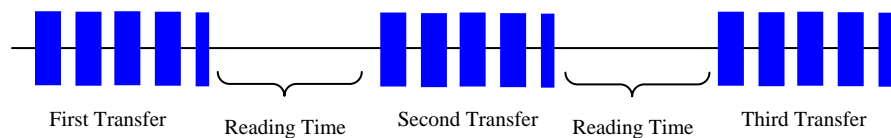
Figure 20: FTP Traffic Patterns

Table 35 provides the model parameters for FTP traffic that includes file downloads as well as uploads [51]-[52].In the case of file uploads, the arrival of new users is Poisson distributed and each user transfers a single file before leaving the network.

The FTP traffic generation process is described in Figure 21. Based on the results on packet size distribution, 76% of the files are transferred using an MTU size of 1500 bytes and 24% of the files are transferred using an MTU size of 576 bytes. Note that these two packet sizes also include a 40 byte IP packet header and this header overhead for the appropriate number of packets must be added to the file sizes calculated from the statistical distributions in
Table **35**. For each file transfer a new TCP connection is used whose initial congestion window size is 1 segment.

1 A user is defined in outage for FTP service if the average packet call throughput is less
2 than the minimum average throughput requirement of 128 kbps. The system outage
3 requirement is such that no more than 3% of users can be in outage. The air link PER of
4 MAC SDUs for FTP traffic should be not be greater than 1%.
5

Component	Distribution	Parameters	PDF
File size (S)	Truncated Lognormal	Mean = 2 Mbytes SD = 0.722 Mbytes Max = 5 Mbytes	$f_x = \dfrac{1}{\sqrt{2\pi}\sigma x}\exp\left[\dfrac{-(\ln x - \mu)^2}{2\sigma^2}\right], x \geq 0$ $\sigma = 0.35, \mu = 14.45$ if x>max or x<min, discard and generate a new value for x
Reading time (D_{pc})	Exponential	Mean = 180 sec.	$f_x = \lambda e^{-\lambda x}, x \geq 0$ $\lambda = 0.006$

6
7 **Table 35: FTP Traffic Parameters**
8
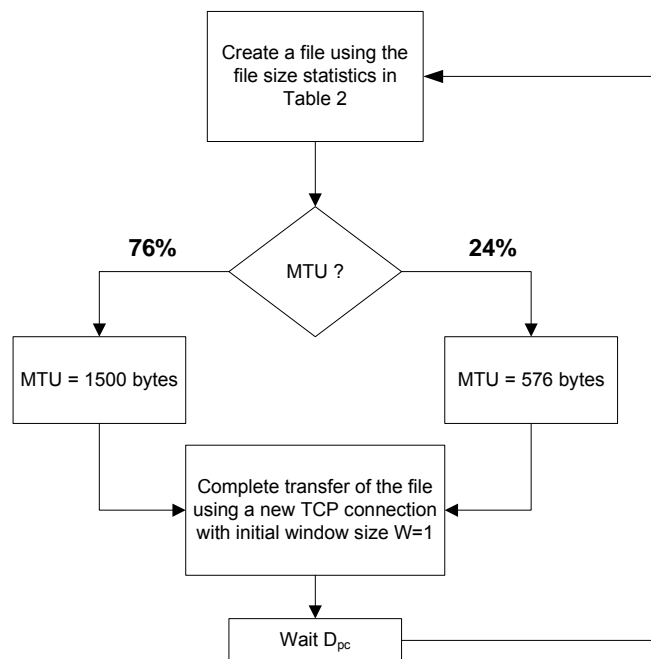
9
10
11 **Figure 21: FTP Traffic Profiles**
12

10.3.   Speech Source Model (VoIP)

VoIP refers to real-time delivery of voice packet across networks using the Internet protocols. A VoIP session is defined as the entire user call time and VoIP session occurs during the whole simulation period.

There are a variety of encoding schemes for voice (i.e., G.711, G.722, G.722.1, G.723.1, G.728, G.729, and AMR) that result in different bandwidth requirements. Including the protocol overhead, it is very common for a VoIP call to require between 5 Kbps and 64 Kbps of bi-directional bandwidth.

10.3.1.   Basic Voice Model

A typical phone conversation is marked by periods of active talking / talk spurts (ON periods) interleaved by silence / listening periods (or OFF periods) as shown in Figure 22.
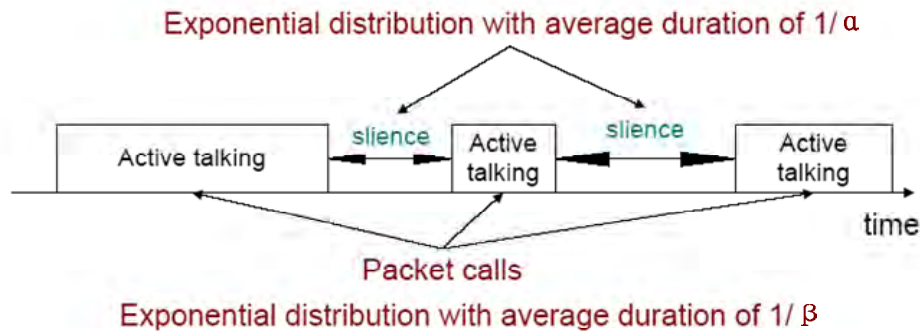
Figure 22: Typical phone conversation profile

Consider the simple 2-state voice activity Markov model shown in Figure 23 [54].
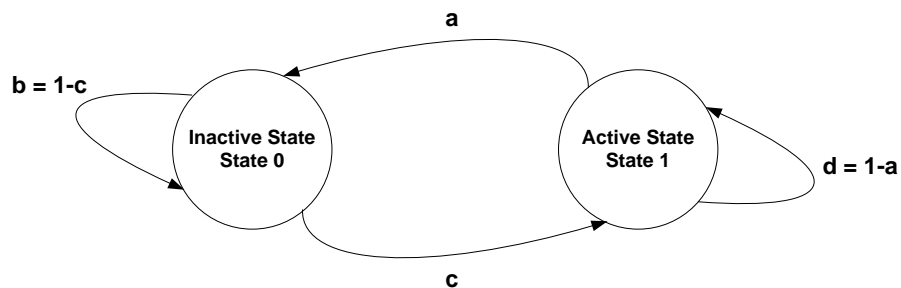
Figure 23: 2-state voice activity Markov model

In the model, the conditional probability of transitioning from state 1 (the active speech state) to state 0 (the inactive or silent state) while in state 1 is equal to a, while the conditional probability of transitioning from state 0 to state 1 while in state 0 is c. The model is assumed to be updated at the speech encoder frame rate $R=1/T$, where T is the encoder frame duration (typically, 20 ms). Packets are generated at time intervals $T+\tau$, where τ is the network packet arrival delay jitter. During the active state, packets of fixed sizes are generated at these intervals, while the model is updated at regular

frame intervals. The size of packet and the rate at which the packets are sent depends on the corresponding voice codecs and compression schemes. Table 36 provides information on some common vocoders.

Vocoder	EVRC	AMR	GSM 6.10	G.711	G.723.1		G.729A
Source Bit rate [Kb/s]	0.8/2/4/8.55	4.75-12.2	13	64	5.3	6.3	8
Frame duration [ms]	20	20	20	10	30	30	10
Information bits per frame	16/40/80/171	95-244	260	640	159	189	80

Table 36: Information on various vocoders

Among the various vocoders in Table 36, a simplified AMR (Adaptive Multi-Rate) audio data compression model can be used to simplify the VoIP modeling process. AMR is optimized for speech coding and was adopted as the standard speech codec by 3GPP and widely used in GSM. The original AMR codec uses link adaptation to select from one of eight different bit rates based on link conditions. If the radio condition is bad, source coding is reduced (less bits to represent speech) and channel coding (stronger FEC) is increased. This improves the quality and robustness of the network condition while sacrificing some voice clarity. In the simplified version in this document, link adaptation has been disabled and the full rate of 12.2 kbps is used in the active state. This model captures the worst case scenario.

Table 37 shows the VoIP packet size calculation for simplified AMR operation with or without header compression when using IPv4 or IPv6. In the table, the MAC CRC of 4 bytes for ARQ is not included and only CRC for HARQ is included because the ARQ process can be assumed to be disabled for VoIP services.

To calculate the total packet size, MAC headers and CRC need to be accounted for (example: there are 6 bytes of MAC header and 2 bytes of HARQ CRC in IEEE 802.16e reference system). Without header compression, an AMR payload of 33 bytes is generated in the active state every $20 + \tau$ ms and an AMR payload of 7 bytes is generated in the inactive state every $160 + \tau$ ms. Assuming IPv4 and uncompressed headers, the resulting VoIP packet size is 81 bytes in the active mode and 55 bytes in the inactive mode.

The voice capacity assumes a 12.2. kbps codec with a 50% activity factor such that the percentage of users in outage is less than 2% where a user is defined to have experienced voice outage if more than 2% of the VoIP packets are dropped, erased or not delivered successfully to the user within the delay bound of 50 ms.

The packet delay is defined based on the 98th percentile of the CDF of all individual users' 98th percentiles of packet delay (i.e., the 98th percentile of the packet delay CDF

1 first determined for each user and then the 98th percentile of the CDF that describes the
2 98th percentiles of the individual user delay is obtained).

3
4
5

Description	AMR without Header Compression IPv4/IPv6	AMR with Header Compression IPv4/IPv6	G.729 without Header Compression IPv4/IPv6	G.729 with Header Compression IPv4/IPv6
Voice Payload (20 ms aggregation interval)	7 bytes for inactive 33 bytes for active	7 bytes for inactive 33 bytes for active	0 bytes for inactive 20 bytes for active	0 bytes for inactive 20 bytes for active
Protocol Headers (including UDP checksum)	40 bytes / 60 bytes	3 bytes / 5 bytes	40 bytes / 60 bytes	3 bytes / 5 bytes
RTP	12 bytes		12 bytes	
UDP	8 bytes		8 bytes	
IPv4 / IPv6	20 bytes / 40 bytes		20 bytes / 40 bytes	
802.16e Generic MAC Header	6 bytes	6 bytes	6 bytes	6 bytes
802.16e CRC for HARQ	2 bytes	2 bytes	2 bytes	2 bytes
Total VoIP packet size	55 bytes/ 75 bytes for inactive 81 bytes / 101 bytes for active	18 bytes/ 20 bytes for inactive 44 bytes / 46 bytes for active	0 bytes for inactive 68 bytes/ 88 bytes for active	0 bytes for inactive 31 bytes/ 33 bytes for active

Table 37: VoIP Packet Calculation for AMR and G.729

6 Bidirectional VoIP capacity is measured in Active Users/MHz/Sector. The total number
7 of active users on the DL and UL is divided by total bandwidth occupied by the system
8 accounting for frequency reuse. For an FDD configuration, the bandwidth is calculated
9 as the sum of the uplink and downlink channel bandwidths. For a TDD configuration, the
10 bandwidth is simply the channel bandwidth.

11 **10.3.2.   VoIP Traffic Model Parameters**

12 During each call (each session), a VoIP user will be in the Active or Inactive state. The
13 duration of each state is exponentially distributed. In the Active/Inactive state, packets of
14 fixed sizes will be generated at intervals of T + τ seconds, where T is the VoIP frame
15 interval of 20 ms, and τ is the DL network delay jitter. For the UL, τ is equal to 0. As the
16 range of the delay jitter is limited to 120 ms, the model may be implemented as packet
17 arrivals at times T+ τ' seconds, where $\tau' = \tau$ + 60 ms and is always positive. Table 38
18 specifies the distributions and parameters associated with the VoIP traffic model.

Component	Distribution	Parameters	PDF
Active state duration	Exponential	Mean = 1 second	$f_x = \lambda\, e^{-\lambda x}$, $x \geq 0$ $\lambda = 1/\,Mean$
Inactive state duration	Exponential	Mean = 1.5 second.	$f_x = \lambda\, e^{-\lambda x}$, $x \geq 0$ $\lambda = 1/\,Mean$
Probability of transition from active to inactive state	N/A	0.02	N/A
Probability of transition from inactive to active state	N/A	0.0133	N/A
Packet arrival delay jitter (Downlink only)	Laplacian	β = TBD	$$f_x = \frac{1}{2\beta}\, e^{-\frac{|\tau|}{\beta}},$$ -60 ms $\leq \tau \leq$ 60ms

Table 38: VoIP traffic model parameters specification

Link adaptation of AMR codec is disabled in order to evaluate performance under worst case, and to simplify the voice traffic model.

During the inactive state, we have chosen to generate comfort noise with smaller packet sizes at regular intervals instead of no packet transmission. This simplified model does not include a feature called hangover, which generates additional seven frames at the same rate as speech to ensure the correct estimation of comfort noise parameters at the receiver side even if there is a silence period at the end of a talk spurt (ON state), and after the hangover period, a SID_FIRST frame is sent. The voice traffic model specifies only one rate during the ON state (talk spurt) of the AMR codec (12.2 kbps) and another rate for the comfort noise (SID_UPDATE) during the OFF state of the AMR codec. SID_UPDATE frames are generated every 8th frame during the silence period.

Table 39 provides the relevant parameters of the VoIP traffic that shall be assumed in the simulations. The details of the corresponding traffic model are described below:

Parameter	Characterization
Codec	RTP AMR 12.2, Source rate 12.2 kbps
Encoder frame length	20 ms
Voice activity factor (VAF)	40%
Payload	Active: 33 bytes (Octet alignment mode)Inactive: 7 bytes SID packet every 160 ms during silence
Protocol Overhead with compressed header	RTP/UDP/IP (including UDP check sum): 3 bytes 802.16 Generic MAC Header: 6 bytes CRC for HARQ: 2 bytes
Total voice payload on air interface	Active: 44 bytes Inactive: 18 bytes

Table 39: Detailed description of the VoIP traffic model for IPv4

10.4. Near Real Time Video Streaming

This section describes a model for streaming video traffic for DL direction. Figure 24 illustrates the steady state of video streaming traffic from the network as observed by the base station. Call setup latency and overhead are not considered in this model.
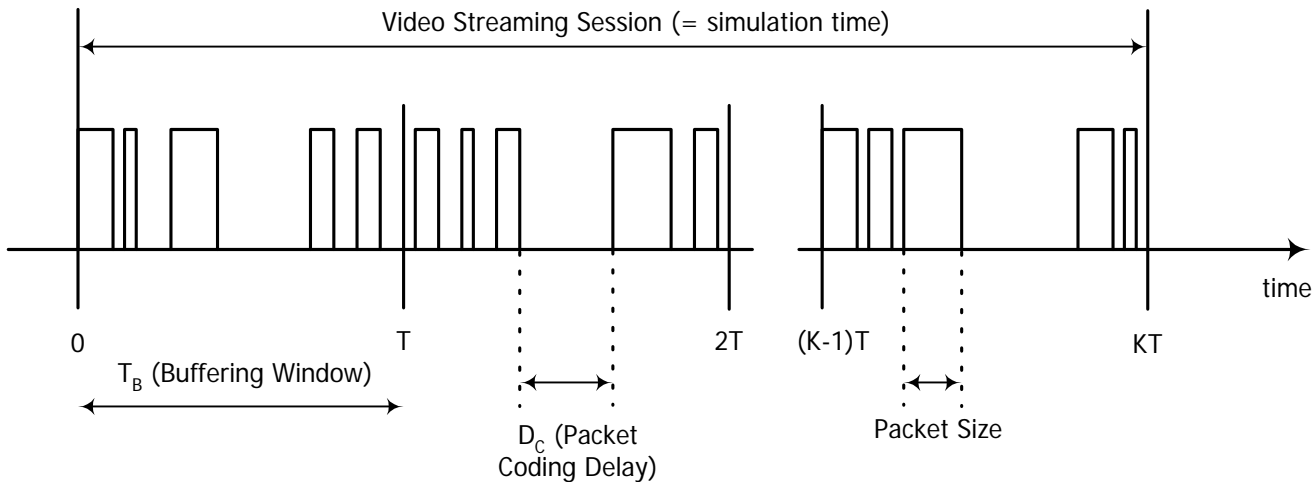
Figure 24: Video Streaming Traffic Model

Each frame of video data arrives at a regular interval T. Each frame can be treated as a packet call and there will be zero OFF duration within a session. Within each frame

1 (packet call), packets (or datagrams) arrive randomly and the packet sizes are random
2 as well.
3
4 To counter the jittering effect caused by the random packet arrival rate within a frame at
5 the MS, the MS uses a de-jitter buffer window to guarantee a continuous display of
6 video streaming data. The de-jitter buffer window for video streaming service is 5
7 seconds. At the beginning of the simulation, the MS de-jitter buffer shall be full with
8 video data. During simulation, data is leaked out of this buffer at the source video data
9 rate and filled as DL traffic reaches the MS from the BS. As a performance criterion, the
10 simulation shall record the length of time, if any, during which the de-jitter buffer runs
11 dry.
12
13 The packet sizes and packet inter-arrival rate can be found in when using a source rate
14 of 64 kbps.
15
16 Table 40 lists the parameters for the video streaming model.
17

Component	Distribution	Parameters	PDF
Inter-arrival time between the beginning of each frame	Deterministic	100 ms (Based on 10 frames per second)	
Number of packets (slices) in a frame	Deterministic	8 packets per frame	
Packet (slice) size	Truncated Pareto	Mean =10 bytes, Max = 250 bytes (before truncation)	$f_x = \dfrac{\alpha k^{\alpha}}{x^{\alpha+1}}, k \le x < m$ $f_x = \left(\dfrac{k}{m}\right)^{\alpha}, x = m$ $\alpha = 1.2, k = 20 bytes, m = 10 bytes$ if x>max, discard and regenerate a new value for x
Inter-arrival time between packets (slices) in a frame	Truncated Pareto	Mean=6 ms, Max=12.5 ms (before truncation)	$f_x = \dfrac{\alpha k^{\alpha}}{x^{\alpha+1}}, k \le x < m$ $f_x = \left(\dfrac{k}{m}\right)^{\alpha}, x = m$ $\alpha = 1.2, k = 2.5 ms, m = 6\,\text{ms}$

			if x>max, discard and regenerate a new value for x

Table 40: Near Real Time Video Streaming Traffic Model Parameters

A user is defined in outage for streaming video service if the 98th percentile video frame delay is larger than 5 seconds. The system outage requirement is such that no more than 3% of users can be in outage.

Parameter	Value
Service	Video Telephony
Video Codec	MPEG-4
Protocols	UDP
Scene Length (sec)	Session duration
Direction	Bi-direction (DL and UL)
Frames/sec	25 frames/sec
GOP	N=12, M=3
Display size	176x144
Color depth (bit)	8
Video Quality	Medium
Mean BW	110 kbps
I frame size (byte)	Weibull($\alpha = 5.15$, $\beta = 863$), shift=3949, μ= 4742 , σ=178 , min=4034, max=5184
P frame size (byte)	Lognormal(μ=259 , σ=134), min=100, max=1663
B frame size (byte)	Lognormal(μ=147 ,σ=74), min=35, max=882

Table 41: Video Telephony Traffic Model

10.5. Video Telephony

Based on the compression efficiency and market acceptance as described in the section 10.4, MPEG 4 has been selected for the video codec. The estimated values for the parameters to model a video stream vary from one trace to another. For parameters associated with the statistical distributions, the estimates depend strongly on the dimensions of the captured frames. For the video telephony traffic model, medium quality of an Office Cam trace is used and the trace library is available at [58]. For the traffic model, two different qualities for the video have been considered; high and

medium quality. For the medium quality encoding the quantization parameters for all three frame types were fixed at 10, and for the high quality encoding the quantization parameters for all three frame types were fixed at 4 [59].

The scene length for the video telephony is assumed to be the entire application session since the background or the main subject may not be so dynamic.

10.6.   Gaming traffic model

Gaming is a rapidly growing application embedded into communication devices, and thus wireless gaming needs to be considered. Games in different genre, such as First Person Shooter (FPS), Role Play Game (RPG), etc., show dramatic different traffic behaviors. FPS model is recommended to represent the gaming traffic model in this document because it posts additional requirements to the system performance, such as real time delay with irregular traffic arrivals.

First Person Shooter (FPS) is a genre of video games. It is a good representation of the modern Massively Multiplayer Online (MMO) game. Due to the nature of the FPS game, it has stringent network delay requirement. For the FPS game, if the client to server to client round trip delay (i.e., ping time, or end to end delay) is below 150 ms, the delay is considered excellent. When the delay is between 150 ms to 200 ms, the delay is noticeable especially to the experienced player. It is considered good or playable. When ping time is beyond 200 ms, the delay becomes intolerable.

This end to end delay budget can be break down into internet delay, server processing delay, cellular network delay, air interface delay, and client processing delay, etc. Let the IP packet delay be the time that the IP packet entering the MAC SDU buffer to the time that the IP packet is received by the receiver and reassembled into IP packet. The IP packet delay is typically budgeted as 50 ms to meet the 200 ms end to end delay.   A gamer is considered in outage if 10% of its packet delay is either lost or delayed beyond the budget, i.e., 50 ms.

The FPS traffic can be modeled by the Largest Extreme Value distribution. The starting time of a network gaming mobile is uniformly distributed between 0 and 40 ms to simulate the random timing relationship between client traffic packet arrival and reverse link frame boundary. The parameters of initial packet arrival time, the packet inter arrival time, and the packet sizes are illustrated in Table 42.

Component	Distribution		Parameters		PDF
	DL	UL	DL	UL	
Initial packet arrival	Uniform	Uniform	a = 0, b = 40 ms	a=0, b=40 ms	$f(x) = \dfrac{1}{b-a} \quad a \le x \le b$

Packet arrival time	Extreme	Extreme	a = 50 ms, b = 4.5 ms	a = 40 ms, b = 6 ms	$f(x) = \frac{1}{b} e^{\frac{x-a}{b}} e^{-e^{\frac{x-a}{b}}}, b > 0$ $[X = \lfloor a - b\ln(-\ln Y)\rfloor]$ $Y \in U(0,1)$
Packet size	Extreme	Extreme	a = 330 bytes, b = 82 bytes	a = 45 bytes, b = 5.7 bytes	$f(x) = \frac{1}{b} e^{\frac{x-a}{b}} e^{-e^{\frac{x-a}{b}}}, b > 0$ $[X = \lfloor a - b\ln(-\ln Y)\rfloor + 2,]$ $[X = \lfloor a - b\ln(-\ln Y)\rfloor]$ $Y \in U(0,1)$

Table 42: FPS Internet Gaming Traffic Model

10.7. Email Traffic Model

Email is an important application that constitutes a high percentage of internet traffic. Email application traffic is included in the UMTS Forum 3G traffic models and ITU R M.2072 [65], [66].

Interactions between email servers and clients are governed by email protocols. The three most common email protocols are POP, IMAP and MAPI. Most email software operates under one of these (and many products support more than one) protocols. The Post Office Protocol (currently in version 3, hence POP3) allows email client software to retrieve email from a remote server. The Internet Message Access Protocol (now in version 4 or IMAP4) allows a local email client to access email messages that reside on a remote server. The Messaging Application Programming Interface (MAPI) is a proprietary email protocol of Microsoft that can be used by Outlook to communicate with Microsoft Exchange Server. It provides somewhat similar but more functionality than an IMAP protocol.

The email traffic model in this section considers both POP3 and MAPI since these protocols generate different traffic patterns. To model POP3, an FTP model can be used, and an email transaction with MAPI protocol can be modeled with multiple MAPI segment transactions in series. Each MAPI fragment is transmitted using the TCP protocol and segmented into smaller segments again based on the TCP configuration. A maximum MAPI fragment size of 16896 bytes has been found so far, and this information is indicated in the first packet of a MAPI fragment. Outlook finishes all the TCP ACK packet transmission for the current MAPI segment and the Exchange server waits for the MAPI fragment completion indication packet before sending the next one. The last packet in the MAPI fragment sets the "PUSH" bit in the TCP packet to transmit all of the packets in the TCP buffer to the application layer at the receiver side [67].

Email traffic can be characterized by ON/OFF states. During the ON-state an email could be transmitted or received, and during the OFF-state a client is writing or reading an email. Figure 25 depicts a simplified email traffic pattern.
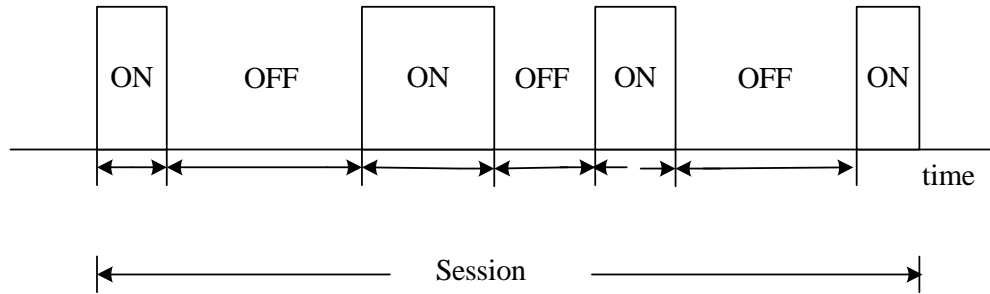
1
2
Figure 25: Email Traffic model
3
4   The parameters for the email traffic model are summarized in Table 43 [67], [68], [69],
5   [70], [71].
6

Parameter	Distribution	Parameters	PDF
E-Mail Protocol	N/A	POP3, MAPI	N/A
E-Mail Average Header Size (Bytes)	Deterministic	1 K	N/A
Number of email receive	Lognormal	Mean μ= 30 Std σ = 17	$f_x = \frac{1}{\sqrt{2\pi}\sigma}\exp\left[\frac{-(\ln x - \mu)^2}{2\sigma^2}\right]$ $x \geq 0$
Number of email send	Lognormal	Mean μ= 14 Std σ = 12	$f_x = \frac{1}{\sqrt{2\pi}\sigma}\exp\left[\frac{-(\ln x - \mu)^2}{2\sigma^2}\right]$ $x \geq 0$
Email reading time (sec)	Pareto	$\alpha = 1.1,, k = 2, m = 65$, mean = 60, maximum = 63	$f_x = \frac{\alpha k^\alpha}{x^{\alpha+1}}, k \leq x < m$ $f_x = \left(\frac{k}{m}\right)^\alpha, x = m$
Email writing time (sec)	Pareto	$\alpha = 1.1, k = 2, m = 125$, mean = 120, maximum = 123	$f_x = \frac{\alpha k^\alpha}{x^{\alpha+1}}, k \leq x < m$ $f_x = \left(\frac{k}{m}\right)^\alpha, x = m$
Size of email receive/send without attachment (Kbytes)	Cauchy	median $\mu = 22.7$ Kbytes, 90%-tile = 80Kbytes	$f_x = \frac{A}{\pi((x-\mu)^2+1)}$, A is selected to satisfy 90%-tile value
Size of email receive/send with attachment (Kbytes)	Cauchy	median $\mu = 227$ Kbytes, 90%-tile = 800 Kbytes	$f_x = \frac{A}{\pi((x-\mu)^2+1)}$, A is selected to satisfy 90%-tile value
Ratio of email with attachment	Deterministic	Without attachment: 80% With attachment: 20%	N/A

7
8
Table 43: Email Traffic Parameters

1   **10.8.   Traffic Mixes**

2   A mobile broadband wireless system is expected to support a mix of simultaneous
3   traffic types. There can be different types of usage scenarios (multi-service v. single-
4   type), different types of devices (notebook PCs, vs. PDAs or smart phones), different
5   usage levels (intense vs. light) and different delay/latency requirements (real-time vs.
6   best-effort).

7   The previous sections are primarily concerned with the traffic models for each of the
8   potential traffic types. As discussed in the previous section, these models are based on
9   statistical analysis of measured traffic that yielded some invariant patterns that are not
10   very dependant on the specific system. It is more difficult to describe a similar invariant
11   mix of traffic types since these tend to depend more heavily on the type of system and
12   the actual deployment mix of user device types.

13   In the context of system performance evaluation, the specific traffic-mix chosen should
14   emphasize different aspects of the system performance, e.g. sustained throughput for
15   file downloads v. faster response times for interactive applications.
16

17   Table 44 contains traffic mixes that should be used in system evaluations. For system
18   level simulation purposes, "traffic mix" refers to the percentage of users in the system
19   generating a particular type of traffic. In this context, each user is assumed to be
20   generating only one type of traffic, recognizing that in an actual network a single user's
21   terminal could support multiple applications and generate several types of traffic
22   simultaneously.
23

24   Mandatory traffic mixes (full buffer data only and VoIP only) shall be required for the
25   evaluation of performance metrics as defined in the 802.16m requirements. For
26   proposals that target improvements in performance metrics related to optional traffic
27   mixes, the proponents should provide simulation results based on the corresponding
28   traffic mixes. The NGMN traffic mix as specified in [63] or a later revision may be used
29   for liaison with NGMN. The following table specifies mandatory and optional traffic
30   mixes required for 802.16m system performance evaluation:

31

	VoIP	FTP	HTTP	NRTV	Gaming	VT	Full Buffer	Mandatory/ Optional
VoIP only	100% * (#users = N_v*)	0%	0%	0%	0%	0%	0%	Mandatory
Full Buffer Data only	0%	0%	0%	0%	0%	0%	100%, 10 users per sector	Mandatory
NGMN Traffic Mix	30%	10%	20%	20%	20%	0%	0%	Optional
FTP only	0%	100%	0%	0%	0%	0%	0%	Optional
HTTP only	0%	0%	100%	0%	0%	0%	0%	Optional
NRTV only	0%	0%	0%	100%	0%	0%	0%	Optional
Gaming only	0%	0%	0%	0%	100%	0%	0%	Optional
VT only	0%	0%	0%	0%	0%	100%	0%	Optional

VoIP & Full Buffer Mix 1	0.5 of N_v	0%	0%	0%	0%	0%	10 users per sector	Optional
VoIP & Full Buffer Mix 2	0.75 of N_v	0%	0%	0%	0%	0%	10 users per sector	Optional

Table 44: Traffic Mixes

* Nv is the system voice capacity that satisfies outage criteria at system and user level

11. Simulation Procedure and Flow

A nineteen cell network topology with wrap-around (as shown in Appendix G) shall be used as the baseline network topology for all system-level simulations.

1. The system is modeled as a network of 7 clusters. Each cluster has 19 hexagonal cells with six cells in the first tier and twelve cells in the second tier surrounding the central cell of each cluster. Each cell has three sectors. Frequency reuse is modeled by planning frequency allocations in different sectors in the network.

2. MSs are dropped independently with uniform distribution throughout the system. Each mobile corresponds to an active user session that runs for the duration of the drop.

3. Mobiles are randomly assigned channel models. Depending on the simulation, these may be in support of a desired channel model mix, or separate statistical realizations of a single type of channel model.

4. MSs are dropped according to the specified traffic mix.

5. For sectors belonging to the center cluster, sector assignment to an MS is based on the received power at an MS from all potential serving sectors. The sector with best path to MS, taking into account slow fading characteristics (path loss, shadowing, and antenna gains) is chosen as the serving sector.

6. Mobile stations are randomly dropped over the 57 sectors such that each sector has the required numbers of users. Although users may be in regions supporting handover each user is assigned to only one sector for counting purposes. All sectors of the system shall continue accepting users until the desired fixed number of users per sector is achieved everywhere. Users dropped within 35 meters of a sector antenna shall be redropped. MS locations for six wrapping clusters are the same as the center cluster.

7. For simulations that do not involve handover performance evaluation, the location of each MS remains unchanged during a drop, and the speed of an MS

is only used to determine the Doppler effect of fast fading. Additionally, the MS is assumed to remain attached to the same BS for the duration of the drop.

8. Fading signal and fading interference are computed from each mobile station into each sector and from each sector to each mobile for each simulation interval.

9. Packets are not blocked when they arrive into the system (i.e. queue depths are infinite).Users with a required traffic class shall be modeled according to the traffic models defined in this document. Start times for each traffic type for each user should be randomized as specified in the traffic model being simulated.

10. Packets are scheduled with a packet scheduler using the required fairness metric. Channel quality feedback delay, PDU errors are modeled and packets are retransmitted as necessary. The HARQ process is modeled by explicitly rescheduling a packet as part of the current packet call after a specified HARQ feedback delay period.

11. .Simulation time is chosen to ensure convergence in user performance metrics. For a given drop the simulation is run for this duration, and then the process is repeated with the MSs dropped at new random locations. A sufficient number of drops are simulated to ensure convergence in the system performance metrics.

12. Performance statistics are collected for MSs in all cells according to the output matrix requirements.

13. All 57 sectors in the system shall be dynamically simulated.

12. Interference Modeling

The reuse of frequencies through planned allocation enables a cellular system to increase capacity with a limited number of channels. The interference model due to frequency reuse should accurately represent the time-frequency selective nature of OFDMA interference. The channel matrices for the desired and interfering signals shall be generated according to the models in Section 3 which account for the pathloss, BS antenna gain, shadowing, and fast fading variations. For simplicity, the same fast fading channel model but a different realization shall be assigned to each link between an MS & all BSs in the network.   This time-frequency modeling can create significant computational complexity in network simulations. To reduce complexity, pathloss and shadowing are calculated to determine the I_{strong} strongest interferers. The strongest interferers are modeled as spatially correlated processes and their channel matrices include pathloss, BS antenna gain, shadowing and fast fading components. The remaining I_{weak} interferers are modeled as spatially white spectrally flat processes. It has been shown that this modeling procedure results in negligible loss in performance.

The procedure for downlink simulations is summarized below:

1. Determine the pathloss, BS antenna gain, and shadowing from all interfering sectors to MS.
2. Rank the interfering sectors in order of received power (based on pathloss, BS antenna gain, and shadowing).
3. Model the channels of the strongest (I_{strong}) interferers as described in Section 3. The channel matrices of the strongest interfering sectors account for the pathloss, BS antenna gain, shadowing, and fast fading variations. For downlink baseline simulations with Matrix A and Matrix B, the value of I_{strong} shall be set to 8.
4. Model the remaining sectors as spatially white Gaussian noise processes whose variances are based on a spectrally flat Rayleigh fading process. The power of the Rayleigh fading process includes the effects of pathloss, BS antenna gain, and shadowing. The fading processes for all links between MS and BS are assumed to be independent, and the Doppler rate is determined by the speed of the mobile. At any instant in time, the total received interference power is the summation of the receive power from of all weak interferers. Hence, the interference power is varying in time during a simulation drop.

13. Performance Metrics

13.1.   Introduction

Performance metrics may be classified as single-user performance metrics or multi-user performance metrics.

13.1.1.   Single User Performance Metrics

13.1.1.1.   Link Budget and Coverage Range (Noise Limited) – single-cell consideration

Link budget evaluation is a well known method for initial system planning that needs to be carried out for BS to MS links. Although a link budget can be calculated separately for each link, it is the combination of the links that determines the performance of the system as a whole. The parameters to be used needs to be agreed upon after obtaining consensus. Using the margins in the link budget, the expected signal to noise ratio can be evaluated at given distances. Using these results, the noise limited range can be evaluated for the system. The link budget template is TBD.

Coverage range is defined as the maximum radial distance to meet a certain percentage of area coverage (x%) with a signal to noise ratio above a certain threshold (target SINR) over y% of time, assuming no interference signals are present. It is proposed that x be 99 and y be 95.

13.1.1.2.   SINR Coverage – interference limited multi-cell consideration

The SINR coverage is defined as the percentage area of a cell where the average SINR experienced by a stationary user is larger than a certain threshold (target SINR).

13.1.1.3.   Data Rate Coverage – interference limited multi-cell consideration

The percentage area for which a user is able to transmit/receive successfully at a specified mean data rate using single-user analysis mentioned above. No delay requirement is considered here.

13.1.2.   Multi-User Performance Metrics

Although a user may be covered for a certain percentage area (e.g. 99%) for a given service, when multiple users are in a sector/BS, the resources (time, frequency, power) are to be shared among the users. It can be expected that a user's average data rate may be reduced by a factor of N when there are N active users (assuming resources are equally shared and no multi-user diversity gain), compared to a single user rate.

For example, assume that there is a system, where a shared channel with a peak rate of 2 Mbps can serve 99% of the area. Consider the scenario where a particular user wants to obtain a video streaming service at 2 Mbps. This user may be able to obtain the service if no other user gets any service during the whole video session (which may extend for more than an hour). Therefore, in this example although 99% area is covered for the video service, this service is not a viable service for the operator and the evaluation of coverage needs to be coupled with the evaluation of capacity in order to reflect viable service solutions. Coverage performance assessment must be coupled with capacity (# of MSs), to obtain a viable metric.

The users having poor channel quality may be provided more resources so that they would get equal service from the cellular operator. This could adversely impact the total cell throughput. Thus, there is a trade-off between coverage and capacity. Any measure of capacity should be provided with the associated coverage. .

Since an operator should be able to provide the service to multiple users at the same time, an increase in the area coverage itself does not give an operator the ability to offer a given service. Therefore, the number of users that can be supported under a given coverage captures actual coverage performance for a given service from a viability point of view.

The suggested performance metric is the number of admissible users (capacity), parameterized by the service (R_{min}), and the coverage (allowable outage probability).

13.2.   Definitions of Performance Metrics

It is assumed that simulation statistics are collected from sectors belonging to the test cell(s) of the 19-cell deployment scenario. Collected statistics will be traffic-type (thus traffic mix) dependent.

In this section, we provide a definition for various metrics collected in simulation runs. For a simulation run, we assume:

1
2   1] Simulation time per drop = T_{sim}
3   2] Number of simulation drops = D
4   3] Total number of users in sector(s) of interest= N_{sub}
5   4] Number of packet calls for user u = p_u
6   5] Number of packets in i^{th} packet call = $q_{i,u}$

7   ### 13.2.1.   Throughput Performance Metrics

8   For evaluating downlink (uplink) throughput, only packets on the downlink (uplink) are
9   considered in the calculations. Downlink and uplink throughputs are denoted by upper
10   case DL and UL respectively (example: R_u^{DL}, R_u^{UL}). The current metrics are given per a
11   single simulation drop.
12
13   The throughput metrics below shall be measured at the following layers:
14   • PHY Layer
15   • MAC Layer
16   • TCP Layer
17
18   The throughput for those layers is measured at the points identified in
19   Figure 26 where the throughput refers to the payload throughput without the overhead.
20
21
22
23
24
25
26
27
28
29
30
31
32
33
34
35
36
37
38
39
40   **Figure 26: Throughput Metrics Measurement Points**
41
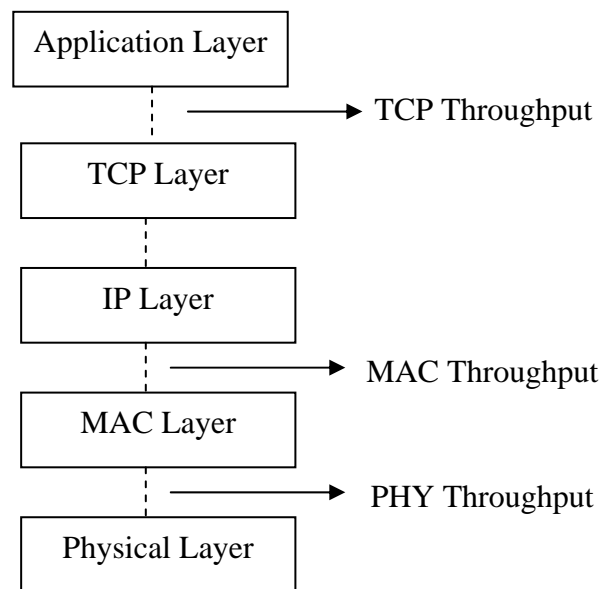
42   ### 13.2.1.1.   Average Data Throughput for User u

43   The data throughput of a user is defined as the ratio of the number of information bits
44   that the user successfully received divided by the amount of the total simulation time. If

user u has $p_u^{DL(UL)}$ downlink (uplink) packet calls, with $q_{i,u}^{DL(UL)}$ packets for the ith downlink (uplink) packet call, and $b_{j,i,u}$ bits for the jth packet; then the average user throughput for user u is

$$R_u^{DL(UL)} = \frac{\sum_{i=1}^{p_u^{DL(UL)}} \sum_{j=1}^{q_{i,u}^{DL(UL)}} b_{j,i,u}}{T_{Sim}} \quad (101)$$

13.2.1.2.   Average Per-User Data Throughput

The average per-user data throughput is defined as the sum of the average data throughput of each user in the system as defined in Section 13.2.1.1, divided by the total number of users in the system.

13.2.1.3.   Sector Data Throughput

Assuming N_{sub} users in sector of interest, and u^{th} user where $u \in N_{sub}$ has throughput $R_u^{DL(UL)}$, then DL or UL sector data throughput is :

$$R_{sec}^{DL(UL)} = \sum_{u=1}^{N_{sub}} R_u^{DL(UL)} \quad (102)$$

13.2.1.4.   Average Packet Call Throughput for User u

Packet call throughput is the total bits per packet call divided by total packet call duration. If user u has $p_u^{DL(UL)}$ downlink (uplink) packet calls, with $q_{i,u}^{DL(UL)}$ packets for the ith downlink (uplink) packet call, and $b_{j,i,u}$ bits for the jth packet; then the average packet call throughput is

$$R_u^{pc,DL(UL)} = \frac{1}{p_u^{DL(UL)}} \left(\sum_{i=1}^{p_u^{DL(UL)}} \frac{\sum_{j=1}^{q_{i,u}^{DL(UL)}} b_{j,i,u}}{(T_{i,u}^{end,DL(UL)} - T_{i,u}^{start,DL(UL)})} \right) \quad (103)$$

where $T_{i,u}^{start,DL(UL)}$ defines the time instant at which the transmission of first packet of the ith downlink (uplink) packet call for user u starts and and $T_{i,u}^{end,DL(UL)}$ defines the time instant at which the last packet of the ith downlink (uplink) packet call for user u is received.

13.2.1.5.   Average Per-User Packet Call Throughput

The average per-user packet call throughput is defined as the sum of the average packet call throughput of each user in the system as defined in Section 13.2.1.4, divided by the total number of users in the system.

13.2.1.6. The Histogram of Users' Average Packet Call Throughput

The histogram will display the distribution of the downlink (uplink) average packet call throughput observed at the MS (BS) for the subscribed users.

13.2.1.7. Throughput Outage

Throughput outage ($O_{thpt}(R_{min})$) is defined as the percentage of users with data rate R_u^{DL}, less than a predefined minimum rate R_{min} (TBD).

13.2.1.8. Cell Edge User Throughput

The cell edge user throughput is defined as the 5th percentile point of the CDF of users' average packet call throughput.

13.2.1.9. Geographical Distribution of Average Packet Call Throughput per User (optional)

The plot will show the geographical distribution of the average packet call throughput observed on the downlink (uplink) by the MS (BS). It provides insight into the throughput variation as a function of distance from the BS. This allows for easy comparison between different reuse scenarios, network loading conditions, smart antenna algorithms, etc.

13.2.2. Performance Metrics for Delay Sensitive Applications

For evaluating downlink (uplink) delay, only packets on the downlink (uplink) are considered in the calculations. Downlink and uplink delays are denoted by upper case DL and UL respectively (example: D_u^{DL}, D_u^{UL}) .

13.2.2.1. Packet Delay

Assuming the jth packet of the ith packet call destined for user u arrives at the BS (SS) at time $T_{j,i,u}^{arr,DL(UL)}$ and is delivered to the MS (BS) MAC-SAP at time $T_{j,i,u}^{dep,DL(UL)}$, the packet delay is defined as

$$Delay_{j,i,u}^{DL(UL)} = T_{j,i,u}^{dep,DL(UL)} - T_{j,i,u}^{arr,DL(UL)} \qquad (104)$$

Packets that are dropped or erased may or may not be included in the analysis of packet delays depending on the traffic model specifications. For example, in modeling traffic from delay sensitive applications, packets may be dropped if packet transmissions are not completed within a specified delay bound. The impact of such dropped packets can be captured in the packet loss rate.

13.2.2.2. The CDF of packet delay per user

CDF of the packet delay per user provides a basis in which maximum latency, x%-tile, average latency as well as jitter can be derived.

13.2.2.3.   X%-tile Packet delay per user

The x%-tile packet delay is simply the packet delay value for which x% of packets have delay below this value.

13.2.2.4.   The CDF of X%-tile Packet Delays

The CDF of x%-tiles of packet latencies is used in determining the y%-tile latency of the x%-tile per user packet delays.

13.2.2.5.   The Y%-tile of X%-tile Packet Delays

The y%-tile is the latency number in which y% of per user x%-tile packet latencies are below this number. This latency number can be used as a measure of latency performance for delay sensitive traffic. A possible criteria for VoIP, for example, is that the 97th %-tile of the 97%-tile of packet latencies per user is 50ms.

13.2.2.6.   User Average Packet Delay

The average packet delay is defined as the average interval between packets originated at the source station (either MS or BS) and received at the destination station (either BS or MS) in a system for a given packet call duration. The average packet delay for user u, $D_u^{avg,DL(UL)}$ is given by:

$$D_u^{avg,DL(UL)} = \frac{\sum_{i=1}^{p_u}\sum_{j=1}^{q_{i,u}}\left(T_{j,i,u}^{dep,DL(UL)} - T_{j,i,u}^{arr,DL(UL)}\right)}{\sum_{i=1}^{p_u}q_{i,u}} \tag{105}$$

13.2.2.7.   CDF of Users' Average Packet Delay

The CDF will reflect the cumulative distribution of the average packet delay observed by all users.

13.2.2.8.   Packet Loss Ratio

The packet loss ratio per user is defined as

$$Packet\ Loss\ Ratio = 1 - \frac{Total\ Number\ of\ Successfully\ \mathrm{Re}ceived\ Packets}{Total\ Number\ of\ Successfully\ Transmitted\ Packets} \tag{106}$$

13.2.3.   System Level Metrics for Unicast Transmission

13.2.3.1.   System data throughput

The data throughput of a BS is defined as the number of information bits per second that a site can successfully deliver or receive via the air interface using the scheduling algorithms.

13.2.3.2. Spectral Efficiency

Both physical layer spectral efficiency and MAC layer spectral efficiency should be evaluated. Physical layer spectral efficiency should represent the system throughput measured at the interface from the physical layer to the MAC layer, thus including physical layer overhead but excluding MAC and upper layer protocols overhead. MAC layer spectral efficiency should represent the system throughput measured at the interface from the MAC layer to the upper layers, thus including both physical layer and MAC protocol overhead. Typical Layer 1 and Layer 2 overheads are described in Appendix I.

The MAC efficiency of the system should be evaluated by dividing the MAC layer spectral efficiency by the physical layer spectral efficiency.

The average cell/sector spectral efficiency is defined as

$$r = \frac{R}{BW_{eff}} \tag{107}$$

Where R is the aggregate cell/sector throughput, BW_{eff} is the effective channel bandwidth. The effective channel bandwidth is defined as

$$BW_{eff} = BW \times TR \tag{108}$$

where BW is the used channel bandwidth, and TR is time ratio of the link. For example, for FDD system TR is 1, and for TDD system with DL:UL=2:1, TR is 2/3 for DL and 1/3 for UL, respectively.

13.2.3.3. CDF of SINR

For uplink simulations, this is defined as the cumulative distribution function (CDF) for the signal to interference and noise ratio (SINR) observed by the BS for each MS on the uplink. For downlink simulations, this is defined as the CDF for the SINR observed by each MS on the downlink. This metric allows for a comparison between different reuse scenarios, network loading conditions, smart antenna algorithms, resource allocation and power control schemes, etc.

13.2.3.4. Histogram of MCS

This histogram will display the distribution of MCS for all subscribed users.

13.2.3.5. Application Capacity

Application capacity (C_{app}) is defined as the maximum number of application users that the system can support without exceeding the maximum allowed outage probability.

13.2.3.6.   System Outage

System outage is defined as when the number of users experiencing outage exceeds 3% of the total number of users. The user outage criterion is defined based on the application of interest in Section 10.

13.2.3.7.   Coverage and Capacity Trade-off Plot

In order to evaluate the coverage and capacity trade-off, system level simulation shall provide a plot of the x% coverage data rate versus sector throughput. The default value of x is 95%.

13.2.4.   System Level Metrics for Multicast Broadcast Service

In order to evaluate the performance of multicast broadcast services, two cases should be considered. The first case consists of all 57 sectors transmitting the same MBS service. In the second case, which is used to evaluate the performance at the MBS zone edge, only the centre cell and the first tier of cells are transmitting the same MBS service. The remaining cells are either transmitting unicast data or a different MBS service. In both cases, the self interference due to effective channel delay exceeding cyclic prefix should be modeled. Both cases should be evaluated with the performance metrics given in the following subsections.

13.2.4.1.   Maximum MBS Data Rate

The maximum MBS data rate is defined as the maximum data rate for 95% coverage with a target packet error rate of 1%.

13.2.4.2.   Coverage versus Data Rate Trade-off

The coverage versus data rate trade-off can be evaluated through a plot of the coverage percentage versus the data rate for a target packet error rate of 1%.

13.2.4.3.   Impact of Multicast/Broadcast resource size on Unicast Throughput

As the MBS resource size increases, the impact on unicast throughput should be provided. Given the total resource budget, the impact of multicast/broadcast resource size on unicast throughput can be evaluated through a plot of the unicast throughput versus the multicast/broadcast throughput for 95% coverage with a target PER of 1%.

13.3.   Fairness Criteria

It may be an objective to have uniform service coverage resulting in a fair service offering for best effort traffic. A measure of fairness under the best effort assumption is important in assessing how well the system solutions perform.

The fairness is evaluated by determining the normalized cumulative distribution function (CDF) of the per user throughput. The CDF is to be tested against a predetermined fairness criterion under several specified traffic conditions. The same scheduling algorithm shall be used for all simulation runs. That is, the scheduling algorithm is not

1   to be optimized for runs with different traffic mixes. The owner(s) of any proposal are
2   also to specify the scheduling algorithm.
3
4   Let $T_{put}[k]$ be the throughput for user k. For a packet call, let $T_{put}[k]$ be defined as the
5   average packet call throughput for user k as defined in Section 13.2.1.4. The
6   normalized throughput with respect to the average user throughput for user k, $\tilde{T}_{put}[k]$ is
7   given by

8
$$\tilde{T}_{put}[k] = \frac{T_{put}[k]}{\text{avg } T_{put}[i]} \qquad (109)$$

9   ### 13.3.1.   Moderately Fair Solution

10 The CDF of the normalized throughputs with respect to the average user throughput for
11 all users is determined. This CDF shall lie to the right of the curve given by the three
12 points in Table 45.
13

Normalized Throughput w.r.t average user throughput	CDF
0.1	0.1
0.2	0.2
0.5	0.5

14
15   **Table 45: Moderately Fair Criterion CDF**

16 ### 13.3.2.   Short Term Fairness Indication

17 During the simulation, the following short-term fairness indicator should be computed
18 and recorded every τ ms (τ is suggested to be 20 or 40):

19
$$F(t) = \frac{\left|\sum_{i \in A} \hat{T}_i(t)\right|^2}{|A|\sum_{i \in A} \hat{T}_i^2(t)} \qquad (110)$$

20 where $\hat{T}_i(t)$ is the amount of service received by the *i*th user in time interval $[t, t+\tau), A$ is
21 the set of users with nonzero buffers in $[t, t+\tau)$, and $|A|$ is the cardinality of A. The
22 minimum of $F(t)$ during the simulation time, defined as $F_{\min} = \min\limits_{t \in \{0, \tau, 2\tau, 3\tau, \dots T_{sim}\}} F(t)$, can serve
23 as an indication of how much fairness is maintained all the time.

24 ## 14. Template for Reporting Results
25

1   Relevant system performance metrics for partial and complete technical proposals
2   should be generated and included in the evaluation report as specified in the following
3   table. For relative performance metrics, results for the reference system should be
4   included. Models and assumptions should be aligned with those listed in this document.
5   Additional assumptions and deviations from required assumptions should be specified.
6
7   System Level results such as the cdf of normalized throughput and Link Level results
8   that are required for performance evaluation should be shown in separate figures.
9

Performance Metric	Value : 802.16m	Value : 802.16e Reference System
Peak Data Rate DL / UL (bps/Hz)		
Maximum Data Latency DL / UL (ms)		
State Transition Latency (ms)		
Maximum Intra-frequency handover interruption time (ms)		
Maximum Inter-frequency handover interruption time (ms)		
Average User Throughput * DL / UL (bps/Hz)		
Cell Edge User Throughput * DL / UL (bps/Hz)		
Sector Throughput * DL / UL (bps/Hz)		
VoIP Capacity ** DL / UL (Active Users/MHz/sector)		
MBS Spectral Efficiency *** 0.5 km site-to-site distance (bps/Hz)		
MBS Spectral Efficiency 1.5 km site-to-site distance (bps/Hz)		
Estimated Layer 1 Overhead DL / UL (%)		
Estimated Layer 2 Overhead DL / UL (%)		

10
11   **Table 46: Evaluation Report**
12   * Applies to full buffer data traffic for all active users
13   ** Applies to VoIP traffic for all active users
14   *** All configuration baseline parameters defined in Section 2 apply to site-to-site distance of 0.5 km

1

Appendix A: Spatial Correlation Calculation

In order to compute the spatial correlation, two methods can be considered here:

Method-1: Using 20 subpaths to approximate the Laplacian PDF

For each path, generate 20 subpaths with some angular offsets from the per-path AoD_n and AoA_n. The angular offsets of the k-th (k=1..20) subpath are determined by (the offsets are the same for all paths)

$$\psi_{k,BS} = \Delta_k AS_{BS,Path}$$
$$\psi_{k,MS} = \Delta_k AS_{MS,Path}$$

where the values of Δ_k are given below.

Sub-path number k	Δ_k
1,2	± 0.0447
3,4	± 0.1413
5,6	± 0.2492
7,8	± 0.3715
9,10	± 0.5129
11,12	± 0.6797
13,14	± 0.8844
15,16	± 1.1481
17,18	± 1.5195
19,20	± 2.1551

Table 47: Value of Δ_k

Derive the antenna spatial correlation at the BS and MS between the p-th and q-th antenna as:

$$r_{n,BS}(p,q) = \frac{1}{20} \sum_{k=1}^{20} \exp\left\{ j \frac{2\pi d_{BS}}{\lambda}(p-q)\sin(AOD_n + \psi_{k,BS} + \theta_{BS}) \right\}$$

$$r_{n,MS}(p,q) = \frac{1}{20} \sum_{k=1}^{20} \exp\left\{ j \frac{2\pi d_{MS}}{\lambda}(p-q)\sin(AOA_n + \psi_{k,MS} + \theta_{MS}) \right\}$$

where d_{BS} (d_{MS}) is the antenna spacing at BS (MS) and λ is the wavelength.

Method-2: Pre-compute the correlation values with quantized AoA, AoD

Pre-calculate the BS spatial correlation matrices for a set of

$AOD \in \{-90^o, -80^o, \cdots, 0^o, \cdots, 80^o, 90^o\}$ and the MS spatial correlation matrices for a set of

$AOA \in \{-90^o, -80^o, \cdots, 0^o, \cdots, 80^o, 90^o\}$

$$R_{BS}(m,p,q) = \int_{-\infty}^{\infty} f(\alpha)\exp\left\{ j\frac{2\pi d_{BS}}{\lambda}(p-q)\sin(AOD[m]+\alpha+\theta_{BS}) \right\} d\alpha$$

$$R_{MS}(m,p,q) = \int_{-\infty}^{\infty} f(\beta)\exp\left\{ j\frac{2\pi d_{MS}}{\lambda}(p-q)\sin(AOA[m]+\beta+\theta_{MS}) \right\} d\beta$$

where m is the quantization step index, α, β are the angular offset at BS and MS, respectively with Laplacian PDF as defined in 3.2.8.

Assuming omni directional antennas and the incoming rays within $\pm\Delta$ of the mean angle of arrival or departure (i.e. the Laplacian PAS is defined over $[\phi_0 - \Delta, \phi_0 + \Delta)$) an exact expression to calculate the spatial correlation coefficient is given by [1]

$$\Re[R_{BS}(m,p,q)] = J_0(D(p-q)) + 2\sum_{r=1}^{\infty} \frac{J_{2r}(D(p-q))}{\left(\frac{\sqrt{2}}{\sigma_\phi^2}\right)^2 + (2r)^2}(\cos(2r\phi_0))\left\{\frac{\sqrt{2}}{\sigma_\phi^2} + \exp\left(-\frac{\Delta\sqrt{2}}{\sigma_\phi^2}\right)\left[2r\sin(2r\Delta) - \frac{\sqrt{2}}{\sigma_\phi^2}\cos(2r\Delta)\right]\right\}$$

$$\Im[R_{BS}(m,p,q)] = 2\sum_{r=0}^{\infty} \frac{J_{2r+1}(D(p-q))}{\left(\frac{\sqrt{2}}{\sigma_\phi^2}\right)^2 + (2r+1)^2}\sin((2r+1)\phi_0)\left\{\frac{\sqrt{2}}{\sigma_\phi^2} - \exp\left(-\frac{\Delta\sqrt{2}}{\sigma_\phi^2}\right)\left[(2r+1)\sin((2r+1)\Delta) + \frac{\sqrt{2}}{\sigma_\phi^2}\cos((2r+1)\Delta)\right]\right\}$$

Where $D = \frac{2\pi d_{BS}}{\lambda}$, $\sigma_\phi = AS_{BS,Path}$, $J_x(\cdot)$ is the x-th order Bessel function of the first kind and ϕ_0 is the AOD. Similarly the expressions for the $R_{MS}(m,p,q)$ can be written with $D = \frac{2\pi d_{MS}}{\lambda}$, and $\sigma_\phi = AS_{MS,Path}$. The infinite sums are truncated at

$$\frac{(r+1) - \text{th term}}{\text{Sum of first r terms}} = 0.1\% .$$

For each path, determine the index m_{BS} corresponding to AoD$_n$,

$$m_{BS} = \left\lfloor \frac{AOD_n}{10} \right\rfloor$$

and the index m_{MS} corresponding to AoA$_n$

$$m_{MS} = \left\lfloor \frac{AOA_n}{10} \right\rfloor$$

The spatial correlation matrix for this path is then

$$r_{n,BS}(p,q) = R_{BS}(m_{BS}, p, q)$$
$$r_{n,MS}(p,q) = R_{MS}(m_{MS}, p, q)$$

1   **Appendix B: Polarized Antenna**

2

3   Correlation between polarized antennas results from the cross polarization power ratio
4   (XPR). The polarization matrix is given by:

5
$$\mathbf{S} = \begin{bmatrix} s_{vv} & s_{vh} \\ s_{hv} & s_{hh} \end{bmatrix},$$

6   where v denotes vertical and h horizontal polarization, the first index denoting the
7   polarization at BS and the second the polarization at MS. The example below assumes
8   -8 dB per-tap power ratio between vertical-to-horizontal and vertical-to-vertical
9   polarisations (also P_{hv}/P_{hh} = -8dB). But the actual XPR value for each scenario should
10 follow the specification in respective CDL model. The -8dB value was adopted from
11 reference [24]. The following derivation of antenna correlation due to polarization with -
12 8dB XPR can also be found in [24]. This results in the following mean power per
13 polarization component

14

15
$$p_{vv} = E\left\{|s_{vv}|^2\right\} = 0\,\mathrm{dB} = 1$$

$$p_{vh} = E\left\{|s_{vh}|^2\right\} = -8\,\mathrm{dB} = 0.1585$$

$$p_{hv} = E\left\{|s_{hv}|^2\right\} = -8\,\mathrm{dB} = 0.1585$$

$$p_{hh} = E\left\{|s_{hh}|^2\right\} = 0\,\mathrm{dB} = 1$$

16 If the MS polarizations are assumed to be vertical and horizontal, but the BS
17 polarizations are slant +45° and -45°. The MS and BS polarization matrices $\mathbf{P}_{MS}$ and $\mathbf{P}_{BS}$
18 respectively are rotation matrices, which map vertical and horizontal polarizations to MS
19 and BS antenna polarizations.

20
$$\mathbf{P}_{MS} = \begin{bmatrix} 1 & 0 \\ 0 & 1 \end{bmatrix}$$

21
$$\mathbf{P}_{BS} = \frac{1}{\sqrt{2}} \begin{bmatrix} 1 & 1 \\ 1 & -1 \end{bmatrix}$$

22 The total channel is the matrix product of the BS polarization, the channel polarization,
23 and the MS polarization:

24
$$\mathbf{Q} = \mathbf{P}_{BS}\,\mathbf{S}\,\mathbf{P}_{MS} = \frac{1}{\sqrt{2}} \begin{bmatrix} s_{vv} + s_{hv} & s_{vh} + s_{hh} \\ s_{vv} - s_{hv} & s_{vh} - s_{hh} \end{bmatrix}$$

25 The covariance matrix of the channel is

$$\Gamma_{UL} = E\{vec(\mathbf{Q}) \cdot vec(\mathbf{Q})^H\}$$

$$= E\left\{ \frac{1}{2} \begin{bmatrix} (s_{vv}+s_{hv})(s_{vv}+s_{hv})^* & (s_{vv}+s_{hv})(s_{vv}-s_{hv})^* & (s_{vv}+s_{hv})(s_{vh}+s_{hh})^* & (s_{vv}+s_{hv})(s_{vh}-s_{hh})^* \\ (s_{vv}-s_{hv})(s_{vv}+s_{hv})^* & (s_{vv}-s_{hv})(s_{vv}-s_{hv})^* & (s_{vv}-s_{hv})(s_{vh}+s_{hh})^* & (s_{vv}-s_{hv})(s_{vh}-s_{hh})^* \\ (s_{vh}+s_{hh})(s_{vv}+s_{hv})^* & (s_{vh}+s_{hh})(s_{vv}-s_{hv})^* & (s_{vh}+s_{hh})(s_{vh}+s_{hh})^* & (s_{vh}+s_{hh})(s_{vh}-s_{hh})^* \\ (s_{vh}-s_{hh})(s_{vv}+s_{hv})^* & (s_{vh}-s_{hh})(s_{vv}-s_{hv})^* & (s_{vh}-s_{hh})(s_{vh}+s_{hh})^* & (s_{vh}-s_{hh})(s_{vh}-s_{hh})^* \end{bmatrix} \right\}$$

$$= \frac{1}{2} \begin{bmatrix} p_{vv}+p_{hv} & p_{vv}-p_{hv} & 0 & 0 \\ p_{vv}-p_{hv} & p_{vv}+p_{hv} & 0 & 0 \\ 0 & 0 & p_{vh}+p_{hh} & p_{vh}-p_{hh} \\ 0 & 0 & p_{vh}-p_{hh} & p_{vh}+p_{hh} \end{bmatrix}$$

1
2
3 Here the property of uncorrelated fading between different elements in **S** (i.e.
4 $E\{s_{ij}s_{kl}^*\}=0,\quad i\neq k, j\neq l$) has been used to simplify the expressions. Plugging the
5 numerical example of -8dB XPD, we have

6 $$\Gamma_{UL} = \frac{1}{2} \begin{bmatrix} 1+0.1585 & 1-0.1585 & 0 & 0 \\ 1-0.1585 & 1+0.1585 & 0 & 0 \\ 0 & 0 & 0.1585+1 & 0.1585-1 \\ 0 & 0 & 0.1585-1 & 0.1585+1 \end{bmatrix} = \begin{bmatrix} 0.5793 & 0.4208 & 0 & 0 \\ 0.4208 & 0.5793 & 0 & 0 \\ 0 & 0 & 0.5793 & -0.4208 \\ 0 & 0 & -0.4208 & 0.5793 \end{bmatrix}$$

7 When all of the diagonal elements are equal, the covariance matrix can be further
8 normalised to correlation matrix:

9 $$\Gamma_{UL} = \begin{bmatrix} 1 & \gamma & 0 & 0 \\ \gamma & 1 & 0 & 0 \\ 0 & 0 & 1 & -\gamma \\ 0 & 0 & -\gamma & 1 \end{bmatrix}$$

10 Value of   depends only on XPR and it is obtained from the previous matrix after the
11 normalization of the diagonal values to "1". With different orientations of MS and BS
12 antenna polarizations, also the covariance matrix structure will be different.
13
14

1   **Appendix C: LOS Option with a K-factor**

2   A single-tap MIMO channel can be added to the TDL channels in this case and then

3 modify the time-domain channels as:

4

5

6

$$
\mathbf{H}_n = \begin{cases} \sqrt{\dfrac{1}{K+1}}\mathbf{H}_n + \sqrt{\dfrac{K}{K+1}}\mathbf{H}^{LOS} & n=1\,(\text{first tap}) \\[4ex] \sqrt{\dfrac{1}{K+1}}\mathbf{H}_n & n \neq 1 \end{cases}
$$

7

8

9

10   where the K-factor is in decimal and the LOS component is defined as, between p-th

11 BS antenna and q-th MS antenna

12

13

$$
\mathbf{H}^{LOS}(p,q) = \exp\left(j\frac{2\pi d_{BS}(p-1)}{\lambda}\sin\left(\theta_{BS}\right)\right) \times \exp\left(j\frac{2\pi d_{MS}(q-1)}{\lambda}\sin\left(\theta_{MS}\right)\right)
$$

14 where d_{BS} and d_{MS} are antenna spacing at the BS and MS, respectively, assuming

15 uniform linear array in this case.

1   **Appendix D: Antenna Gain Imbalance and Coupling**

2   Overall receive correlation matrix is

3
$$\mathbf{H}_n^{'} = \begin{bmatrix} \sqrt{\dfrac{1}{c+1}} & \sqrt{\dfrac{c}{c+1}} \\ \sqrt{\dfrac{c}{c+1}} & \sqrt{\dfrac{1}{c+1}} \end{bmatrix} \begin{bmatrix} 1 & 0 \\ 0 & \sqrt{a} \end{bmatrix} \mathbf{H}_n$$

4

5   where antenna-1 to antenna-2 coupling coefficient (leakage of ant-1 signal to ant-2) is
6   "c" (linear) and the antenna-1 and antenna gain ratio is "a" (linear).
7

Appendix E: WINNER Primary Model Description

This appendix describes the primary model from which the CDL models were derived. The primary model is an accurate representation of the true MIMO radio channel. The CDL modes are a simplification of the primary model in order to save simulation time. The use of the primary model is optional but encouraged for further simulation.

The primary model is a double-directional model. Geometric based modeling of the radio channel enables separation of propagation parameters and antennas.

The channel parameters for individual snapshots are determined stochastically, based on statistical distributions extracted from channel measurement. Antenna geometries and field patterns can be defined properly by the user of the model. Channel realizations are generated with geometrical principle by summing contributions of rays (plane waves) with specific small scale parameters like delay, power, angle-of-arrival (AoA) and angle-of-departure (AoD). Superposition results to correlation between antenna elements and temporal fading with geometry dependent Doppler spectrum.

A number of rays constitute a cluster. In the terminology of this document we equate the cluster with a propagation path diffused in space, either or both in delay and angle domains. For a discussion of the word cluster, see Section 3.2.5.

The WINNER generic model is a system level model, which can describe an infinite number of propagation environment realizations. The generic model can describe single or multiple radio links for all the defined scenarios and arbitrary antenna configurations. This is done by applying different parameter sets to a single common mathematical framework. The generic model is a stochastic model with two (or three) levels of randomness. The first level, known as large scale (LS), parameters like Shadow fading, delay and angular spreads are drawn randomly from tabulated distribution functions. LS parameters have cross-correlation between different parameters and auto-correlation between different transceiver locations. Next, the small scale parameters like delays, powers and directions arrival and departure are drawn randomly according to tabulated distribution functions and the random LS parameters (second moments). At this stage the geometric setup is fixed and the only free variables are the random initial phases of the scatterers. By picking (randomly) different initial phases, an infinite number of different realizations of the model can be generated. When the initial phases are also fixed, there is no further randomness.

Channel segment (drop) represents period of quasi-stationarity in witch probability distributions of low-level parameters are not changed. During this period all large-scale control parameters, as well as velocity and direction-of-travel for mobile station (MS), are held constant. Motion within a segment is only virtual and causes fast fading and the Doppler effect by superposition of rotating phasors, rays. To be physically feasible, the channel segment must be relatively confined in distance. The size depends on the environment, but it can be at maximum few meters. Although the large scale

1   parameters can be correlated between the channel segments, the radio channel is
2   discontinuous from segment to segment.

3   A detailed description of the WINNER model is given in [13]. An implementation of the
4   primary model is available at [25].

Appendix F: Generic Proportionally Fair Scheduler for OFDMA

The proportionally fair scheduler (PFS), in its simplest form, computes a metric for all active users at for a given scheduling interval. The user with the highest metric is allocated the resource available in the given interval, the metrics for all users are updated before the next scheduling interval, and the process repeats. To adapt this simple algorithm for OFDMA systems, the definition of scheduling interval and scheduling resource must be extended to apply to a two-dimensional OFDMA frame resource. Furthermore, this PFS applies only to baseline full buffer traffic simulations and zones which use a distributed subcarrier permutation such as PUSC.

For OFDMA systems, the scheduling interval is typically a frame, and multiple users may be allocated in the same frame. Therefore, in the simplest extension to OFDMA systems, two modifications must be made to the PFS: (i) Frames must be equi-partitioned into regular, fixed scheduling resources that must be scheduled sequentially until all available resources are assigned. (ii) The metric must be updated after scheduling each partition. Note that the number of resources eventually allocated to a user depends on the metric update process, and does not preclude a single user from getting multiple or all the resources in a frame. For system simulations with an assumption of fixed overhead allowing for up to $N_{partition}$ resource partitions, each partition assignment should be considered as a separate packet transmission.

To promote fair comparison, each proponent should evaluate system performance with full-buffer traffic using this generic PFS. If this scheduler is not used, the proponent must justify the use of an alternate scheduler, and describe the algorithm in detail. The number of partitions, $N_{partition}$, the time constant of the filter used in the metric computation, and number of active users are all simulation parameters that must be specified by the proponent.

For informative purposes, the metric for a simple proportionally fair scheduler, in which a single user is scheduled in a given scheduling interval, is described in the remainder of this appendix.

At any scheduling instant t, the scheduling metric $M_i(t)$ for subscriber i used by the proportional fair scheduler is given by

$$M_i(t) = \frac{T\_inst_i(t)}{T\_average_i(t)}$$

where $T\_inst_i(t)$ is the data rate that can be supported at scheduling instant t for subscriber i, $T\_inst_i(t)$ is a function of the CQI feedback, and consequently of the modulation and coding scheme that can meet the PER requirement. $T\_average_i(t)$ is throughput smoothed by a low-pass filter at the scheduling instant t for user i. For the scheduled subscriber, $T\_average_i(t)$ is computed as

$$T\_average_i(t) = \frac{1}{N_{PF}}*T\_inst_i(t) + (1-\frac{1}{N_{PF}})*T\_average_i(t-1)$$

and for unscheduled subscriber,

$$T\_average_i(t) = (1-\frac{1}{N_{PF}})*T\_average_i(t-1)$$

The latency scale of the PF scheduler, N_{PF}, is given by

$$N_{PF} = T_{PF} N_{Partitions} / T_{Frame}$$

where T_{PF} represents the latency time scale in units of seconds and T_{Frame} is the frame duration of the system.

In some implementations, the scheduler may give priority to HARQ retransmissions.

1   **Appendix G: 19 Cell Wrap Around Implementation**

2   **G-1.   Multi-Cell Layout**
3   In Figure 27, a network of cells is formed with 7 clusters and each cluster consists of 19
4   cells. Depending on the configuration being simulated and required output, the impact
5   of the outer 6 clusters may be neglected. In such cases, only 19 cells of the center
6   cluster may be modeled.
7
8   For the cases where modeling outer-cells are necessary for accuracy of the results, the
9   wrap around structure with the 7 cluster network can be used. In the wrap around
10   implementation, the network is extended to a cluster of networks consisting of 7 copies
11   of the original hexagonal network, with the original hexagonal network in the middle
12   while the other 6 copies are attached to it symmetrically on 6 sides, as shown in Figure
13   27. The cluster can be thought of as 6 displacements of the original hexagon. There is a
14   one-to-one mapping between cells/sectors of the center hexagon and cells/sectors of
15   each copy, so that every cell in the extended network is identified with one of the cells in
16   the central (original) hexagonal network. Those corresponding cells have thus the same
17   antenna configuration, traffic, fading etc. except the location. The correspondence of
18   those cells/sectors is illustrated in
19   Figure 28.
20
21   An example of the antenna orientations in case of a sectorized system is defined in
22   Figure 28. The distance from any MS to any base station can be obtained from the
23   following algorithm: Define a coordinate system such that the center of cell 1 is at (0,0).
24   The path distance and angle used to compute the path loss and antenna gain of a MS
25   at (x,y) to a BS at (a,b) is the minimum of the following:
26
27   a.   Distance between (x,y) and (a,b);
28   b.   Distance between (x,y) and $(a+3R, b+8\sqrt{3}R/2)$;
29   c.   Distance between (x,y) and $(a-3R, b-8\sqrt{3}R/2)$;
30   d.   Distance between (x,y) and $(a+4.5R, b-7\sqrt{3}R/2)$;
31   e.   Distance between (x,y) and $(a-4.5R, b+7\sqrt{3}R/2)$;
32   f.   Distance between (x,y) and $(a+7.5R, b+\sqrt{3}R/2)$;
33   g.   Distance between (x,y) and $(a-7.5R, b-\sqrt{3}R/2)$,
34   Where, R is the radius of a circle which connects the six vertices of the hexagon.

35

Useful Link

Interference Link
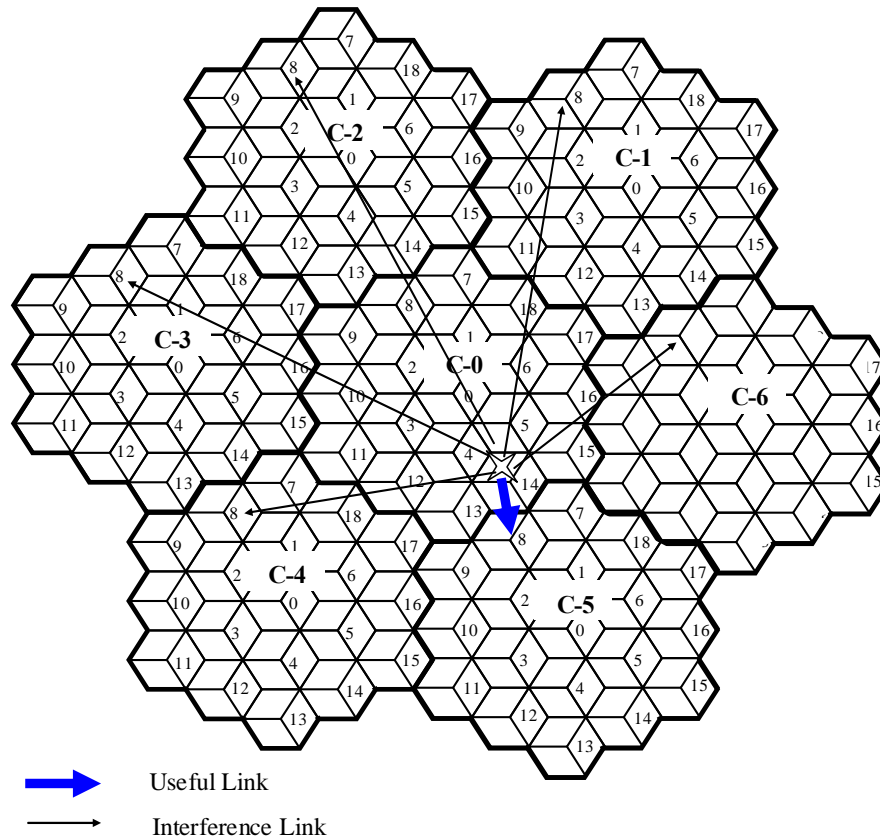
Figure 27: Multi-cell Layout and Wrap Around Example

G-2.   Obtaining virtual MS locations

The number of MSs is predetermined for each sector, where each MS location is
uniformly distributed. The MS assignment is only done for the cluster-0 from where the
decided MSs are replicated in the other six clusters. The purpose to employ this wrap-
around technique, as will be discussed in later section, is to easily model the
interferences from other cells.

G-3.   Determination of serving cell/sector for each MS in a wrap-around multi-cell
network

The determination of serving cell for each MS is carried out by two steps due to the
wrap-around cell layout. The first step is to determine the 19 shortest distance cells for
each MS from all seven logical cells clusters, and the second step is to determine the
serving cell/sector among the nearest 19 cells for each MS based on the strongest link
according to the path-loss and shadowing.

To determine the shortest distance cell for each MS, the distances between the target
MS and all logical cell clusters should be evaluated and the 19 cells with a shortest
distance in all 7 cell clusters should be selected. Figure 27 illustrates an example for
determination of the shortest distance cell for the link between MS and cell-8. It can be

1 seen that the cell-8 located in cluster-5 generates the shortest distance link between MS
2 and cell-8.
3
4 To determine the serving cell for each MS, we need to determine 19 links, whereby we
5 may additionally determine the path-loss, shadowing and transmit/receive antenna gain
6 in consideration of antenna pattern corresponding to the nearest 19 cells/sectors. The
7 serving cell for each MS should offer a strongest link with a strongest received long-
8 term power. It should be noted that the shadowing experienced on the link between MS
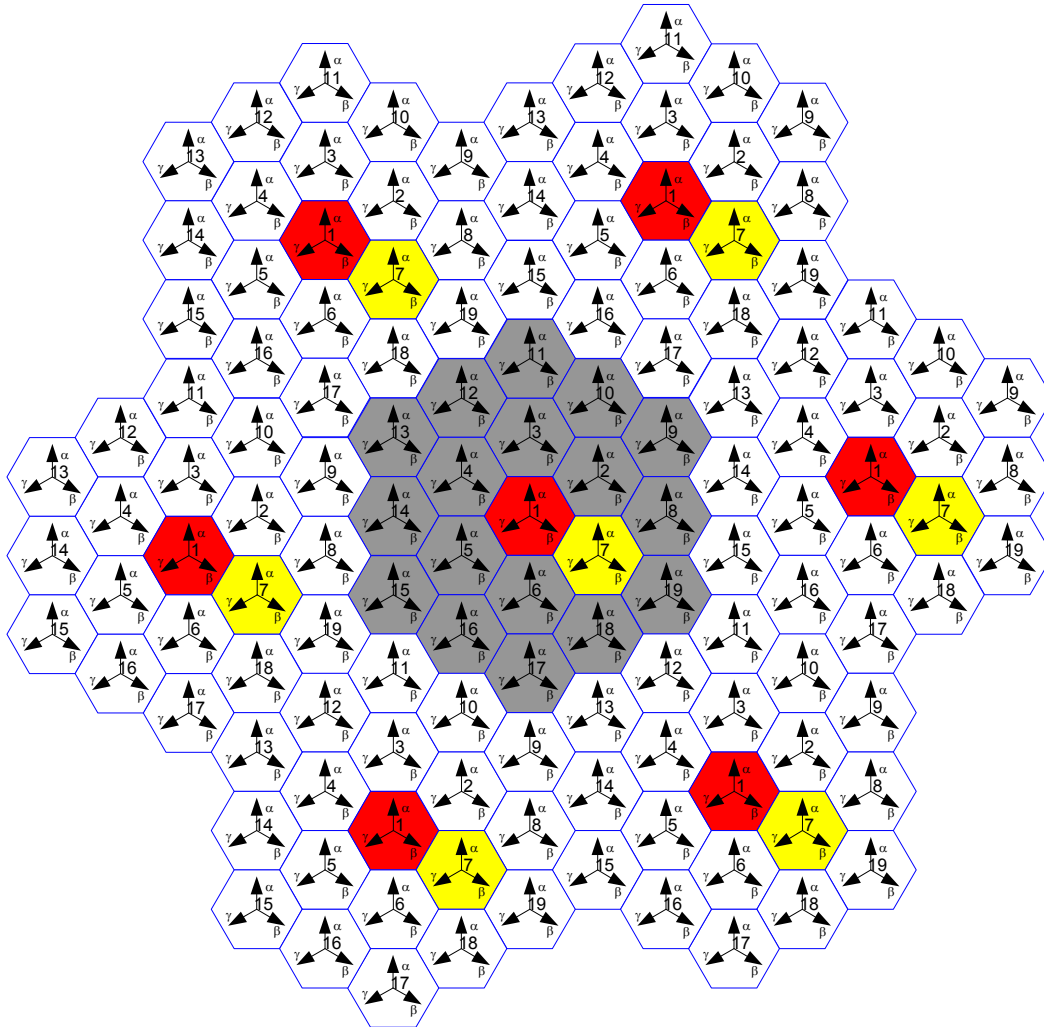9 and cells located in different clusters is the same.

Figure 28: Antenna orientations for a sectorized system in wrap around simulation *

* The arrows in the figure show the directions that the antennas are pointing

1   **Appendix H: Path Loss Calculations**

2

3   The modified COST231 Hata model define the following pathloss

$$PL[dB] = \left(44.9 - 6.55\log_{10}(h_{bs})\right)\log_{10}(\frac{d}{1000}) + 45.5 +$$

4

$$\left(35.46 - 1.1 h_{ms}\right)\log_{10}(f) - 13.82\log_{10}(h_{bs}) + 0.7 h_{ms} + C$$

5

6   where 'd' is expressed in meters and that 'f' is expressed in MHz. The constant C = 3 dB
7   for urban macro.

8   Assuming MS height of 1.5m and at f=2GHz carrier frequency, the model becomes

$$PL = \left(44.9 - 6.55\log_{10}(h_{BS})\right)\log_{10}(d) + 26.46$$

9

$$+ 5.83\log_{10}(h_{BS})$$

10   In addition, a frequency scaling factor of $26\log_{10}(f_c)$ is used to account for the path loss
11   change according to the carrier frequency. The frequency correction factor was taken
12   from some work done by Jakes and Reudink [17] where they used measurement data
13   taken in New Jersey at frequencies of 450MHz, 900MHz, 3.7GHz, and 11.2GHz. They
14   showed a frequency dependence for path loss of $f^{2.6}$, which is larger than the frequency
15   correction being employed by the WINNER models (f^2). Note that the original Hata
16   model has a frequency dependence of $(26.16-1.1h_{ms}+1.56)\log(f)$ (=26.07 when
17   h_{ms}=1.5m) , which is very close to the dependence found by Jakes and Reudink. So the
18   proposed path loss model becomes

$$PL = \left(44.9 - 6.55\log_{10}(h_{BS})\right)\log_{10}(d) + 26.46$$

19

$$+ 5.83\log_{10}(h_{BS}) + 26\log_{10}(f[GHz]/2)$$

$$with \quad 50m < d < 5km \quad h_{BS} > 30m \quad f = 2...6GHz$$

20   With both a default BS and MS heights 32m and 1.5 respectively, the model reduces to

21

$$PL = 35.2 + 35\log_{10}(d) + 26\log_{10}(f[GHz]/2)$$

22

23   For the COST 231 Hata suburban path loss model the path loss equation is identical to
24   that of the urban macro model in (ref except for a C=0dB correction factor instead of
25   3dB. However, this offset itself is somewhat contradictory with the suburban offset used
26   in the original Hata model derived for 150-1500MHz. The original Hata offset for
27   suburban areas was [19]. The offset between urban and suburban path loss models
28   applies to 2.5 GHz only.

29

$$PL_{Suburban} = PL_{Urban} - 2\left[\log\left(\frac{f(MHz)}{28}\right)\right]^2 - 5.4$$

30   Since the original Hata offset matches well with the experiments reported in the Erceg
31   model [3], it is adopted here. Again, a frequency scaling factor of $26\log_{10}(f_c)$ is used to
32   account for the path loss change according to the carrier frequency.

1

2

3   The recommended urban microcellular LOS path loss model is the following [20]:

$$\frac{P_r(r)}{P_t} = -20\log\left(\frac{e^{sr}\,4\pi r D(r)}{\lambda}\right)$$

where,

$P_t = \text{Transmit Power}$

$P_r(r) = \text{Received power}$

$r = \text{Distance between Tx and Rx antennas}$

$e^{sr} = \text{Visibility factor }(s = 0.002)$

$\lambda = \text{Wavelength}$

$$D(r) = \begin{cases} 1 & \text{if } r \leq r_{bp} \\ \dfrac{r}{r_{bp}} & \text{if } r > r_{bp} \end{cases}$$

$$r_{bp} = \frac{4(h_t - h_0)(h_r - h_0)}{\lambda} = \text{breakpoint distance}$$

$h_t = \text{Height of transmit antenna above the road}$

$h_r = \text{Height of transmit antenna above the road}$

4

$h_0 = \text{Effective road height} = 1.0\text{m}$

5

6   This is effectively a two ray model, which has an effective road height to account for the
7   effect of traffic on the ground reflected ray. It also includes a visibility factor, which adds
8   additional path loss at longer ranges as visibility in the street becomes more obscured.
9   The model has been validated by measurements at several frequencies in Japan [20].
10

11   The WINNER path loss model for this case assumes that the dominant propagation
12   path is around the streets, and therefore only has a 'round-the-streets' component.
13   However, in practice there is also an over-the-rooftop component, as given in the ETSI
14   model for UMTS in [21]. The ETSI model combines a round-the-streets model (Berg
15   model) with an over-the-rooftop model, taking the minimum of these two models at any
16   given mobile location. The ETSI model was modified to include the advanced LOS
17   model [20].

1   **Appendix I: Modeling Control Overhead and Signalling (Informative)**

2

3   **I-1.Overhead Channels**

4   **I-1.1.   Dynamic Simulation of the Downlink Overhead Channels**

5

6   Dynamic simulation of the overhead channels is essential to capture the dynamic nature
7   of these channels. The simulations should be done as follows:

8

9   The performance of the overhead channels shall be included in the system level
10   simulation results unless the overhead channel is taken into account as part of fixed
11   overhead e.g., if an overhead channel is time division multiplexed, and takes all the
12   bandwidth, the percentage of time used translates into the same percentage decrease
13   in throughput.

14

15   There are two possible types of overhead channels depending on the proposal: static
16   and dynamic. A static overhead channel requires fixed base station power and
17   bandwidth. A dynamic overhead channel requires dynamic base station power and (or)
18   bandwidth.

19

20   Layer 1 (L1) and Layer 2 (L2) overhead should be accounted for in time and frequency
21   for the purpose of calculation of system performance metrics such as spectral
22   efficiency, user throughput, etc. Examples of L1 overhead include synchronization,
23   guard and DC subcarriers, guard/switching time (in TDD systems), pilots and cyclic
24   prefix. Examples of L2 overheads include common control channels, HARQ ACK/NACK
25   signaling, channel feedback, random access, packet headers and CRC. It must be
26   noted that in computing the overheads, the fraction of the available physical resources
27   used to model control overhead in L1 and L2 should be accounted for in a non-
28   overlapping way. Power allocation/boosting should also be accounted for in modeling
29   resource allocation for control channels.

30

31   The demodulation performance (i.e., frame error rate) of the downlink control channel
32   could be assessed using the link abstraction method used to model traffic channels,
33   with proper modifications, if necessary, to reflect any difference in the transmission or
34   coding format of the control channel.

35

36   The system level simulations need not directly include the coding and decoding of
37   overhead channels. The link level performance should be evaluated off-line by using
38   separate link-level simulations. The link level performance is characterized by curves of
39   detection, miss, false alarm, and error probability (as appropriate).

40

41   For static overhead channels, the system simulation should compute the received SINR
42   and predict the demodulation performance.

43

1   For dynamic modeling of overhead channels with open-loop control (if used), the
2   simulations should take into account the required downlink power or bandwidth for
3   transmission of the overhead channels. During the reception of overhead information,
4   the system simulation should compute the received SINR.
5
6   Once the received SINR is obtained and the frame error rate is predicted, then the
7   impact of the detection, miss, false alarm, error probability should be appropriately
8   taken into account in system-level simulation.
9
10   All overhead channels should be modeled or accounted for. If a proposal adds
11   messages to an existing channel (for example sending control on a data channel), the
12   proponent shall justify that this can be done without creating undue loading on this
13   channel. The system level and link level simulation required for this modified overhead
14   channel as a result of the new messages shall be performed.

15   **I-1.2.   Uplink Modeling in Downlink System Simulation**
16   The proponents shall model feedback errors (e.g. power control, acknowledgements,
17   rate indication, etc.) and measurements (e.g. C/I measurement). In addition to supplying
18   the feedback error rate average and distribution, the measurement error model and
19   selected parameters, the estimated power level required for the physical reverse link
20   channels shall be supplied.

21   **I-1.3.   Signalling Errors**
22   Signaling errors shall be modeled and specified as in the following table.
23

Signaling Channel	Errors	Impact
ACK/NACK channel (if proposed)	Misinterpretation, missed detection, or false detection of the ACK/NACK message	Transmission (frame or encoder packet) error or duplicate transmission
Explicit Rate Indication (if proposed) / mode selection	Misinterpretation of rate)/ mode selection	One or more Transmission errors due to decoding at a different rate (modulation and coding scheme) or selection of a different mode
User identification channel (if proposed)	A user tries to decode a transmission destined for another user; a user misses transmission destined to it.	One or more Transmission errors due to HARQ/IR combining of wrong transmissions
Rate or C/I feedback channel(if proposed)	Misinterpretation of rate or C/I	Potential transmission errors
Transmit sector indication, transfer of HARQ states etc.(if proposed)	Misinterpretation of selected sector; misinterpretation of frames to be retransmitted.	Transmission errors

24
25   **Table 48: Signaling Errors**
26

1   Proponents shall quantify and justify the signaling errors and their impacts in the
2   evaluation report.

1   **Appendix J: Optional Test Scenarios (Informative)**

2   The following table summarizes the channel environments and associated assumptions

3   and parameters for optional test scenarios.

4

Scenario/ Parameters	Suburban Macrocell	Urban Microcell	Indoor Small Office	Indoor Hotspot	Outdoor to Indoor	Rural
Requirement	Optional	Optional	Optional	Optional	Optional	Optional
Site-to-Site distance	1.5 km	0.5 km	50 m	80m	TBD	10 km
Carrier Frequency	2.5 GHz	2.5 GHz	2.5 GHz	2.5 GHz	2.5 GHz	2.5 GHz
Operating Bandwidth	10 MHz for TDD / 5 MHz per uplink and downlink for FDD	10 MHz for TDD / 5 MHz per uplink and downlink for FDD	10 MHz for TDD / 5 MHz per uplink and downlink for FDD	10 MHz for TDD / 5 MHz per uplink and downlink for FDD	10 MHz for TDD / 5 MHz per uplink and downlink for FDD	10 MHz for TDD / 5 MHz per uplink and downlink for FDD
BS Height	32 m	12.5 m	1-2.5m	1~2.5m	TBD	50 m
BS Tx Power	46 dBm TDD 43 dBm FDD	46 dBm TDD 43 dBm FDD	TBD	TBD	46 dBm	46 dBm
MS Tx Power	23 dBm	23 dBm	23 dBm	23 dBm	23 dBm	23 dBm
MS Height	1.5 m	1.5 m	1.5m	1.5m	1.5m	1.5m
Penetration Loss	10 dB	10 dB	0 dB	TBD	0 dB	10 dB
Path Loss Model	Refer to Section 3.2.3.2	Refer to Section 3.2.3.3	Refer to Section 3.2.3.4	Refer to Section 3.2.3.5	Refer to Section 3.2.3.6	Refer to Section 3.2.3.7
Lognormal Shadowing Standard Deviation	NLOS: 8 dB	NLOS: 4 dB LOS: 3 dB	NLOS (Room to corridor): 8 dB NLOS (Through light wall): 6 dB NLOS (Through heavy wall): 8 dB	LOS: TBD NLOS: TBD	7 dB	LOS (near) 4dB LOS (far) 6 dB NLOS 8 dB
Correlation distance for shadowing	50m	50m	TBD	TBD	TBD	LOS 40 m NLOS 120 m
Mobility	TBD	TBD	TBD	0-3 km/hr	TBD	0-350 km/hr
Channel Mix	0-350 kmph	Stationary 0 km/hr - 60%, 3 km/hr -20%, 30 km/hr- 20%	Stationary 0 km/hr - 80%, 3 km/hr -20%	Stationary 0 km/hr - 80%, 3 km/hr -20%	TBD	Stationary 0 km/hr - 30%, ITU Ped B 3 km/hr - 30%, ITU Veh A 30 km/hr - 20%, ITU Veh A 120 km/hr –

						20%
Spatial Channel Model	Refer to Section 3.2.5.2	Refer to Section 3.2.5.3	Refer to Section 3.2.5.4	Refer to Section 3.2.5.5	Refer to Section 3.2.5.6	Refer to Section 3.2.5.7

Table 49: Optional Test Scenarios

1   **Appendix K: Transmit Power and EVM**
2
3   Different modulation methods may have different PAPR and spectral characteristics,
4   affecting the maximum transmit output power. Table 3 specifies the baseline output
5   power and EVM values for the BS and MS, which are applicable for OFDM
6   transmission. This section may be used for evaluating the proposed techniques
7   affecting maximum output power such as PAPR and spectral characteristics
8
9   In the case that a proposed modulation method yields different PAPR and/or different
10   spectral characteristics which affect the maximum output power, these numbers shall be
11   calibrated accordingly. Table 50 contains the reference parameters required for
12   calibration.
13
14

Parameter	Value	Notes
PA model	RAPP-2 (*s*=2)	AM/AM compression model. See below.
Spectral masks	FCC	See appendix XX
EVM (error vector magnitude)	To be specified in the proposal	May be chosen to optimize performance per MCS
Over sampling	≥4	
RBW (resolution bandwidth)	1% of signal bandwidth (100Khz for 10Mhz BW)	For emission measurement. See appendix XX
Reference OFDM transmission	Full bandwidth UL/DL PUSC	

15   **Table 50: Reference parameters for transmit power calibration**
16
17
18   Equation (111) defines the RAPP model. $x(t)$, $y(t)$ are the complex baseband
19   representations of the PA input and output respectively, and the parameter s controls
20   the smoothness of the curve. A value of s=2 will be used by default. It is also
21   recommended to supply results for s=30 to represent a linearized PA. C is the
22   saturation amplitude of the PA.

23
$$y(t) = \frac{x(t)}{\left(1 + \left|\frac{x(t)}{C}\right|^{2s}\right)^{1/2s}}$$
                                                                        (111)

24
25   The proponents should provide simulation results where the modulated signal is passed
26   through a PA compression model and the spectral masks and EVM are computed. The
27   maximum transmit power is the maximum power which meets the spectral masks and
28   the required EVM. The maximum transmit power of flat, full bandwidth modulated
29   OFDM reference signal shall be compared with the maximum effective transmit power
30   of the proposed modulation (with the same PA and mask parameters), and the

difference (power gain or loss) will be added to the BS/MS transmit power as defined in Table 3. The saturation power C shall be set so that the maximum power that the reference OFDM system can transmit is according to the power defined in Table 3.The EVM may be chosen per MCS/mode and results in potentially different maximum transmit power per MCS. The EVM required for the reference OFDM system is as defined in Table 3. Effective transmit power and EVM are defined below.

EVM is defined as the ratio between the effective transmit power and the power of the error vector, both described below. Error vector power is measured over all subchannels, including unmodulated sub-channels. Sub-carriers which do not carry information for any user (guard, DC sub-carriers, and reserved sub-carriers for PAPR reduction) are not included (neither for the error calculation nor for the power calculation). The error signal may be computed using pilot based equalization (as described in [67] 802.16e-2005, subclause 8.4.12.3), or by comparing the transmitted signal with an undistorted (but possibly filtered) signal. In the second case since the distortion error is correlated with the signal, a suitable gain should be applied to undistorted signal such that the error signal becomes uncorrelated with the undistorted signal (and the error vector could be abstracted as additive uncorrelated noise).

The effective transmit power is defined as the power of the distorted signal which is correlated to the ideal signal (so that the power does not include either the error vector or any extra energy for PAPR reduction).

The error vector power and effective transmit power are accumulated in linear domain and their ratio is converted to dB. The EVM is accumulated over a single transmission time interval. In case the EVM varies between different cases in the same transmission mode (e.g. between different sub-channels), the 10% percentile shall be used.

Appendix L: TCP Modeling (Informative)

The widespread use of TCP as a transport protocol in the internet requires an accurate model of TCP behavior to better characterize traffic flow. The major behaviors that need to be accounted for in the TCP model are the session establishment and release and TCP slow start.

L-1.   TCP Session Establishment and Release

TCP uses a 3-way handshake to establish and release a TCP session. The sequences of establishing and releasing a TCP session on the downlink and the uplink are shown in Figure 29 and Figure 30 respectively.

A TCP session is established by the transmitter sending a 40 byte SYNC control segment to the remote server. In response, the server sends a 40 byte SYNC/ACK control segment. The final acknowledgement is sent by the transmitter by setting the ACK flag in the first TCP segment of the TCP session, which is then started in slow start mode [60].

The TCP session is released by the transmitter setting the FIN flag in the last TCP segment. In response, the receiver sends by a FIN/ACK control segment. The session is concluded by the transmitter sending a final ACK message [60].
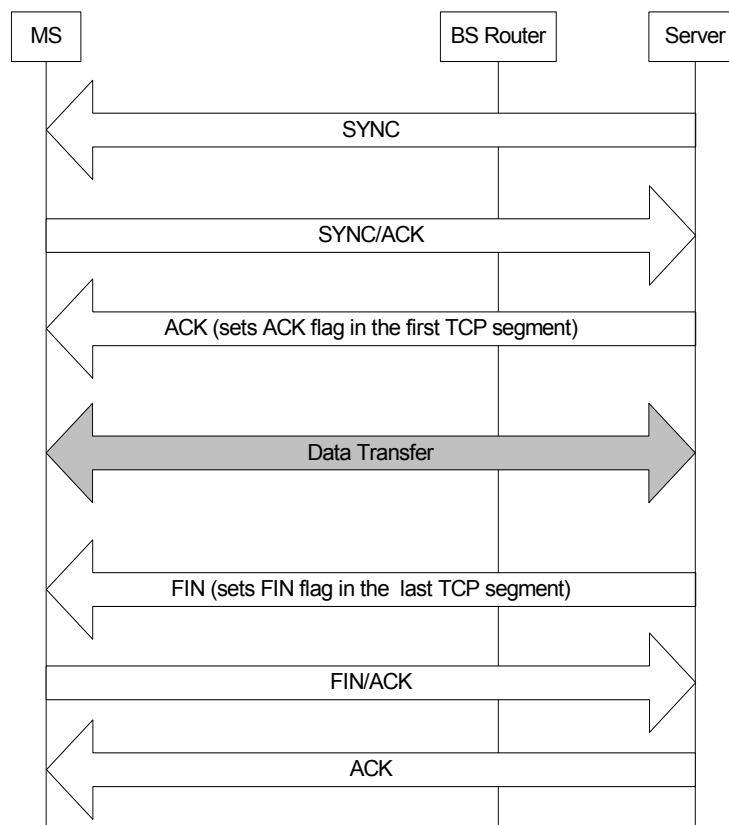
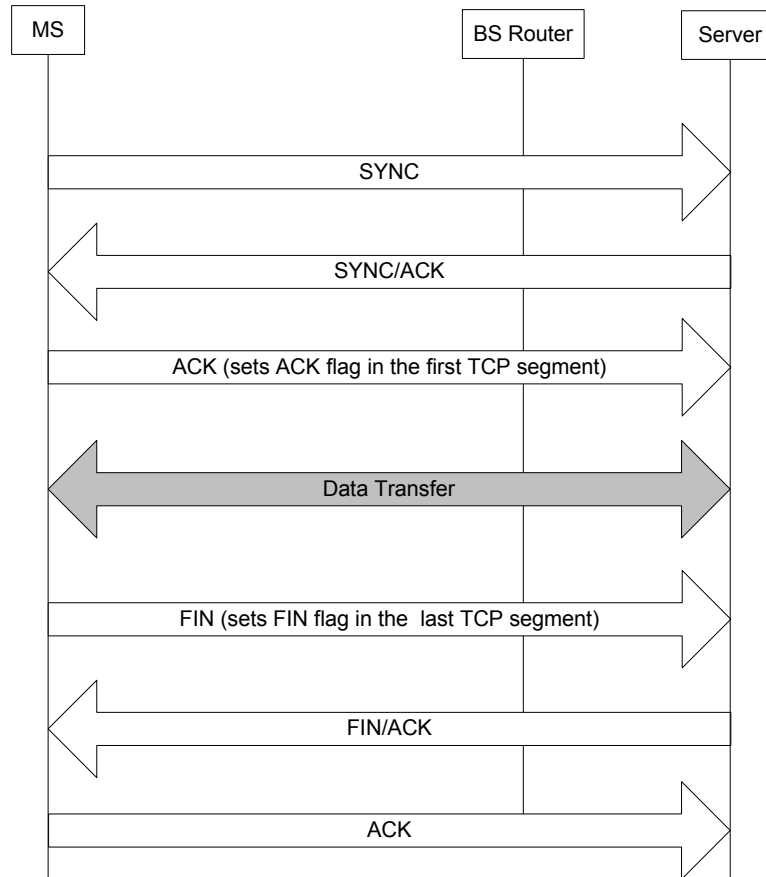**Figure 29: TCP Connection establishment and release on the downlink**

Figure 30: TCP Connection establishment and release on the uplink

L-2.   TCP Slow Start Modeling

TCP slow start is part of the congestion control mechanism implemented in the TCP protocol. Congestion control is implemented using a window flow control mechanism, which tracks the maximum amount of unacknowledged or outstanding data at the transmitter.

The amount of outstanding data that can be sent without receiving an acknowledgement (ACK) is determined by the minimum of the congestion window size and the receiver window size. After the TCP session is established, the transfer of data starts in slow-start mode with an initial congestion window size of 1 segment. The congestion window size is subsequently increased by one with each arriving ACK for a successfully received packet. This increase occurs regardless of whether the packet is correctly received or not, and regardless of whether the packet is out of order or not. This results in an exponential growth of the congestion window.

Figure 31 explains the packet transmission sequence in a TCP session. The round trip time (RTT) for the TCP slow start model consists of:

RTT = $\tau 1 + \tau 2$

where:

$\tau 1$: Time taken by an ACK packet to travel from the client (server) to Base Station + Time taken by an ACK packet to travel from Base Station to server (client) + Time taken by TCP segment to travel from server (client) to Base Station.

$\tau 2$: Time taken by ACK segment to travel from Base Station to Client (server).

$\tau 1$ is assumed to be a random variable of exponential distribution, while $\tau 2$ is determined by the air link throughput . This model only accounts for the slow start process, while congestion control and avoidance have not been modeled. Additionally, the receiver window size is assumed to be large, and thus not a limiting factor.
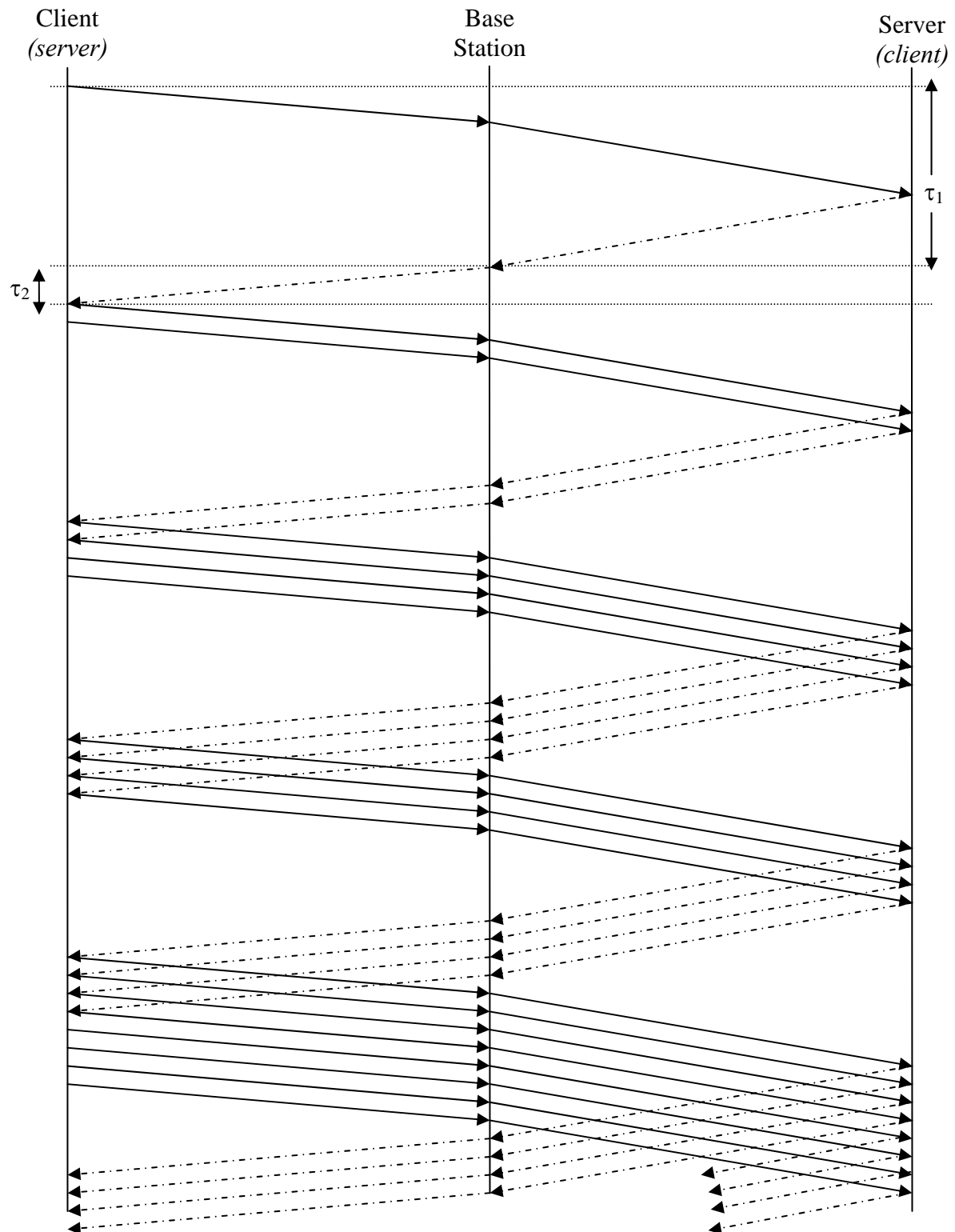
Client
(server)

Base
Station

Server
(client)

τ_1

τ_2

Figure 31: TCP Slow Start Process

1   **Appendix M: Trace Based Model for Streaming Video (Informative)**
2
3   There is no silver bullet on the synthetic traffic generation for streaming video. Multiple
4   analytical algorithms are proposed but no single reference algorithm is ideal for the task.
5   Generally, long rang dependency is recognized for the probability distributions of frame
6   sizes. By using self-similar traffic generator, some of the characteristics of the
7   streaming video traffic can be reproduced. However, the synthetic video traces
8   generated by the analytical model are so different from the reference traces that it is
9   difficult to convince people that synthetic traces have captured the core characteristics
10   of the streaming video traffic.
11
12   Since streaming video traces are easy to obtain and they are easy to use in the
13   simulation environment, a trace based streaming video traffic model is recommended.
14   In this model, a set of 12 MPEG4 traces are selected from the ASU video library. They
15   are representative of the typical mix supported in the network. Among the 12 traces, 6
16   of them are from the major movie genre, such as drama, action, SciFi, and carton; 2 of
17   them are from major sport events; 1 is from MTV, 2 are from talk show with and without
18   commercial, and 1 is from TV sitcom. For a simulation run, each user with video traffic
19   is randomly assigned one video trace out of the 12 available traces. The first packet in
20   the trace is not limited to the start of the trace but is picked at random. Starting from this
21   packet, the trace should continue to evolve sequentially to the end and then wrap
22   around from the beginning back to this starting point. The key characters of these
23   streaming video traces are listed in Table 51.

MPEG4 Video Library*

	Name	Hurst Parameter	Mean Bit Rate (Kbps)	Quantization (I-P-B)	CBR/VBR
Movie					
1	Citizen Kane	0.84	52	30-30-30	VBR
2	Citizen Kane		128		CBR
3	Die Hard	0.72	70	30-30-30	VBR
4	Jurassic Park	0.61	78.5	24-24-24	VBR
5	Star War IV	0.78	65	24-24-24	VBR
6	Aladdin	0.86	91	30-30-30	VBR
Sports					
7	Football With Commercials	0.74	267.5	24-24-24	VBR
8	Baseball With Commercials	0.58	74.2	30-30-30	VBR
MTV					
9	MTV	0.85	212.4	24-24-24	VBR
Talk Show					
10	Tonight Show With Commercials (Jay Leno)	0.8	482	24-24-24	VBR
11	Tonight Show Without Commercials (Jay Leno)	0.93	55	24-24-24	VBR
Sitcom					
12	Friends vol4	0.77	53	24-24-24	VBR

24   * From ASU video library. URL: http://trace.eas.asu.edu/
25
26   **Table 51: MPEG4 video library**

1
2   A user is defined in outage for streaming video service if the 98th percentile video frame
3   delay is larger than 5 seconds. The system outage requirement is such that no more
4   than 3% of users can be in outage.

1   # Appendix N: FCC Spectral Mask (Informative)

2   The following table specifies FCC spectral mask regulations for mobile stations taken
3   from [62].
4

Frequency band	Maximum signal power	RBW
First 1 MHz from channel edge	-13 dBm/RBW,	1% of signal BW, for example 100 KHz for 10 MHz signal
1 MHz to 5.5 MHz from channel edge	-13 dBm/RBW	1 MHz
5.5 MHz or more from edge	-25 dBm/RBW	1 MHz

5   **Table 52: FCC Spectral Mask**
6
7
8

1
2

Appendix O: Per-tone Post Processing SINR for MISO and MIMO with Cyclic Delay Diversity (Informative)

3

4 Cyclic delay diversity (CDD) is a technique that transforms spatial diversity into
5 frequency diversity. The new effective CDD or composite channel frequency response
6 that incorporates the physical channel gains $H_m^{(0)}(n)$ and the artificially induced frequency
7 selectivity associated with a CDD cyclic shifts $e^{-j2\pi n \delta_m / N}$ is given by

8
$$\tilde{H}^{(0)}(n) = \frac{1}{\sqrt{N_T}} \sum_{m=0}^{N_T-1} H_m^{(0)}(n) e^{-j2\pi n \delta_m / N}$$

9 where $\delta_m = m$, $m = 0,1,2,\ldots,N_T - 1$ is the delay applied to the *m*-th antenna, with $\delta_0 = 0$ is
10 assumed to be the reference antenna in a CDD implementation.

11

12 For MISO (multi-input, single-output) and MIMO proposals with CDD implementations
13 the effective CDD or composite channel gains should be used for per tone SINR
14 computations. For example, the n-th tone post processing SINR for a MISO system with
15 a CDD implementation may be defined as

16
$$SINR^{(0)}(n) = \frac{P_{tx}^{(0)} P_{loss}^{(0)} \left| \tilde{H}^{(0)}(n) \right|^2}{\sigma^2 + \sum_{j=1}^{N_I} P_{tx}^{(j)} P_{loss}^{(j)} \left| H^{(j)}(n) \right|^2} \; .$$

17
18